



DoD Corrosion Prevention and Control Program

Corrosion/Degradation Monitoring Technology for Composite Materials Used to Extend Building Service Life

Final Report on Project F07-AR03

Michael K. McInerney, Orange S. Marshall, L.D. Stephenson, Ashok Kumar, Lawrence Clark, Chris Olaes, and Vishal Shinde July 2014



The U.S. Army Engineer Research and Development Center (ERDC) solves the nation's toughest engineering and environmental challenges. ERDC develops innovative solutions in civil and military engineering, geospatial sciences, water resources, and environmental sciences for the Army, the Department of Defense, civilian agencies, and our nation's public good. Find out more at www.erdc.usace.army.mil.

To search for other technical reports published by ERDC, visit the ERDC online library at http://acwc.sdp.sirsi.net/client/default.

Corrosion/Degradation Monitoring Technology for Composite Materials Used to Extend Building Service Life

Final Report on Project F07-AR03

Michael K. McInerney, Orange Marshall, L.D. Stephenson, and Ashok Kumar

Construction Engineering Research Laboratory U.S. Army Engineer Research and Development Center 2902 Newmark Drive Champaign, IL 61822

Lawrence Clark and Chris Olaes

Mandaree Enterprise Corporation. 812 Park Drive Warner Robins, GA 31088

Vishal Shinde

Physical Acoustic Corporation 195 Clarksville Road Princeton Junction, NJ 08550

Final report

Approved for public release; distribution is unlimited.

Prepared for Office of the Secretary of Defense (OUSD(AT&L))

3090 Defense Pentagon

Washington, DC 20301-3090

Under Project F07-AR03, "Corrosion/Degradation Monitoring for FRP Composites

Used for Service Life Extension of Buildings"

Abstract

Fiber-reinforced polymer (FRP) composites offer cost and performance advantages for patching concrete structures that have corroded reinforcing steel, but the Army largely avoids structural composite repair applications because of the lack of long-term performance data. Established composite patch inspection methods are fast but highly subjective. This report describes the demonstration of acoustic guided wave (AGW) technology as a nondestructive evaluation (NDE) methodology for assessing the condition of FRP composite structural patches. The technology uses a hand-guided rolling probe to collect ultrasonic inspection data that can then be analyzed to determine patch condition.

The technology was used to evaluate more than 250 composite seismic upgrade patches installed in 1999 at historic Michie Stadium, U.S. Military Academy. The amplitude difference between the probe's emitted signal and the measured reflection provides data about bond quality and potential material defects. The technology identified several patches needing follow-up attention and possible rehabilitation. When considering costs for equipment procurement, logistics, labor, and field contingencies, an average patch-inspection time of 1.5 hours was estimated. The calculated lifecycle return on investment for this application was 11.91.

DISCLAIMER: The contents of this report are not to be used for advertising, publication, or promotional purposes. Citation of trade names does not constitute an official endorsement or approval of the use of such commercial products. All product names and trademarks cited are the property of their respective owners. The findings of this report are not to be construed as an official Department of the Army position unless so designated by other authorized documents.

DESTROY THIS REPORT WHEN NO LONGER NEEDED. DO NOT RETURN IT TO THE ORIGINATOR.

Contents

Abs	stract			ii	
Fig	gures a	and Tab	les	v	
Pre	eface.			vi	
Exe	ecutiv	e Sumn	nary	vii	
Uni	it Con	version	Factors	viii	
1	Intro	duction	1	1	
	1.1	Proble	em statement	1	
	1.2	Object	tive	2	
	1.3	Approa	ach	3	
2	Technical Investigation				
	2.1	Techn	ology overview	4	
	2.2	Field v	work	7	
	2.3	Data a	analysis	11	
3	Discussion				
	3.1	Metric	S	12	
		3.1.1	Data imaging	12	
		3.1.2	Statistical analysis		
	3.2		ts		
	3.3	Lesso	ns learned		
		3.3.1	Site selection		
		3.3.2	Inspection		
		3.3.3	Unforeseen issues		
		3.3.4	Data management		
		3.3.5	Analysis software	18	
4	Ecor	nomic S	ummary	19	
	4.1	Costs	and assumptions	19	
	4.2	Returr	n on investment (ROI) computation	20	
5	Cond	clusions	and Recommendations	22	
	5.1	Conclu	usions	22	
	5.2	Recon	nmendations	23	
		5.2.1	Applicability	23	
		5.2.2	Implementation	23	
Ref	feren	ces		25	

Appendix A: Full-Tier Drawings Showing Locations of Inspected Patches	A1
Appendix B: Inspected Locations	B1
Appendix C: Statistical Analysis Results	C1
Appendix D: C-scan Results With Digital Pictures	D1
Appendix E: Original ROI Projection From Project Management Plan (PMP)	E1
Report Documentation Page	

Figures and Tables

Figures

Figure 1. Structural support beams with FRP composite patches and	
piezoelectric sensors under Michie Stadium.	
Figure 2. Pocket AU scanning system	5
Figure 3. Workspace for composite patch evaluation.	7
Figure 4. Composite wraps at column tops.	8
Figure 5. Patch naming convention for data logging.	9
Figure 6. List of inspected locations.	10
Figure 7. Inspection in progress.	10
Figure 8. A-scan graph showing amplitude response	13
Figure 9. C-scan image.	13
Figure 10. AU color scale.	14
Figure 11. Statistical toolbox.	15
Figure 12. Sample C-scan image statistical content.	16
Figure 13. Lower-tier amplitude distribution	16
Figure 14. Middle-tier amplitude distribution.	17
Figure 15. Upper-tier amplitude distribution	17
Tables	
Table 1. Breakdown of total project costs	
Table 2. Project field demonstration costs	19
Table 3. ROI calculation.	21

Preface

This demonstration was performed for the Office of the Secretary of Defense (OSD) under Department of Defense (DoD) Corrosion Prevention and Control Project F07-AR03, "Corrosion/Degradation Monitoring for FRP Composites used for Service Life Extension of Buildings." The proponent was the U.S. Army Office of the Assistant Chief of Staff for Installation Management (ACSIM), and the stakeholder was the U.S. Army Installation Management Command (IMCOM). The technical monitors were Daniel J. Dunmire (OUSD(AT&L)), Bernie Rodriguez (IMPW-FM), and Valerie D. Hines (DAIM-ODF).

The work was performed by the Engineering and Materials Branch (CEERD-CF-M), Facilities Division (CF), U.S. Army Engineer Research and Development Center, Construction Engineering Research Laboratory (ERDC-CERL). The ERDC CPC Program Manager was Michael K. McInerney, CEERD-CF-M. Mandaree Enterprise Corporation (MEC), Warner Robins, GA, provided project management and onsite process assessments. At the time this report was prepared, Vicki L. Van Blaricum was Chief, CEERD-CF-M; L. Michael Golish was Chief, CEERD-CF; and Kurt Kinnevan (CEERD-CV-T) was the Acting Technical Director for Adaptive and Resilient Installations. The Deputy Director of ERDC-CERL was Dr. Kirankumar Topudurti and the Director was Dr. Ilker Adiguzel.

The following personnel are gratefully acknowledged for their support and assistance in this project:

- Mr. Jeffery Friese, U.S. Army Engineer District New York, CENAN-EN-MM
- Mr. Pete McGaughran, Directorate of Public Works (DPW) EP&S, USMA West Point
- Mr. Randy McMurtrie, Directorate of Public Works (DPW) EP&S, USMA West Point.

COL Jeffrey R. Eckstein was the Commander of ERDC, and Dr. Jeffery P. Holland was the Director.

ERDC/CERL TR-14-9 vii

Executive Summary

Aging reinforced concrete buildings in the Army inventory often have severely corroded reinforcing steel that necessitates structural upgrades for conformance to current safety codes. Fiber-reinforced polymer (FRP) composites offer many cost and performance advantages for patching degraded reinforced concrete, but the Army largely avoids using them because of the lack of long-term performance data. Improved material inspection methods could help the Army better manage risks and information gaps associated with composite structural reinforcement materials.

This report describes the demonstration of acoustic guided wave (AGW) technology as a nondestructive evaluation (NDE) methodology for assessing the condition of FRP composite structural patches. The technology was used to evaluate patches applied in a 1999 seismic upgrade of historic Michie Stadium at the U.S. Military Academy, West Point, NY. The objective of the inspection was to verify the quality of the bond between the patches and the concrete, and also to check for evidence of delamination within the patches.

The demonstrated AGW technology measures variations in the propagation of acoustic energy used to probe the composite patch. A manually directed rolling-sensor probe emits acoustic energy (100–500 kHz) into the patch and measures the reflected energy. The amplitude difference between the emitted and reflected signal provides data about bond quality and potential material defects. In this study, 250 randomly selected patches were scanned, and the acquired data were statistically analyzed.

Considering all implementation factors and contingencies (e.g., wet patches) encountered during the project, the average patch-inspection time is 1.5 hours. The technology provides objective results, as compared with visual and finger-tap acoustic evaluation by inherently subjective individual inspectors. Results indicate that the technology is effective at identifying composite/concrete bond defects that may need repair. The return on investment for implementing AWG NDE inspection, as compared with conventional inspection methods, was calculated to be 11.91.

ERDC/CERL TR-14-9 viii

Unit Conversion Factors

Multiply	Ву	To Obtain	
degrees Fahrenheit	(F-32)/1.8	degrees Celsius	
Feet	0.3048	meters	
gallons (U.S. liquid)	3.785412 E-03	cubic meters	
Inches	0.0254	meters	
Mils	0.0254	millimeters	
square feet	0.09290304	square meters	

1 Introduction

1.1 Problem statement

Structural degradation of buildings is a facility sustainment problem of immense scope for the Department of Defense (DoD), with the U.S. Army alone being responsible for more than 143,000 buildings. These include thousands of barracks buildings and many historically significant structures. Aging reinforced concrete buildings in the Army inventory often have severely corroded reinforcing steel that necessitates structural upgrades for conformance to current safety codes.

Advanced structural composites, such as fiberglass-reinforced polymer (FRP) materials, offer many cost and performance advantages over conventional upgrade systems for reinforced concrete. They can significantly reduce life-cycle costs, including up to a 50 percent reduction in first costs. They are also easier to install than conventional upgrades and provide improved occupant safety. However, they are typically characterized by a brittle (i.e., non-ductile) failure mode, which could lead to catastrophic structural failure with little forewarning. For this reason, and because of the lack of long-term performance data, the Army largely avoids using composite patches.

Improved material inspection methods could provide Army engineers and facility operators more reliable and current information about composite patch service life. Established methods of composite patch assessment—visual inspection and finger-tap acoustic evaluation—are fast, but they depend on the inherently subjective judgment of each individual inspector.

The U.S. Military Academy (USMA) has installed FRP composite structural upgrades for Michie Stadium at USMA, West Point, NY. This stadium, constructed in 1924, is a historically significant structure. The upgrades are intended to help restore the stadium's resistance to seismic motions that can accelerate structural degradation, often in difficult-to-detect locations. The structural patches need to be monitored using a method that can predict long-term degradation rates on the basis of short-term nondestructive testing. Several of the stadium upgrades were originally installed with embedded piezoelectric sensors (Figure 1), but those can affect the strength and performance of composites. An improved, nondestructive evaluation (NDE) method—one that does not affect material perfor-

mance—is needed to track and document the in situ condition of FRP composites.



Figure 1. Structural support beams with FRP composite patches and piezoelectric sensors under Michie Stadium.

Acoustic guided wave (AGW) inspection is an emerging technology for NDE of FRP composites. Short-term AGW data can be extrapolated to predict long-term material performance and service life. This technology requires no manual intrusion into or physical sampling of the composite repair material, unlike piezoelectric sensors. The DoD Corrosion Prevention and Control Program sponsored a demonstration of AGW technology on selected composite structural patches at Michie Stadium to investigate and validate its efficacy in the in situ monitoring composite material integrity.

1.2 Objective

The objective of this demonstration is to conduct a proof-of-performance evaluation of AGW technology by inspecting a large sample of FRP composite patches installed at Michie Stadium.

1.3 Approach

The U.S. Army Engineer Research and Development Center, Construction Engineering Research Laboratory (ERDC-CERL) coordinated with the USMA Directorate of Public Works (DPW) to select the specific patches to be inspected. The team performed a preliminary visual inspection of the patches and selected candidates for AGW testing. From the patches that were considered easily accessible for AGW testing, 250 were randomly selected for testing. The group contained a cross section of ages, patches with obvious debonding or delamination*, and patches with no obvious debonding or delamination.

The selected patches were indexed and scanned for defects. A scissors lift and articulated manlift were used to perform the inspections, which involved sites located above grade and in cramped quarters beneath the stadium seats.

The scan results were analyzed and bond quality determined based on previous theoretical, laboratory, and field studies (Godínez-Azcuaga 2004, Trovillion et al. 2004).

* Debonding is the separation of two materials adhered to each other. Delamination is the separation of layers in a single laminated material, sometimes caused by manufacturing flaws or stress in service.

-

2 Technical Investigation

2.1 Technology overview

The NDE technology used in this demonstration was the FRP-Concrete Inspection System (FRPCIS) from Physical Acoustics Corporation, Princeton Junction, NJ. This technology was first developed by Physical Acoustics Corporation under a 2004 Small Business Innovative Research (SBIR) Project funded through ERDC-CERL (Godínez-Azcuaga 2004, Trovillion et al. 2004).

The system uses a sonic emitter to send out a short-duration sound pulse and a sensor that captures returning echoes. A defect will change the propagation characteristics of the pulse and the return signal will be modified based on the size and orientation of the defect. Pulse-echo ultrasonic measurements can determine the location of a discontinuity in a part or structure by accurately measuring the time required for a short ultrasonic pulse generated by the rolling-sensor probe to travel through a thickness of material, reflect from the back or the surface of a discontinuity, and be returned to the probe.

One common method of displaying ultrasonic data is termed an "A-scan." For an A-scan, the probe is fixed in position and the strength of the returning echoes as a function of time (or, equivalently of penetration depth) is displayed. The A-scan presentation displays the amount of received ultrasonic energy as a function of time. The relative amount of received energy is plotted along the vertical axis, and the elapsed time (which may be related to the sound energy travel time within the material) is displayed along the horizontal axis. Most instruments with an A-scan display allow the signal to be displayed in its natural radio frequency (RF) form, as a fully rectified RF signal; or as either the positive or negative half of the RF signal. In the A-scan presentation, relative discontinuity size can be estimated by comparing the signal amplitude obtained from an unknown reflector to that from a known reflector. Reflector depth can be determined by the position of the signal on the horizontal sweep.

Another common data display type is the ultrasonic C-scan. In a C-scan, the probe is manually rolled in two dimensions across the surface of the specimen being inspected. The display typically shows the peak response within a time or depth interval of interest as a function of probe position.

The C-scan presentation provides a plan-type view of the location and size of test specimen features. The plane of the image is parallel to the scan pattern of the probe. C-scan presentations are produced with an automated data acquisition system. Typically, a data collection gate is established on the A-scan, and the amplitude or the time of flight of the signal is recorded at regular intervals as the probe is rolled over the test piece. The relative signal amplitude or the time of flight is displayed as a shade of gray or a color for each of the positions where data was recorded. The C-scan presentation provides an image of the features that reflect and scatter the sound within and on the surfaces of the test piece.

The scanning system used in this demonstration was the Physical Acoustics Pocket Guided Wave Acousto-Ultrasonics (AU) system (Figure 2), which is designed for NDE of composite materials that are difficult to inspect using conventional ultrasonic or other evaluation methods. The Pocket AU system includes a scanner unit with 1 Gb onboard flash memory and a USB computer interface (see center picture below). A-scan or C-scan data can be exported as ASCII files so a third-party application can be used to view and analyze the data. The exported ASCII files are saved in *.TXT format.



Figure 2. Pocket AU scanning system.

The Pocket AU system includes a unique dry-coupled rolling-sensor probe (Figure 2, right-hand picture) that contains two wide-band acoustic rolling sensors—one working as a pulser and the other as a receiver. These sensors are spring loaded to maintain a constant contact pressure of 20 lb against the structure, while four guide wheels are used to stabilize the scanner during the inspection procedure.

The rear guide wheels incorporate a rotary encoder that tracks the distance the scanner travels during the scanning process. The position information is necessary to generate the C-scan images.

The rolling-sensor probe also contains a multipurpose button that allows the operator to scale the acoustic signal displayed on the scanner unit screen when working in the A-scan mode, to save A-scan files to memory, or to begin a new scanning line when working in the C-scan mode. A light-emitting diode (LED) mounted on top of the rolling-sensor probe is automatically turned on during scanning and turned off to indicate that the probe has reached the end of a scanning line during a C-scan inspection. The electronics necessary for the LED, multipurpose button, and a 26 dB preamplifier to boost the received acoustic signal are included in a connection board housed inside an ergonomically designed enclosure.

A 2 m interface cable is provided to connect the rolling sensor probe to the Pocket AU scanner unit. This cable has three connectors at each end: two SMB coaxial connectors for the analog acoustic signals and a single DB9 serial connector for the encoder and other digital signals. It is very important that the pulser output from the scanner unit be connected to the pulsing input on the probe; if instead it is connected to the receiver port of the probe, the internal preamplifier on the probe may be damaged.

The technology works by directing acoustic waveform bursts (100–500 kHz) into the material being inspected via the pulser sensor on the rolling-sensor probe. The receiver sensor on the rolling-sensor probe receives the reflected waves, and the scanner unit processes the results and displays them as A-scan waveforms and C-scan image maps. The acoustic signal features include gated amplitude and time-of-flight parameters that change when the acoustic bursts travel through the material and encounter defects or discontinuities such as cracks, material property changes, delamination, and debonding. Defects can be identified from the C-scan images.

The probe's AU emitter can be excited in two ways: fixed or swept frequency. The duration of the pulse is also selectable. Fixed frequency enables the user to select the frequency at which the pulsing sensor will send out a signal. The user can also specify the duration of this signal. By choosing this mode, the signal used to excite the pulsing sensor will be a square wave burst of the frequency and duration chosen.

Swept frequency enables the user to specify a lower and upper range for the frequency of the pulsing sensor. The system will automatically set up the required number of cycles and their durations based on user input to the frequency values. As before, the user can also specify the duration of this signal.

2.2 Field work

Access to the patches, which are installed at the underside of the stadium structure, was provided with a scissors lift and an articulating manlift. The use of ladders was not acceptable because two hands and a stable platform are required to operate the scanning instrument. Scaffolding was not feasible because the uneven ground and debris in the work space would hinder scaffold assembly and relocation. The manlift provided the best combination of stability and mobility between work locations; an entire section between support columns could be completed by moving the arm without repositioning the lift. Figure 3 shows one of the space-constrained work locations. Figure 4 shows examples of the composite wraps (light-gray bands) at the tops of columns beneath the seating.



Figure 3. Workspace for composite patch evaluation.



Figure 4. Composite wraps at column tops.

Two technicians and two support personnel inspected 250 FRP composite patches over 24 days from 15 October to 8 November 2007. The technicians operated the scanning systems while the support personnel operated the lifts. When all tasks and delays in the field operation are included (setup, staging, scanning, teardown, rain, humidity), the average inspection time was about 1.5 hours per patch.

For the inspection of the Michie Stadium patches, the pulser waveform was a 230 kHz square wave of 50 μS duration. Five random FRP patches were selected in the lower tier to calibrate the unit. The received amplitude from all five patches was recorded, and the patch returning the maximum amplitude was used as the calibration benchmark. (The maximum-amplitude return signal corresponded to a good patch—one with minimal to no debonding or delamination.) The A-scan screen height was then adjusted to the maximum detected amplitude of the waveform. The AU unit was used to generate A-scan and C-scan images for each of the inspected patches.

Figure 5 shows the naming convention used for data logging purposes. The entire inspection was divided according to tiers (upper, middle and lower), and each tier was further divided into sections. Every location has two sub patches—an elevation and a bottom patch. Figure 6 shows the number of locations per section that were inspected between October and November. In addition to the 250 preselected locations, 18 additional locations were

inspected. Diagrams of inspected locations and fully marked stadium tier drawings are shown in Appendix A and Appendix B, respectively.

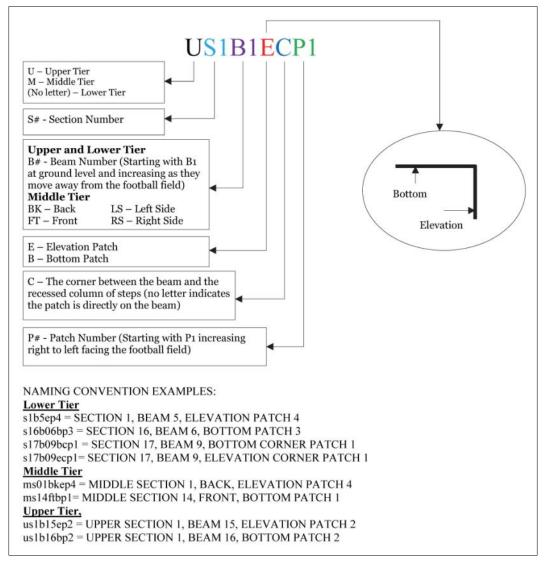


Figure 5. Patch naming convention for data logging.

Section Locations/Section Section Locations/Section Lower Upper Tier Tier Section Locations/Section Middle

Figure 6. List of inspected locations.

Each inspection was subdivided into two scans: one for the bottom patch and one for the elevation patch. Figure 7 shows the inspection of a bottom patch, with labels indicating both the bottom and elevation patches.



Figure 7. Inspection in progress.

2.3 Data analysis

When the scan results were analyzed, bond and lamination qualities were determined based on previous theoretical, laboratory, and field studies by Godínez-Azcuaga (2004) and Trovillion et al. (2004). The statistical analysis of the acquired data is based on the 6 dB drop method—the principle that when ultrasonic waves travel through a delamination, the amplitude of the wave decreases (IAEA 1988). A 6 dB decrease corresponds to a 50% reduction in amplitude.

Appendix C contains all of the statistical results for each inspected location. Appendix D contains all of the C Scan images and accompanying photographs of each inspected location.

3 Discussion

3.1 Metrics

3.1.1 Data imaging

The direct metric for evaluating the qualities of the bond and lamination of an FRP patch is change in AU signal amplitude (emitted versus returned) across each patch. Five FRP patches in the lower tier were selected randomly to calibrate the unit. The received amplitude from each patch was recorded, and the patch returning the maximum amplitude was used as the calibration benchmark. (The maximum amplitude return signal corresponded to a good patch—one with minimal or no debonding or delamination.) The A-scan screen height was then adjusted to the maximum detected amplitude of the waveform.

As discussed previously, AU scanner data were displayed as A- and C-scans. Statistical analysis of the acquired data was based on the 6 dB drop method (IAEA 1988).

In an A-scan, the closer the returned-signal amplitude is to the emitted-signal amplitude, the better are the qualities of the bond and lamination. Examples of good and poor bonds are shown in Figure 8. The evaluation is qualitative because (1) the maximum amplitude of a good bond is determined from a random sampling of patch A-scans (it is assumed that a good bond does exist and that it will be found), and (2) a bond of lesser quality has lesser amplitude. The quantitative bond strength* is not known, just that the bond is of lesser quality.

* One quantitative method of measuring bond strength is ASTM D7522 / D7522M – 09, which determines the greatest perpendicular force (in tension) that an FRP system can bear before a plug of material is detached.

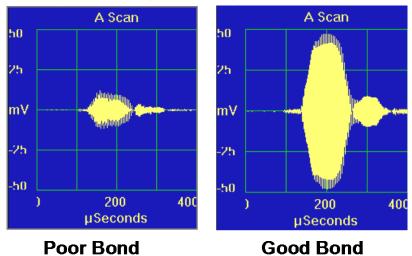


Figure 8. A-scan graph showing amplitude response.

The C-scan image provides information in terms of time of flight and amplitude of the received signals as a raster scan along the X-Y plane of a test sample. Figure 9 shows a C-scan image of a scanned FRP patch. The acquired data are post-processed using UTwin*, a Windows-based data acquisition, imaging, and analysis software system for C-Scan images. (Note that this software required much time and effort to configure before reading the exported data file produced by the AU scanner unit.)

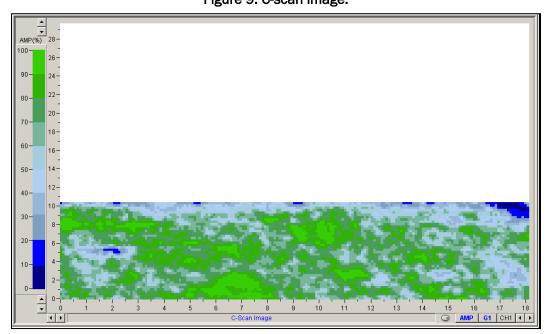


Figure 9. C-scan image.

^{*} UTwin is a trademark of MISTRAS Group, Inc, Princeton Junction, NJ.

Figure 10 shows the AU scanner bar scale that is used to plot the C-scan image. Generally, blue or light-blue colors signify lower AU signal amplitude values that indicate defect-containing areas; and greenish or bright-green colors represent defect-free regions.

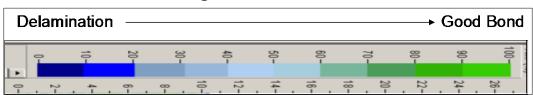


Figure 10. AU color scale.

3.1.2 Statistical analysis

The statistical analysis of the acquired data is based on the 6 dB drop method (IAEA 1988), also known as the K9.3 length. This method is a standard used in ultrasonic testing to analyze flaws. As the rolling-sensor probe passes from a flawless area to a debonded or delaminated area, the amplitude decreases. When the decrease in amplitude is equal to 6 dB, the scanner has moved halfway off of the flawless area. By traversing the flawless area and measuring 6 dB drop dimensions, the approximate dimensions of debonded and delaminated areas may be obtained.

The maximum screen height is set to 100% on the AU color bar in Figure 10 (which indicates a flawless area), and the 6 dB drop is set to 40%* on the color bar. In order to indicate debonded and delaminated areas on the C-scan, whenever the relative amplitude falls below 40% on the A-scan graph shown in Figure 8, a blue pixel is plotted on the C-scan.

The statistical analysis tool allows a quantitative assessment of the C-scan data. Before the acquired data are analyzed, the statistical toolbox (Figure 11) is configured in two steps. In the first step, the feature to analyze is selected; in the second step, the threshold values are set along with the desired C-scan area (the complete scan, in this case).

^{*} Although a 6 dB drop corresponds to 50%, experience has shown that 40% is a better factor to use when inspecting FRP composite patches on concrete.

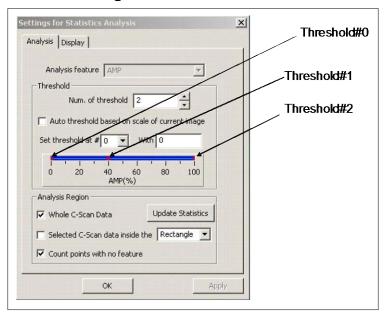


Figure 11. Statistical toolbox.

As seen in Figure 11, three thresholds were used. Threshold#0 was set to 0.0%, threshold#1 was set to 40.0%, and threshold#2 was set to 100%. The statistical tool analyzes the entire C-scan data set and shows the minimum, maximum, average, standard deviation results for the data, along with the distribution (percentage) of the data in the selected thresholds.

3.2 Results

Appendix C shows the statistical results for all 250 locations in a tabular format. Appendix D contains all C-scan images of inspected patches, with the corresponding digital photographs. Figure 12 shows the statistical features extracted from a C-scan image.

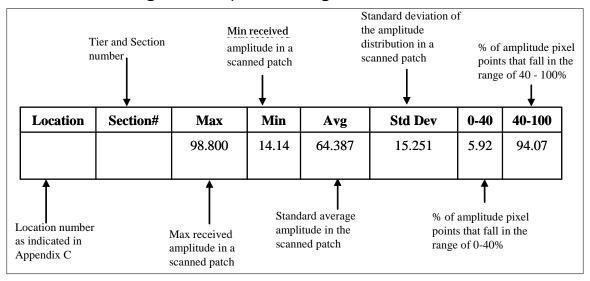


Figure 12. Sample C-scan image statistical content.

All detected flaws were determined to be caused by patch debonding, not delamination. This conclusion was reached using time-of-flight data, which can be used to determine the depth of the flaw beneath the surface. All scans indicated that the flaws were beneath the FRP composite material. As discussed previously, the better the bond between the FRP and the concrete beam, the higher the average amplitude per patch (maximum = 100%). Within each section, 4-10 randomly selected patches were inspected. For each section, the average amplitude is calculated as shown below:

$$Average \ Amplitude / Section = \frac{\sum_{0}^{Total \ inspected \ Patches / Section} Average \ Amplitude / \ patch}{Total \ number \ of \ Patches \ per \ section}$$

Figure 13 – Figure 15 show the amplitude distribution per section.

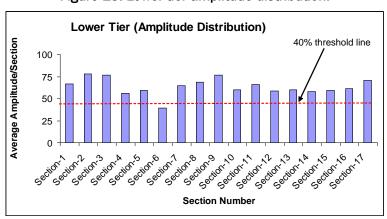


Figure 13. Lower-tier amplitude distribution.

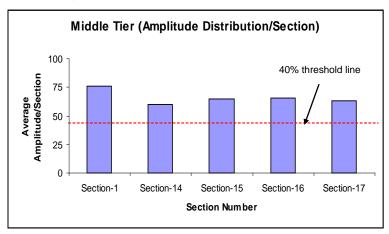
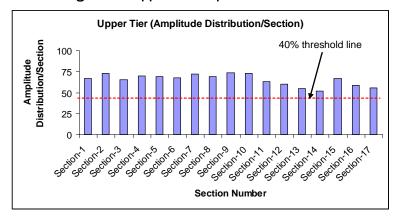


Figure 14. Middle-tier amplitude distribution.

Figure 15. Upper-tier amplitude distribution.



3.3 Lessons learned

3.3.1 Site selection

A pre-inspection site visit was useful to select the patches to be inspected and to identify possible obstacles to field work.

3.3.2 Inspection

Inspection of all the patches was completed within the scheduled time frame. Patches on which surface moisture (e.g., dew) had accumulated produced less signal attenuation than dry ones, which produced skewed readings. Inspection was delayed to wait for wet patches to dry in order to obtain an accurate scan for bond strength.

Patches with protruding resins damaged the encoder on the rolling-sensor probe. No inspection time was lost because a spare probe was available.

The problem was eliminated with a design change to the spare encoder assembly.

3.3.3 Unforeseen issues

Rain caused inspection delays because the work areas are not enclosed and the concrete slabs that make up the seating area are not sealed, allowing rain to get into the inspection area. Rainwater also accumulated on patch surfaces, slowing the drying.

3.3.4 Data management

Data collection, management, and analysis for this project were scoped to suit the purposes of technology demonstration and validation. A detailed examination of the numerical and photographic records indicates a small number of gaps and inconsistencies. When the demonstrated technology is applied to a formal engineering study, the use of data-management best practices is essential in order to accurately track every potentially degraded structural patch. However, even given data-management limitations in the current project, identify several patches requiring expert inspection and possible repair were unambiguously identified.

3.3.5 Analysis software

The UTwin analysis software was selected based on the capabilities stated in the manufacturer's product bulletin, but it was not ready to use "out of the box." Much time and effort was needed to configure this software to read the exported data file produced by the AU scanner unit.

4 Economic Summary

4.1 Costs and assumptions

Total project costs were \$940K. A rough breakdown of project expenses is presented in Table 1.

Description **Amount** Labor \$250,000 Materials \$95,000 Contracts \$425,000 Travel \$80,000 Reporting \$80,000 Air Force and Navy Participation \$10,000 Total \$940,000

Table 1. Breakdown of total project costs.

The field demonstration costs for this CPC project are shown in Table 2.

Item	Description	Amount
1	Labor for two equipment operators (30 days)	\$63,520
2	Travel for two equipment operators (30 days)	\$23,030
3	Rental for two manlifts	\$41,410
4	Personal protective equipment (PPE)	\$3,550
5	Miscellaneous (equipment operations)	\$4,140
6	Labor for two people (Research Engineer I) for preparation and inspection (30 days)	\$90,000
7	Travel for two people for inspection (25 days)	\$15,480
8	Travel for two people for preparation (5 days)	\$5,964
9	AU Handheld Rental 2-units + chargers	\$10,000
10	Consumables and supplies (inspections)	\$500
11	Labor for one person (Research Engineer I) for analysis and reporting (25 days)	\$37,500
	Total	\$295,094

Table 2. Project field demonstration costs.

Alternative 1 (Baseline Scenario). Structural components of the West Point Michie Stadium require complete replacement at Year 8, at a cost of

\$25.5M, as shown in Table 3 (column B). Average annualized maintenance cost of the existing structural components is \$280K, which drops to \$6.5K after complete replacement of the components.

Alternative 2 (New Technology Application). The application of corrosion/degradation monitoring and degradation sensing technologies in Year 1 at a total project cost of \$940K is projected to extend the life of the structural components over the conventional maintenance schedule by another 30 years. Data from maintenance personnel indicate that early detection and subsequent preventive measures result in maintenance cost savings of 50%, which means that the new system cost will be \$140K. The annual cost of operating the sensors would be \$10K, resulting in a total cost of \$150K (Table 3, column D). Under this alternative, the structural components must be replaced in Year 30 at a cost of \$25.5M.

4.2 Return on investment (ROI) computation

The ROI for this technology was computed using methods prescribed by Office of Management and Budget (OMB) Circular No. A-94, *Guidelines and Discount Rates for Benefit-Cost Analysis of Federal Programs*. Comparing the costs and benefits of the two alternatives, the 30-year return on investment after implementing the new technology (Alternative 2) is projected to be about 12 (11.91 as shown in Table 3).

This is very close to the original estimated ROI of 11.98 (see Appendix 1). The difference comes from reconsidering the \$10K annual expense for use of the new technology in the maintenance of the replaced structural components (Alternative 1). Since the primary use for FRP composite patches is for structural upgrades, once the components are replaced, the patches would not be required.

Table 3. ROI calculation.

Return on Investment Calculation

	Investment Required				[940,000	
			Return on Inv	estment Ratio	11.91	Percent	1191%
	Net Present Value of Costs and Benefits/Savings 5,192,295 16,391,820				16,391,820	11,199,525	
						_	
Α	В	С	D	E	F	G	н
Future	Baseline Costs	Baseline	New System	New System	Present Value of	Present Value of	Total Present
Year		Benefits/Savings	Costs	Benefits/Savings	Costs	Savings	Value
1	280.000		150,000.0		140.190	261.688	121,498
2	280,000		150,000.0		131,010	244,552	113,542
3	280,000		150,000.0		122,445	228,564	106,119
4	280,000		150,000.0		114.435	213,612	99.177
5	280,000		150,000.0		106,950	199,640	92,690
6	280,000		150,000.0		99,945	186,564	86,619
7	280,000		150,000.0		93,405	174,356	80,951
8	25,500,000		150,000.0		87,300	14,841,000	14,753,700
9	6,500		150,000.0		81,585	3,535	-78,050
10	6,500		150,000.0		76,245	3,304	-72,941
11	6,500		150,000.0		71,265	3,088	-68,177
12	6,500		150,000.0		66,600	2,886	-63,714
13	6,500		150,000.0		62,250	2,698	-59,553
14	6,500		150,000.0		58,170	2,521	-55,649
15	6,500		150,000.0		54,360	2,356	-52,004
16	6,500		150,000.0		50,805	2,202	-48,603
17	6,500		150,000.0		47,490	2,058	-45,432
18	6,500		150,000.0		44,385	1,923	-42,462
19	6,500		150,000.0		41,475	1,797	-39,678
20	6,500		150,000.0		38,760	1,680	-37,080
21	6,500		150,000.0		36,225	1,570	-34,655
22	6,500		150,000.0		33,855	1,467	-32,388
23	6,500		150,000.0		31,635	1,371	-30,264
24	6,500		150,000.0		29,565	1,281	-28,284
25	6,500		150,000.0		27,630	1,197	-26,433
26	6,500		150,000.0		25,830	1,119	-24,711
27	6,500		150,000.0		24,135	1,046	-23,089
28	6,500		150,000.0		22,560	978	-21,582
29	6,500		150,000.0		21,090	914	-20,176
30	6,500		25,500,000		3,350,700	854	-3,349,846

5 Conclusions and Recommendations

5.1 Conclusions

Using the demonstrated acoustic guided wave technology, two technicians and two support personnel inspected 250 FRP composite patches over 24 days at Michie Stadium. When all tasks and delays in the field operation are included (setup, staging, scanning, teardown, rain, humidity), the average inspection time was about 1.5 hours per patch at a cost of about \$1,180 (\$295,100/250) per patch. An average inspection time of 1.5 hours per patch using this technology (when setup, staging, and teardown are included) seems like a reasonable estimate for planning other inspections.

Patches on which surface moisture (e.g., dew) had accumulated produced less signal attenuation than dry ones, which produced skewed readings. Inspection was delayed to wait for wet patches to dry in order to obtain an accurate scan for bond strength.

Considerable effort was required to configure the commercial analysis software to read the data file exported by the AU scanner unit.

The inspection results were documented in the form of C-scan images. All of the detected flaws were determined to be caused by patch debonding, not composite material delamination. Results indicate that section 6 on the lower tier and section 14 on the upper tier should be fully investigated for patch-bond failures. Specifically, the identified patches of interest are numbers L1–L5 in section 6, and L1–L6 in section 14. Their locations in the stadium are noted in Appendices A and B.

Acoustic guided wave (AGW) inspection technology has been shown to be an objective method for detecting composite patch debonding. This is a substantive and critical benefit when compared with present evaluations, which rely on visual inspection and finger-tap acoustic testing. These methods can be executed rapidly, but they are subjective in terms of assessing of bond condition. The ROI ratio calculated based on the results of this demonstration was 11.91.

5.2 Recommendations

Efforts should be initiated to characterize and model debonding failures of FRP composite patches that will lead to significant progress in understanding the modes and mechanisms of debonding failures. A pilot study should be conducted to directly correlate the reduction in the bonding strength of the patches with the change in AU signal amplitude. This will help in determining the remaining service life of the patches.

Even without a laboratory correlation study, degradation rates can be empirically derived through linear extrapolation of the results of multiple inspections over time to give a first-order degradation rate. The debonding and delamination rates may then be used to predict when the patch will need maintenance or total replacement. Environmental parameters, such loading, temperature, and humidity can be included in the degradation model to increase accuracy.

5.2.1 Applicability

Acoustic guided wave (AGW) technology can be used to inspect FRP-retrofitted components of concrete infrastructure and masonry structures (both reinforced and unreinforced). Suitable applications include beams, columns, slabs, and walls of structures such as bridges, buildings, parking garages, piers, and tunnels.

5.2.2 Implementation

Implementation of this technology throughout DoD could be facilitated through revisions of Unified Facilities Guide Specification (UFGS) Section 04 01 21, *Rehabilitation of Reinforced and Unreinforced Masonry Walls Using Surface-Applied FRP Composites.* Section 3.8.3, "Void Detection," could be modified with the following language:

NOTE: Acoustic guided wave (AGW) inspection technology has been shown to be an objective method for detecting voids.

Section 3.8.4, "Delaminations," could be modified with the following language:

NOTE: Acoustic guided wave (AGW) inspection technology has been shown to be an objective method for detecting delaminations.

Implementation could further be supported through efforts to incorporate this technology into

- American Concrete Institute ACI 440.2R (2008; Errata 2009), Guide for the Design and Construction of Externally Bonded FRP Systems for Strengthening Concrete Structures
- ACI 440.3R (2004), Guide Test Methods for Fiber Reinforced Polymer (FRP) for Reinforcing or Strengthening Concrete Structures.

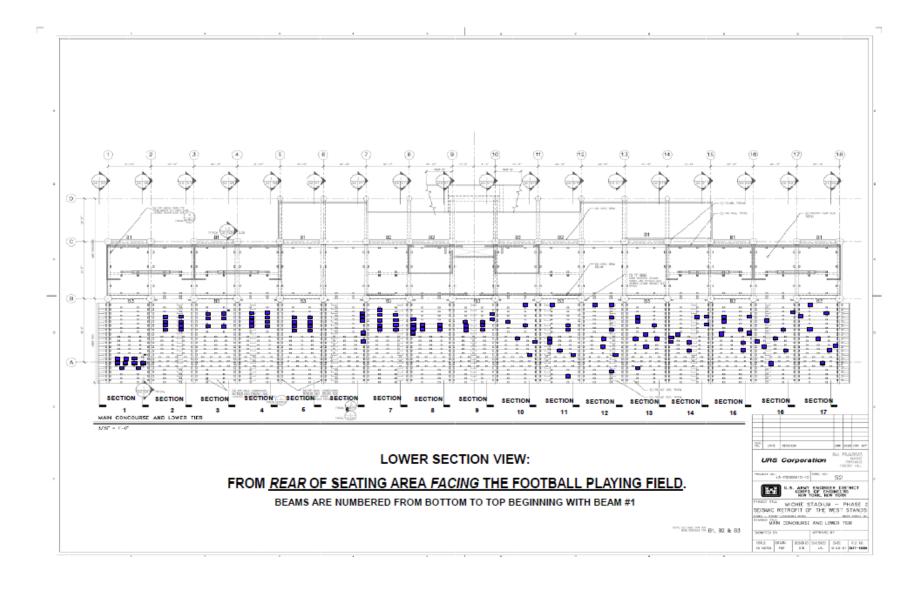
References

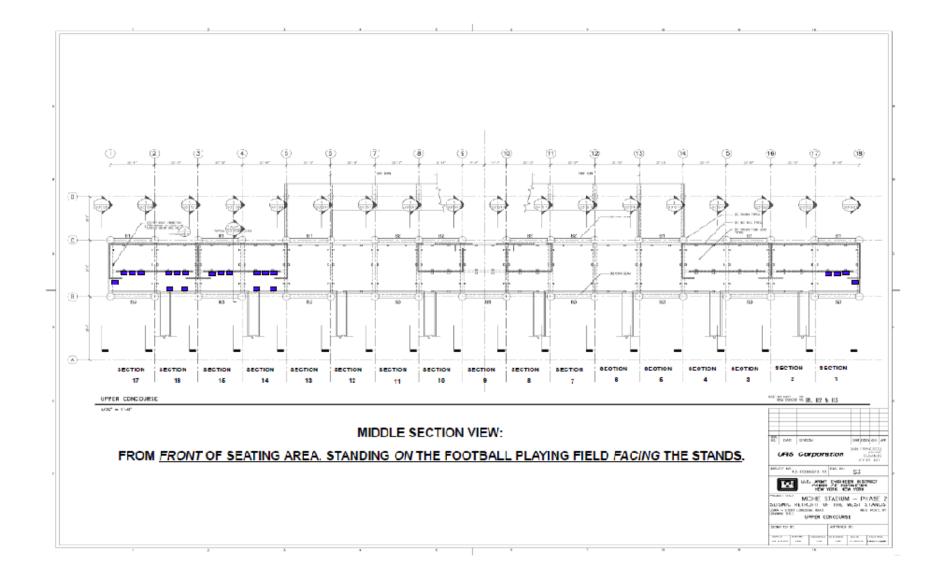
- ASTM D7522 / D7522M 09, "Standard Test Method for Pull-Off Strength for FRP Bonded to Concrete Substrate."
- Godínez-Azcuaga, Valery F. January 2004. Field Portable Infrastructure Fiber-Reinforced Polymer Composite Inspection & Evaluation System Using Ultrasound Technologies. PHASE II Final Report, Contract Number DACA42-02-C-0018.
- International Atomic Energy Agency (IAEA). 1988. "Ultrasonic Testing of Materials at Level 2," Ref. Number 19100874. *INIS* 19:23.
- Office of Management and Budget (OMB) Circular No. A-94. 1992. "Guidelines and Discount Rates for Benefit-Cost Analysis of Federal Programs." Washington, DC: Office of Management and Budget.
- Trovillion, Jonathan C., Valery Godinez-Azcuaga, and Richard Finlayson, "A Nondestructive Evaluation Technique for Fiber Reinforced Polymer (FRP) Composites Using Acoustic Guided Waves (AGW) Conference Proceedings," 24th Army Science Conference, November 2004.

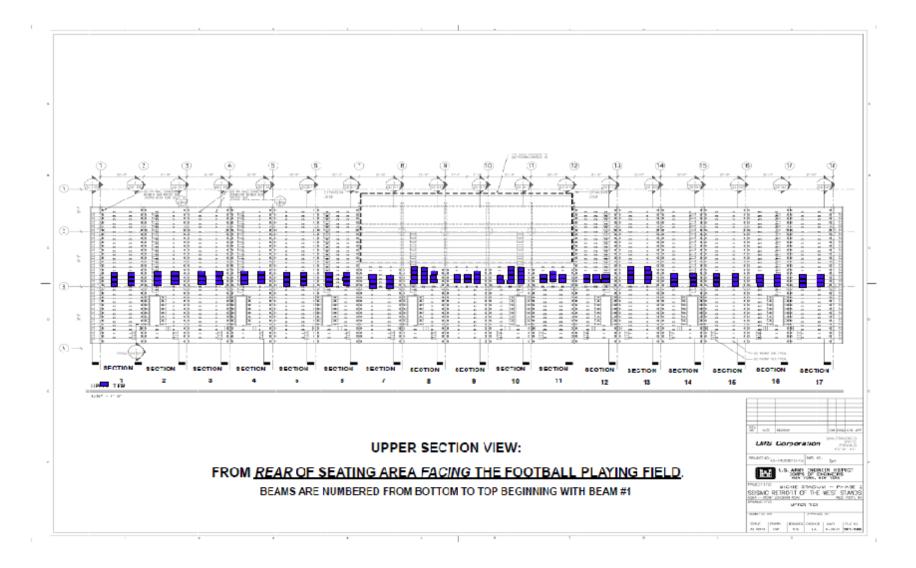
Appendix A: Full-Tier Drawings Showing Locations of Inspected Patches

The drawings in Appendix A show the inspected locations as small blue rectangles in the context of each entire tier. The Lower and Upper Tiers are numbered from left to right, as if the viewer were standing behind the seats looking toward the playing field. The view adopted for the Middle Tier was oriented as if the viewer were standing on the football playing field looking toward at the stands. This "flipped" view was selected for the Middle Tier because rear access to it did not allow an observer to accurately identify the inspected locations using the marked drawing while simultaneously looking at the tier.

Six of the inspected locations are not indicated on these drawings. They are L7 and L8 in Section 3 of the Lower Tier, L9 in Section 5 of the Lower Tier, L6 and L7 in Section 6 of the Lower Tier, and L10 in Section 7 of the Lower Tier. These data gaps are addressed in section 3.3.4 under "Lessons learned."



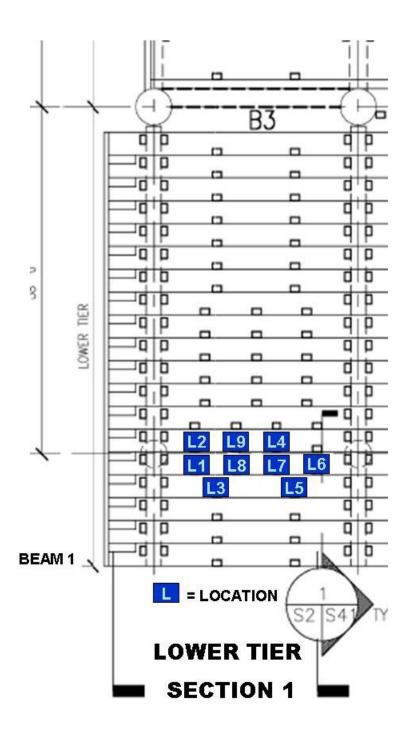


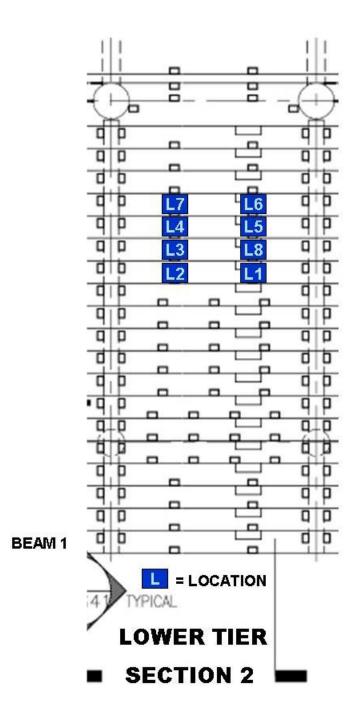


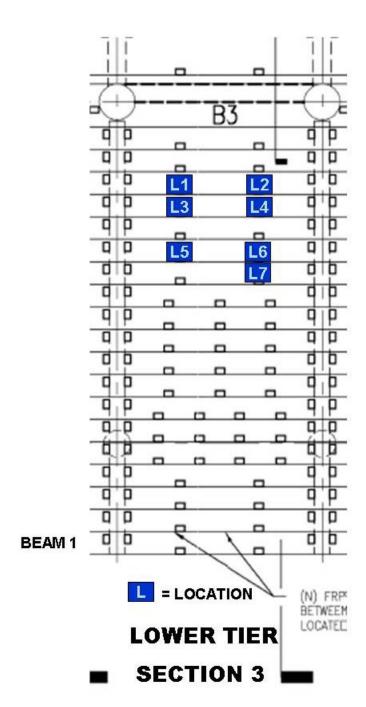
Appendix B: Inspected Locations

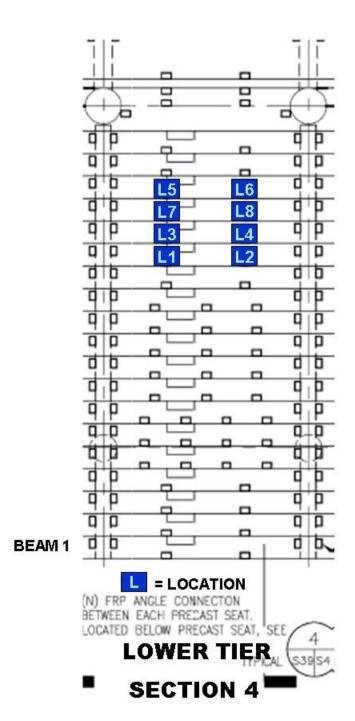
The drawings in this appendix show section-level detail of the inspected locations. They are derived from the drawings in Appendix A.

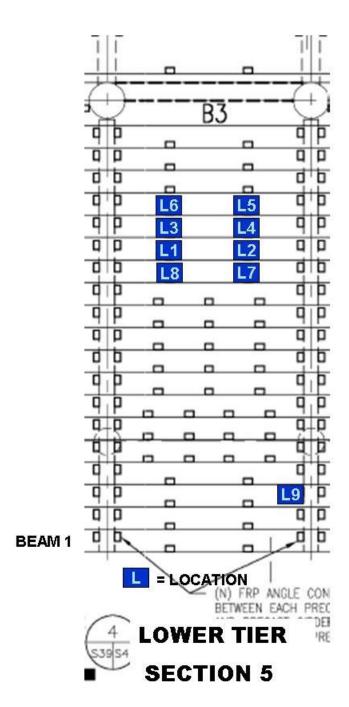
Five of the inspected locations are not indicated on these drawings. They are L8 in Section 3 of the Lower Tier, L6 and L7 in Section 6 of the Lower Tier, L10 in Section 7 of the Lower Tier, and L8 in Section 13 of the Upper Tier. These data gaps are addressed in section 3.3.4 under "Lessons learned."

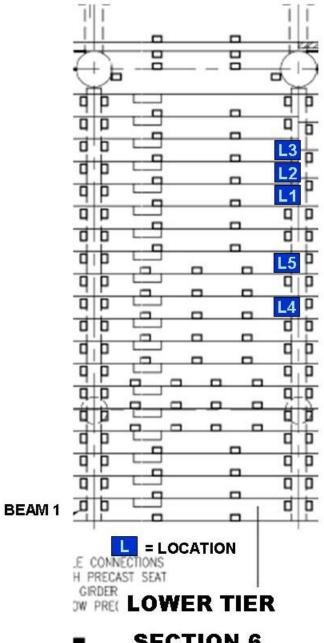




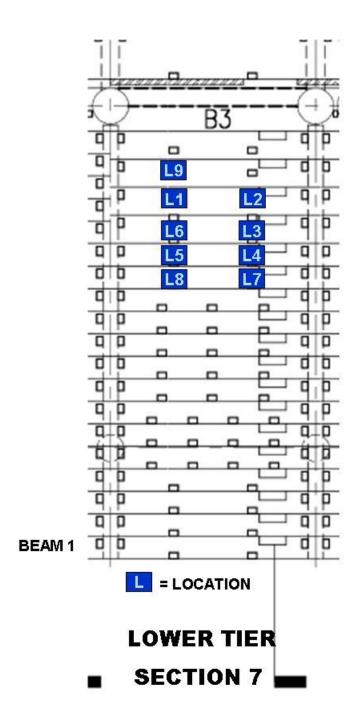


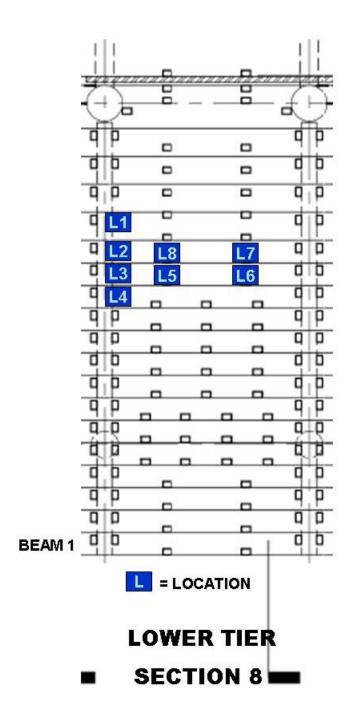


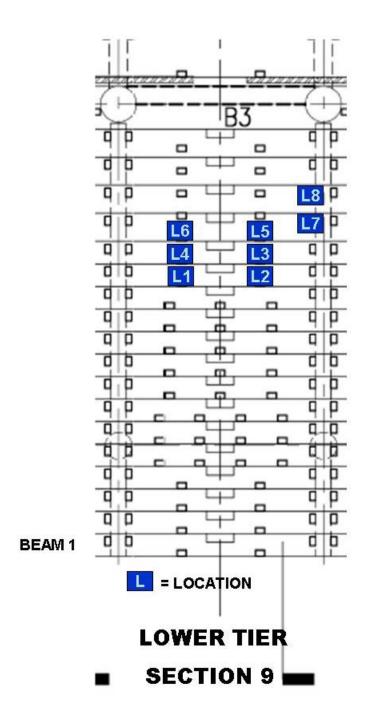


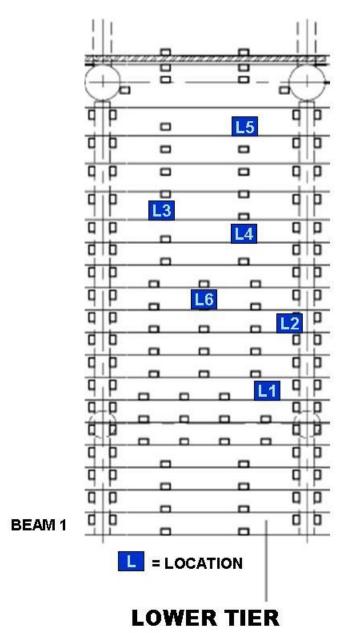


SECTION 6

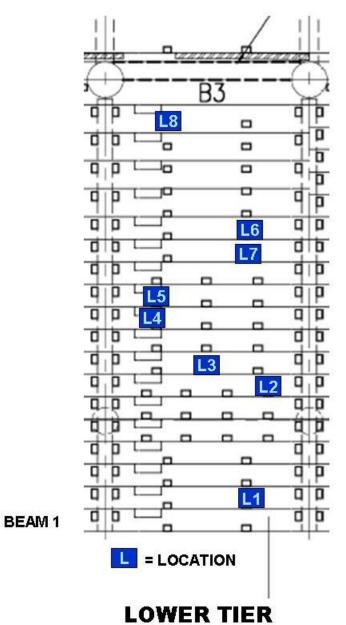




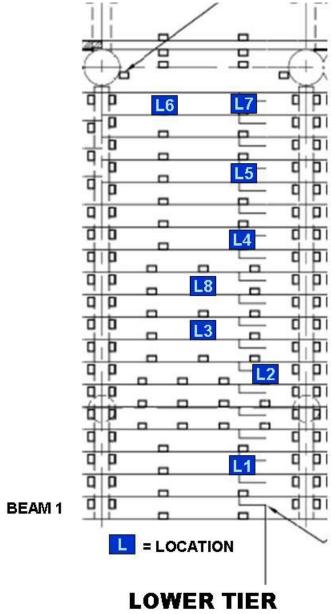




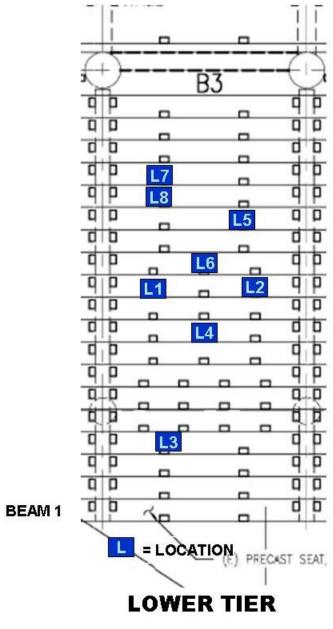
SECTION 10



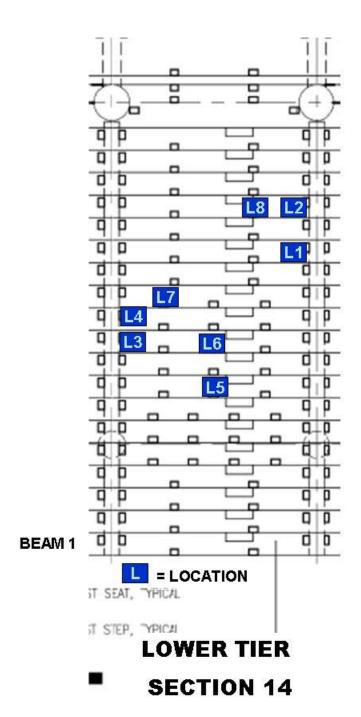
■ SECTION 11

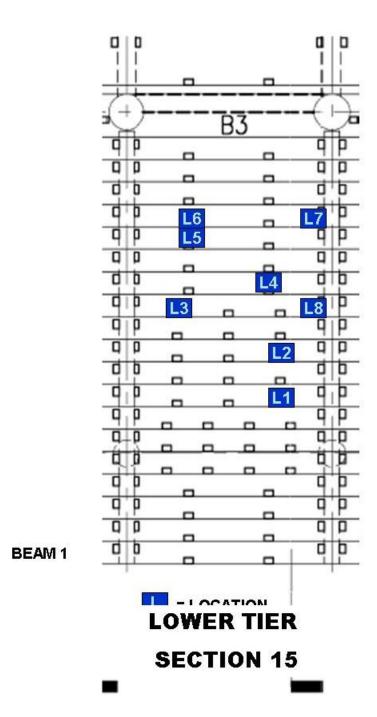


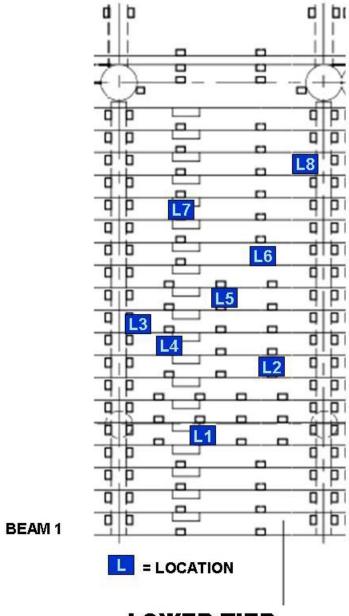
SECTION 12



SECTION 13

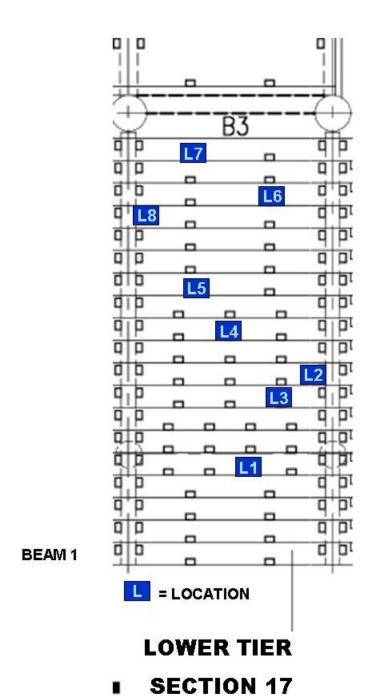


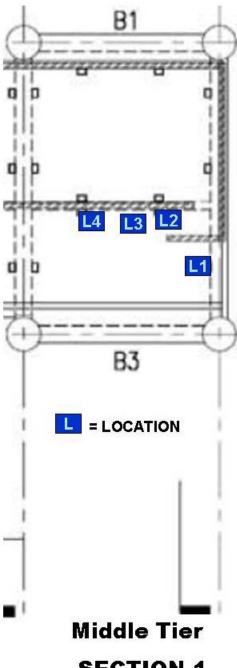




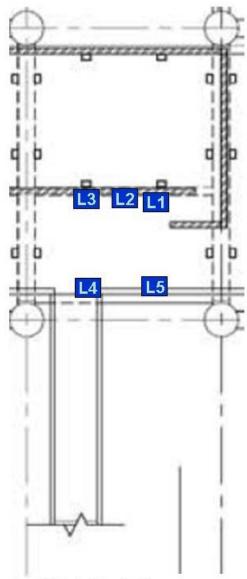
LOWER TIER

SECTION 16



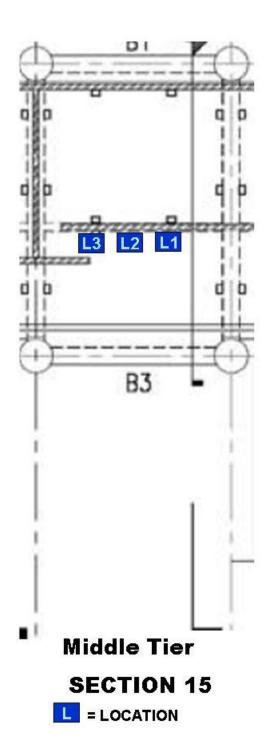


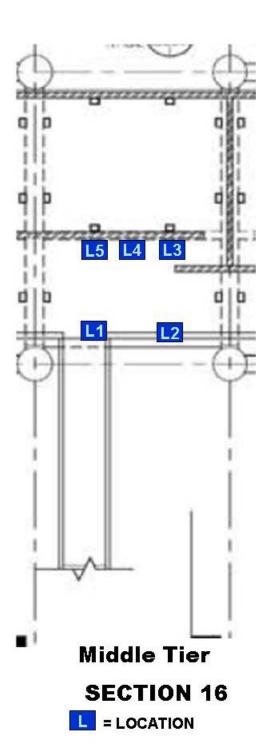
SECTION 1

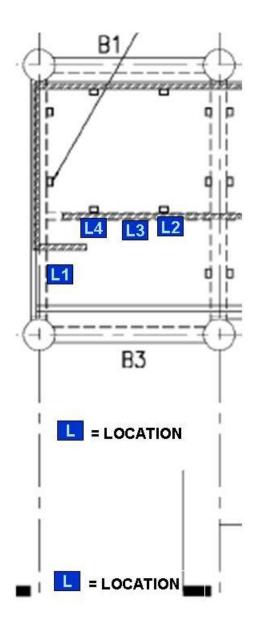


Middle Tier SECTION 14

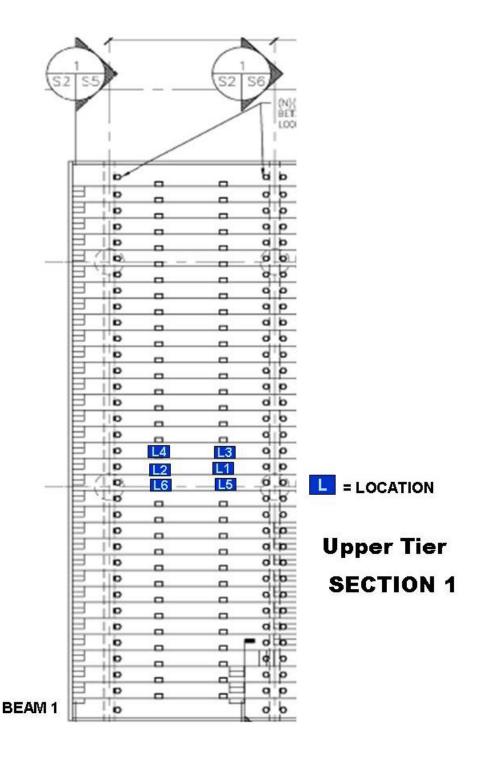
L = LOCATION

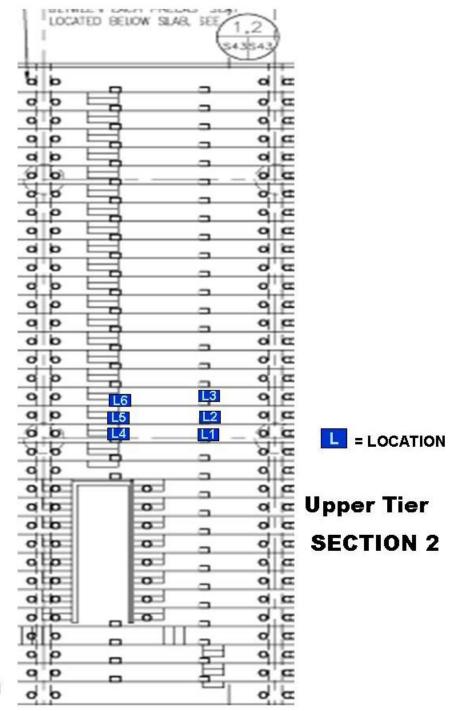


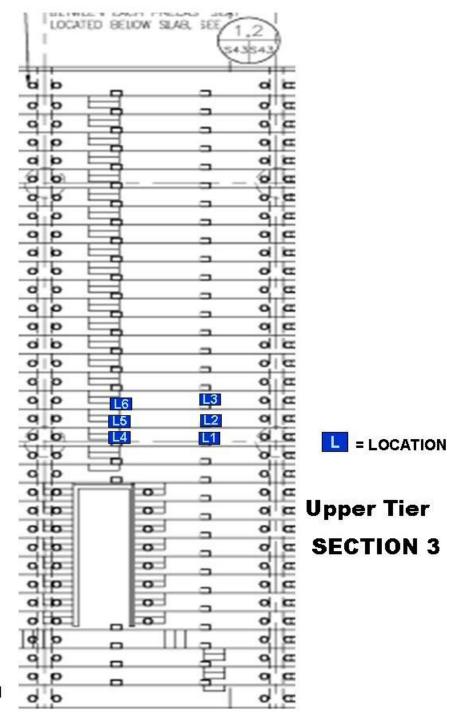


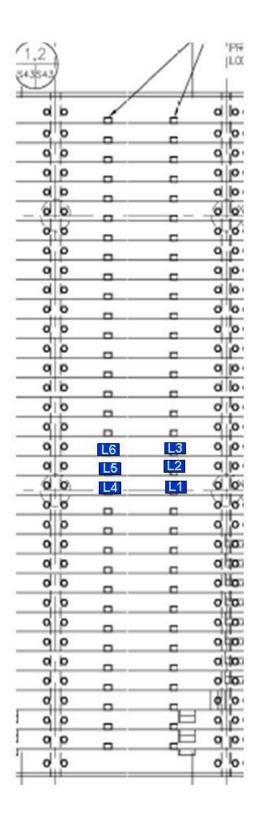


Middle Tier SECTION 17



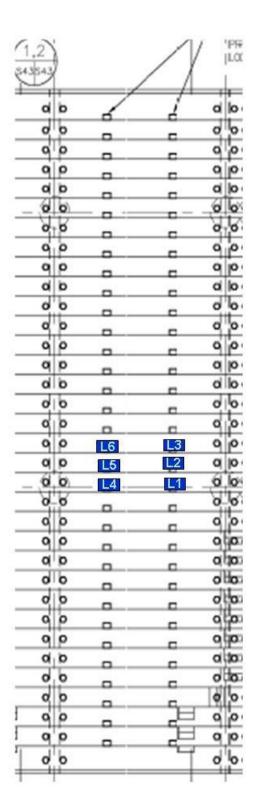






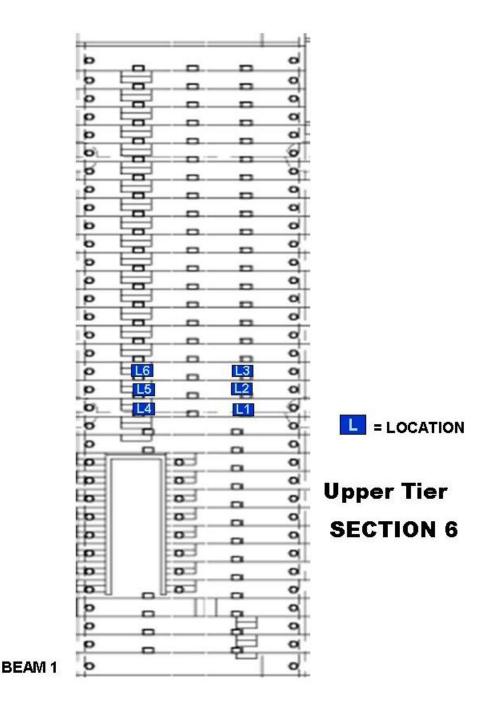
L = LOCATION

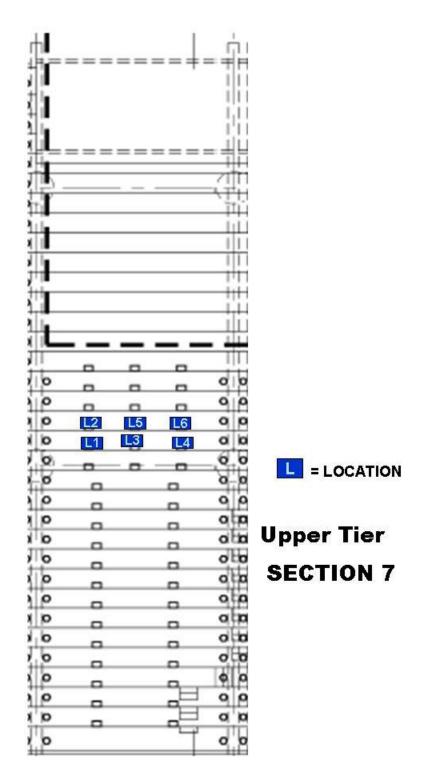
Upper Tier SECTION 4

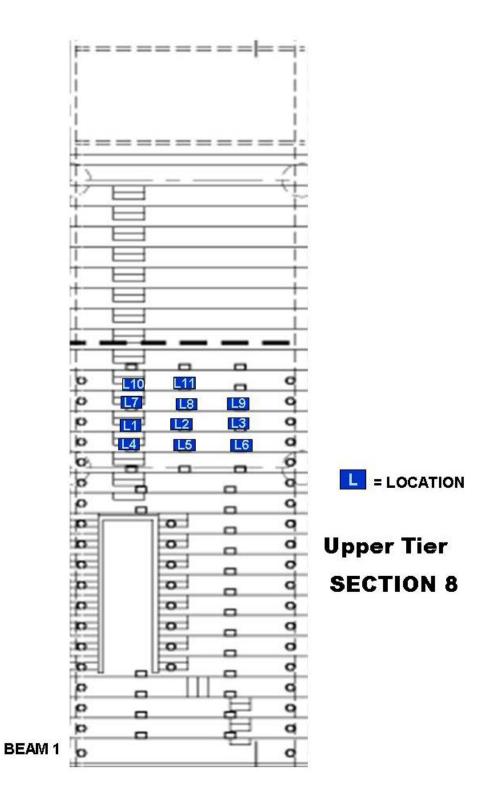


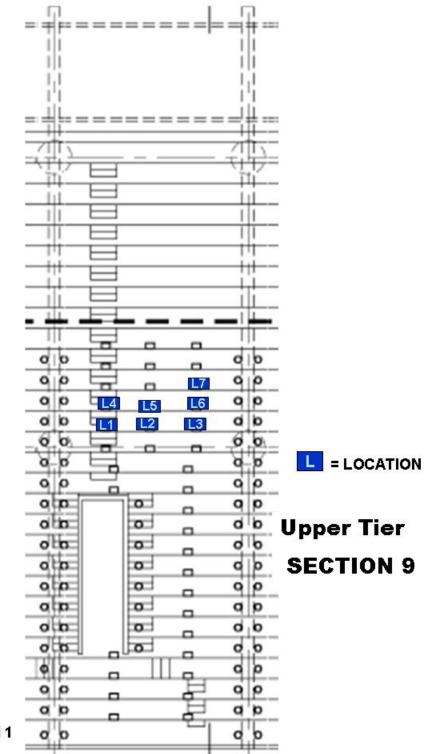
L = LOCATION

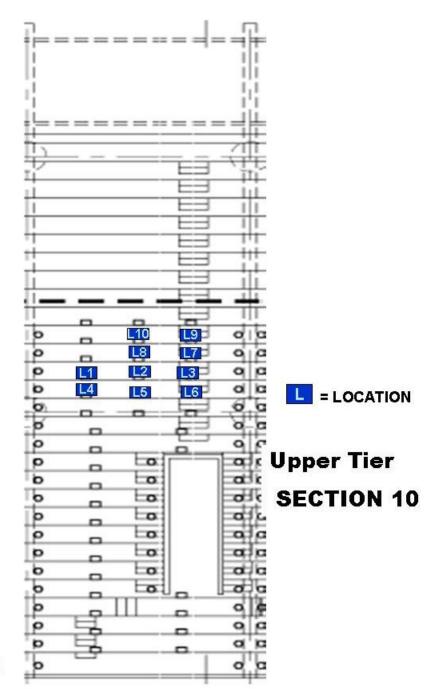
Upper Tier SECTION 5

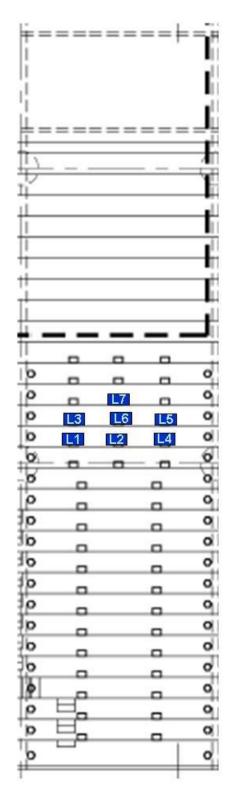






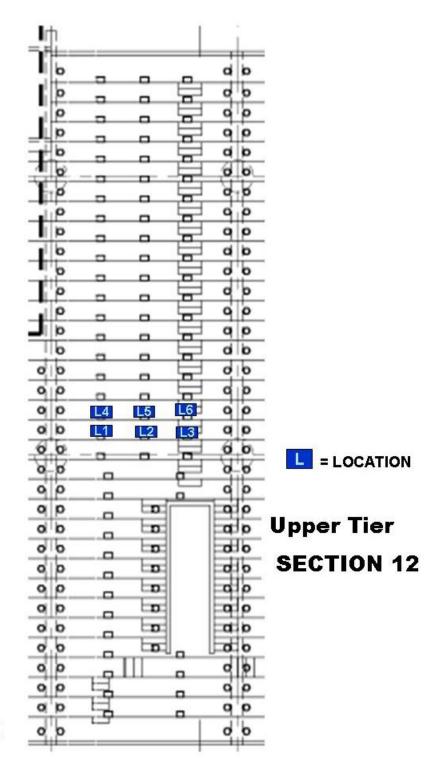


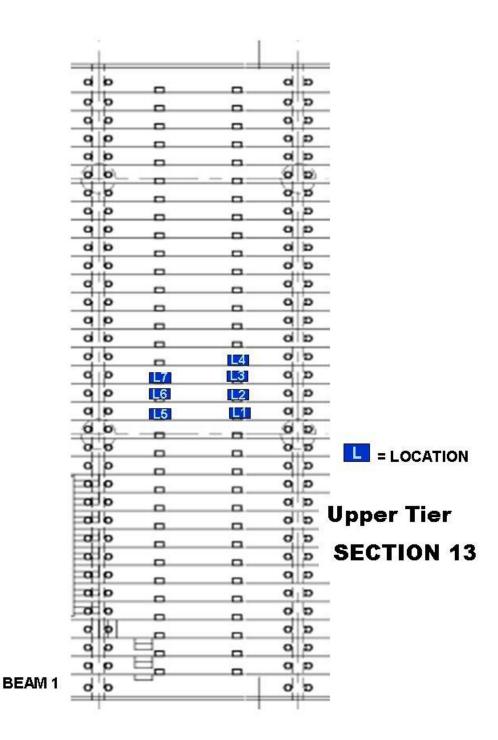




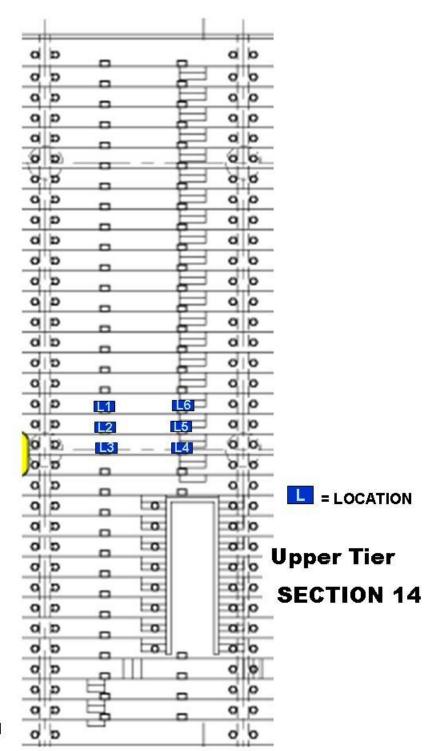
L = LOCATION

Upper Tier
SECTION 11

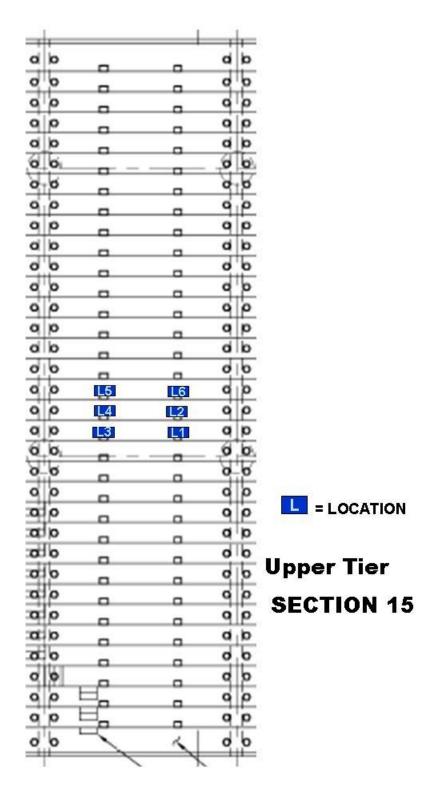


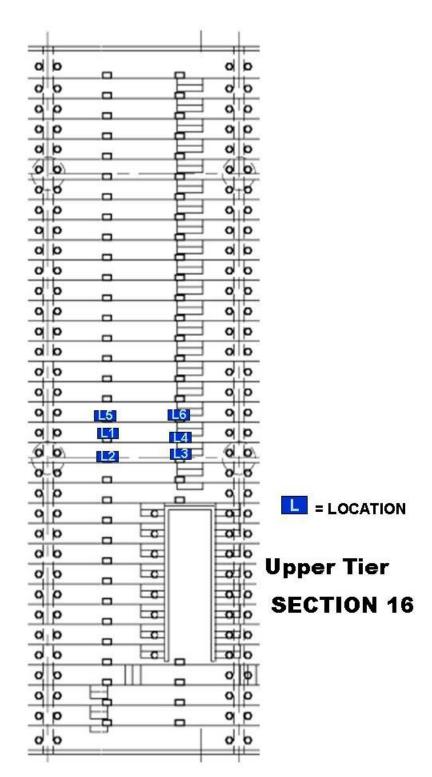


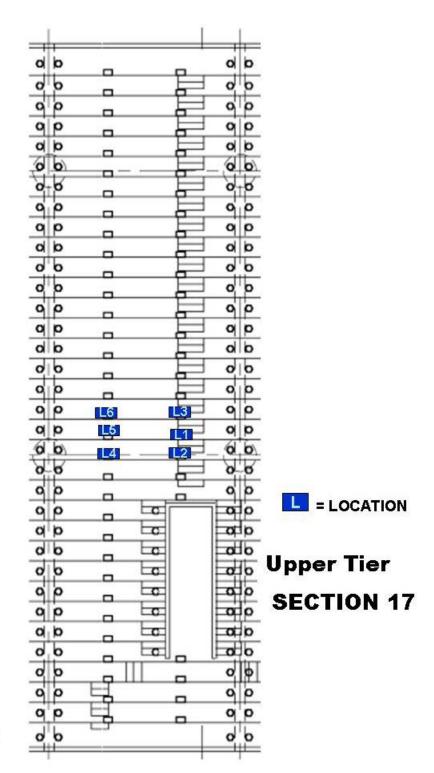
+



BEAM 1







Appendix C: Statistical Analysis Results

Lower Tier

Location	Section-1	Max	Min	Avg	Std	0-40%	0-100%
1	s1b5ep4	99.759	1.737	73.102	18.65	7.44	92.56
	s1b6bp4	99.924	9.389	79.886	16.04	2.86	97.14
2	s1b6ep4	99.716	17.817	74.553	15.89	3.37	96.63
2	s1b7bp4	98.364	1.081	70.047	16.71	5.45	94.55
	•						
3	s1b4ep2	100	10.736	71.71	19.92	7.66	92.34
	s1b5bp2	99.274	13.483	67.864	14.68	4.17	95.83
4	01bCon2	00.42	1 022	64.24	24.22	10.5	06 AE
4	s1b6ep2	99.42	1.923	61.34	21.32	13.5	86.45
	s1b7bp2	98.8	14.164	64.387	15.25	5.92	94.08
5	s1b4ep1	94.954	14.725	62.821	13.86	6.93	93.07
	s1b5bp1	99.756	13.7	67.278	16.11	3.15	96.85
6	s1b5ep1	95.046	1.92	56.674	17.94	13.8	86.18
	s1b6bp1	98.358	4.933	64.203	15.36	6.63	93.38
7	s1b5ep2	98.617	0.586	55.005	21.83	23.7	76.3
	s1b6bp2	96.688	15.43	65.491	14.27	4.96	95.04
8	s1b5ep3	100	2.005	67.541	22.25	10.5	89.45
0	s1b3ep3	99.985	29.911	78.093	13.35	0.75	99.25
	STOODPS	99.900	29.911	70.093	13.33	0.75	99.25
9	s1b7bp3	98.394	1.239	56.662	14.25	11.9	88.1
	s1b6ep3	99.707	3.187	68.314	16.05	6.21	93.8
Location	Section-2	Max	Min	Avg	Std	0-40%	0-100%
1	s2b13ep1	99.985	6.395	77.526	16.71	2.97	97.03
	s2b14bp1	99.179	20.281	74.833	12.74	0.81	99.19
	01.10	400	1.000	74.000	04.07	7.0-	00.47
2	s2b13ep2	100	1.236	74.829	21.24	7.85	92.15
	s2b14bp2	100	28.776	79.254	12.49	0.11	99.89
3	s2b14ep1	99.771	9.365	73.594	11.34	1.31	98.69
-	s2b15bp1	99.838	12.344	80.548	13.4	1.41	98.59
	01.44		0.1.00		100:		
4	s2b14ep2	100	24.509	83.73	13.34	0.56	99.45
	s2b15bp2	99.933	27.338	84.85	10.43	0.32	99.68

5	-0h4F0	100	20.42	04 407	44.00	0.04	00.00
5	s2b15ep2	100	22.43	81.497	11.63	0.64	99.36
	s2b16bp2	99.6	24.371	76.531	12.7	1.09	98.91
	20h1Fam1	00.040	07.000	70.00	10.10	0.05	00.25
6	s2b15ep1	98.049	27.268	73.29	12.12	0.65	99.35
	s2b16bp1	99.277	19.902	71.309	13.55	2.25	97.76
7	s2b16ep1	100	13.95	72.929	13.66	1.7	98.3
	s2b17bp1	99.737	34.289	76.872	13.02	0.33	99.67
8	s2b16ep2	100	24.417	86.269	12.97	0.19	99.82
	s2b17bp2	99.841	25.583	84.313	11.89	0.32	99.68
Location	Section-3	Max	Min	Avg	Std	0-40%	0-100%
1	s3b17ep2	93.724	0.662	46.304	16.21	35.5	64.52
	s3b18bp2	97.909	10.031	61.238	15.56	9.14	90.86
2	s3b17ep1	100	3.208	76.934	18.2	4.34	95.66
	s3b18bp1	94.988	9.835	55.575	15.01	16.2	83.79
3	s3b16ep2	100	8.922	82.11	16.28	2.81	97.19
	s3b17bp2	100	4.753	75.526	20.5	6.53	93.47
4	s3b16ep1	100	7.857	85.836	15.14	2.41	97.59
	s3b17bp1	100	12.805	87.635	14.05	1.06	98.94
	-0-440	00.00	00.000	00.075	40.05	0.40	00.54
5	s3b14ep2	99.93	20.226	82.275	13.85	0.46	99.54
	s3b15bp2	100	31.12	83.046	12.41	0.36	99.64
6	s3b14ep1	100	0.733	80.57	22.82	7.4	92.6
-	s3b15bp1	100	12.421	86.028	13.24	1.37	98.63
7 [§]	s3b13ep2*	99.948	16.361	82.576	14.72	1.68	98.32
	s3b14bp2	100	7.515	81.891	16.21	3.07	96.93
8 ^{§,‡}	s3b13ep1	99.557	10.922	76.34	16.36	3.47	96.53
	s3b14bp1	99.875	20.375	80.464	15.03	1.65	98.35
Location	Section-4	Max	Min	Avg	Std	0-40%	0-100%
1	s4b14ep2	94.075	16.984	60.104	14.84	10.8	89.23
	s4b15bp2	94.518	11.99	59.443	13.47	8.78	91.22
2	s4b14ep1	95.754	6.651	52.292	13.96	17.9	82.15
	s4b15bp1	88.996	16.804	51.82	11.94	15.9	84.14

-

^{*} Associated C-scan result with digital photograph not provided

[§] Location not indicated on Full Tier Drawing

[‡] Location not indicated on Section Level Drawing

		1					
3	s4b15ep2	92.402	0.842	52.271	15.26	21.5	78.49
	s4b16bp2	89.328	20.708	52.858	9.447	7.64	92.36
4	s4b15ep1	95.809	7.561	55.111	17.33	19.8	80.2
•	s4b16bp1	91.395	13.077	55.492	11.6	8.72	91.28
5	s4b17ep2	96.422 97.405	10.553	60.745	14.62	8.11	91.9
	s4b18bp2	97.405	8.773	60.645	14.8	9.83	90.17
6	s4b17ep1	94.243	0.968	52.771	16.35	24	76.01
	s4b18bp1	93.275	21.215	55.434	12.13	9.03	90.97
7	0.4h16an2	89.802	4.267	48.023	15.44	31.3	68.7
1	s4b16ep2 s4b17bp2	88.858	15.424	52.349	13.44	21.6	78.37
	34017002	00.000	13.424	32.343	13.07	21.0	70.57
8	s4b16ep1	99.09	1.996	61.846	17.47	10.8	89.21
	s4b17bp1	95.195	12.204	64.123	14.01	4.13	95.87
Location	Section-5	Max	Min	Avg	Std	0-40%	0-100%
1	s5b14ep2	90.861	6.227	48.292	16.19	33.3	66.7
	s5b15bp2	93.541	18.107	48.594	13.82	30.2	69.81
2	s5b14ep1	86.911	4.64	45.826	12.39	30	70.04
_	s5b15bp1	92.216	2.427	50.178	15.28	27	73.05
3	s5b15ep2	98.318	18.703	68.689	15.09	2.65	97.35
	s5b16bp2	88.318	8.538	40.894	11.04	47.8	52.18
4	s5b15ep1	96.716	5.592	60.154	14.6	6.95	93.06
	s5b16bp1	98.956	24.057	59.262	13.6	5.13	94.87
	-51.404	07.700	0.07	44.000	40.00	50.0	40.70
5	s5b16ep1	87.793	6.67	41.386	12.06	53.2	46.79
	s5b17bp1	87.888	9.069	46.297	12.23	30.4	69.6
6	s5b16ep2	99.008	15.836	65.15	14.93	5.71	94.29
	s5b17bp2	99.679	20.25	70.132	13.77	1.1	98.9
7	oEh12on1	00.007	15 110	02.226	15.57	1 55	00.45
7	s5b13ep1 s5b14bp1	99.997	15.443 36.941	83.326 82.322	15.57 11.72	1.55 0.04	98.45 99.96
	300140P1	100	30.341	02.322	11.12	0.04	33.30
8	s5b13ep2	100	11.096	75.685	18.09	4.61	95.39
	s5b14bp2	99.78	7.747	74.943	17.33	3.68	96.32
9 [§]	o Erob and	07.040	7 405	EC 220	11.45	10.7	07.04
9°	s5r3bcp2	97.643	7.485	56.326	14.45	12.7	87.34
	s5r3ecp2	99.093	6.511	48.402	16.1	31.2	68.83

_

[§] Location not indicated on Full Tier Drawing

Location	Section-6	Max	Min	Avg	Std	0-40%	0-100%
1	s6b15bcp1	92.021	3.648	40.617	12.84	51.6	48.36
	s6b15ecp1	90.47	2.375	43.897	14.49	41.9	58.15
2	s6b16bcp1	99.557	11.419	59.689	15.44	10.4	89.57
	s6b16ecp1	53.364	1.786	20.469	8.103	97.6	2.375
3	s6b17bcp1	99.212	15.815	72.611	14.66	2.74	97.26
	s6b17ecp1	99.936	1.016	42.14	20.95	50.1	49.87
4	s6b10bcp1	78.7	10.672	40.283	12.52	53.6	46.42
	s6b10ecp1	71.587	4.655	23.669	12.84	87.8	12.2
5	s6b12bcp1	80.281	7.817	31.841	9.928	81.3	18.67
	s6b12ecp1	88.959	2.005	39.526	19.16	50.7	49.29
6 ^{§,‡}	s6b10bcp1	78.7	10.672	40.283	12.52	53.6	46.42
	s6b10ecp1	71.587	4.655	23.669	12.84	87.8	12.2
					1 1 1 1	0.10	
7 ^{§,‡}	s6b12bcp1	80.281	7.817	31.841	9.928	81.3	18.67
-	s6b12ecp1	88.959	2.005	39.526	19.16	50.7	49.29
	,						
Location	Section-7	Max	Min	Avg	Std	0-40%	0-100%
1	s7b16ep2	99.719	5.317	60.926	16.75	9.87	90.13
	s7b17bp2	100	9.927	65.918	19.63	11.5	88.52
2	s7b16ep1	99.496	6.847	67.221	17.99	9.08	90.92
_	s7b17bp1	99.655	9.121	73.149	15.39	3.21	96.79
3	s7b15ep1	98.239	19.219	66.931	15.68	6.01	93.99
	s7b16bp1	99.835	15.668	77.58	15.72	2.47	97.53
	·						
4	s7b14ep1	100	18.996	62.765	17.85	8.86	91.14
	s7b15bp1	99.887	12.341	76.962	14.41	1.88	98.13
5	s7b14ep2	94.985	5.452	49.707	17.39	30.7	69.27
	s7b15bp2	96.407	16.731	58.682	13.29	5.8	94.2
6	s7b15ep2	99.249	8.51	57.359	15.9	13.2	86.79
	s7b16bp2	99.814	13.755	70.579	16	4.61	95.39
		_			4 - 00	000	77.04
7	s7b13ep1 s7b14bp1	96.944 99.597	9.191 14.429	54.438 71.896	17.38 15.71	22.8 3.2	77.21 96.81

_

[§] Location not indicated on Full Tier Drawing

[‡] Location not indicated on Section Level Drawing

^{*} Associated C-scan result with digital photograph not provided

8	s7b13ep2	92.668	9.066	48.818	16.07	30.2	69.81
	s7b14bp2	98.877	9.222	66.569	14.23	5.12	94.88
9	s7b17ep2	99.719	5.317	60.926	16.75	9.87	90.13
	s7b18bp2	100	9.927	65.918	19.63	11.5	88.52
10 ^{§,‡}	s7b17ep1 [*]	99.496	6.847	67.221	17.99	9.08	90.92
	s7b18bp1 [*]	99.655	9.121	73.149	15.39	3.21	96.79

Location	Section-8	Max	Min	Avg	Std	0-40%	0-100%
1	s8b15bcp2	96.926	22.213	66.579	12.94	2.61	97.39
	s8b15ecp2	87.311	10.885	38.03	12.18	70.1	29.94
2	s8b14bcp2	100	23.965	82.699	15.12	1.97	98.03
	s8b14ecp2	91.725	0.528	49.084	15.76	30.2	69.78
3	s8b13bcp2	100	26.261	79.644	13.61	0.82	99.18
	s8b13ecp2	96.618	3.681	46.555	20.13	43.9	56.11
4	s8b12bcp2	99.792	24.802	81.652	14.51	1.71	98.29
7	s8b12ecp2	97.469	1.804	33.258	20.1	69.5	30.51
		011100		00.200		00.0	
5	s8b13ep2	99.976	8.034	77.235	15.7	2.43	97.57
	s8b14bp2	99.884	9.118	75.062	16.91	4.69	95.31
6	s8b13ep1	100	8.791	74.497	16.72	4.05	95.95
	s8b14bp1	99.982	7.915	72.212	18.97	6.26	93.75
7	a0b44am4	00.070	04.070	70 700	44.04	0.77	00.04
/	s8b14ep1	99.976	21.276	79.726	14.81	0.77	99.24
	s8b15bp1	99.915	24.28	72.738	14.84	2.06	97.94
8	s8b14ep2	100	11.606	81.989	17.8	4.18	95.82
	s8b15bp2	100	13.968	87.449	12.45	0.42	99.58
Location	Section-9	Max	Min	Avg	Std	0-40%	0-100%
1	s9b13ep2	100	30.687	83.86	12.97	0.38	99.62
	s9b14bp2	100	17.213	83.249	13.75	0.79	99.21
2	s9b13ep1	100	6.905	70.723	18.89	7.48	92.52
	s9b14bp1	99.676	8.669	67.023	15.45	6.09	93.91

_

[§] Location not indicated on Full Tier Drawing

[‡] Location not indicated on Section Level Drawing

^{*} Associated C-scan result with digital photograph not provided

3	s9b14ep1	99.985	3.455	68.377	17.51	5.76	94.24
	s9b15bp1	99.109	5.687	68.34	19.12	10.3	89.69
	·						
4	s9b14ep2	100	17.213	81.421	16.21	1.95	98.05
	s9b15bp2	100	15.69	82.538	13.67	0.67	99.33
5	s9b15ep1	99.918	20.153	76.243	14.8	1.35	98.65
	s9b16bp1	99.985	5.021	70.692	17.24	5.24	94.76
6	s9b15ep2	100	20.601	81.679	14.24	0.79	99.21
	s9b16bp2	100	6.743	80.866	17.17	3.07	96.93
7	0.454	400	44.400	00.004	40.00	0	400
7	s9b15bcp1	100	44.469	88.834	10.23	0	100
	s9b15ecp1	100	6.148	67.25	18.83	9.89	90.11
8	s9b16bcp1	100	41.23	86.809	11.13	0	100
0	s9b16bcp1	99.811	1.09	72.581	18.75	5.82	94.18
	Sapioechi	33.011	1.03	72.301	10.73	3.02	34.10
	0 11 10			_	0.1	0.400/	0.4000/
Location	Section-10	Max	Min	Avg	Std	0-40%	0-100%
1	s10b7ep1	94.606	0.379	45.755	23.12	31.7	68.31
	s10b8bp1	97.726	18.507	62.049	14.1	6.75	93.25
	101.101	22		22.22.4	22.22	40.0	04.00
2	s10b10bcp1	99.573	1.194	63.984	26.02	18.6	81.38
	s10b10ecp1	95.162	8.846	49.399	16.91	30	70
3	s10b15ep2	96.722	10.458	55.907	13.89	11.3	88.75
3	s10b13ep2	99.075	20.324	69.86	14.97	2.87	97.13
	310010002	99.013	20.324	09.00	14.31	2.01	37.13
4	s10b14ep1	95.266	4.451	51.606	15.87	21.7	78.31
	s10b15bp1	99.96	9.505	70.293	15.8	3.43	96.57
5	s10b18ep1	98.031	14.905	68.788	15.68	4.66	95.34
	s10b19bp1	98.458	9.826	70.948	14.13	2.64	97.36
•	010011000	06.040	7.050	EQ 44E	12.00	177	00.00
6	s10b11ep2 s10b12bp2	96.218 92.991	7.259 1.734	52.145 56.757	13.63 15.88	17.7 15	82.26 85.02
	\$100120p2	92.991	1.734	30.737	13.00	15	00.02
				_			
Location	Section-11	Max	Min	Avg	Std	0-40%	0-100%
1	s11b2ep1	99.402	12.473	68.035	19.91	11.3	88.69
	s11b3bp1	94.444	7.158	55.794	16.15	16.8	83.25
2	s11b7ep1	97.735	1.093	42.701	15.75	41.5	58.54
	s11b8bp1	98.477	8.196	64.749	18.12	11.3	88.74
		00.555			00 ==	0	
3	s11b8ep2	99.969	7.68	74.843	20.53	9.56	90.44
	s11b9bp2	100	20.58	89.119	10.4	0.36	99.64

4	s11b10ep3	99.89	0.464	62.601	26.14	19.1	80.9
	s11b11bp3	99.988	16.593	67.344	16.73	5.35	94.65
5	s11b11ep3	98.08	2.668	50.798	17.88	29.7	70.31
	s11b12bp3	100	14.918	69.852	14.93	3.32	96.68
6	s11b14ep1	99.478	14.832	60.157	16.8	11.3	88.66
	s11b15bp1	98.477	16.963	63.884	13.69	4.13	95.87
7	s11b13ep1	99.667	6.126	67.99	19.58	11	88.98
	s11b14bp1	99.878	21.947	84.95	11.59	0.36	99.64
8	s11b18ep2	98.883	8.733	68.271	18.33	8.98	91.02
	s11b19bp2	99.377	21.978	69.559	16.84	5.69	94.31

Location	Section-12	Max	Min	Avg	Std	0-40%	0-100%
1	s12b3ep1	96.78	5.888	59.822	14.76	9.67	90.33
	s12b4bp1	97.817	24.008	67.084	12.55	1.68	98.32
2	s12b7ep1	94.606	0.379	45.755	23.12	31.7	68.31
	s12b8bp1	97.726	18.507	62.049	14.1	6.75	93.25
3	s12b9ep2	99.112	1.071	56.252	17.48	15.5	84.51
	s12b10bp2	95.702	9.539	63.036	14.42	6.05	93.96
4	s12b13ep2	96.734	0.949	47.832	18.07	27.4	72.6
	s12b14bp2	95.003	9.686	58.38	15.23	12.1	87.89
5	s12b16ep1	96.832	9.383	55.774	15.29	15	85.05
	s12b17bp1	96.645	25.824	66.878	12.46	2.11	97.89
6	s12b19ep2	94.145	2.601	51.975	15.61	19.5	80.46
	s12b20bp2	98.773	19.051	68.352	12.48	2.18	97.82
	101.10	22.222		00.010	1= 0.1	100	20.4
7	s12b19ep1	98.288	8.04	62.813	17.81	10.6	89.4
	s12b20bp1	98.431	2.198	62.64	15.72	6.12	93.88
0	012611002	96.218	7.259	52.145	13.63	177	82.26
8	s12b11ep2 s12b12bp2	90.218	1.734	56.757	15.88	17.7 15	85.02
	\$120120p2	92.991	1.734	30.737	15.66	10	05.02
Location	Section-13	Max	Min	Avg	Std	0-40%	0-100%
1	s13b11ep3	98.443	7.335	54.607	14.02	13.1	86.89
	s13b12bp3	98.48	11.606	64.339	14.8	5.54	94.46
2	s13b11ep1	99.368	5.372	49.537	15.42	28.1	71.95
	s13b12bp1	100	15.186	59.998	15.66	11.4	88.56

		T	ı	I	1		1
3	s13b3ep1	96.972	2.176	53.136	18.37	24.6	75.43
	s13b4bp1	99.396	9.93	66.573	21.08	12.8	87.17
4	s13b9ep2	96.456	13.547	56.4	13.04	8.8	91.2
-	s13b10bp2	96.92	14.289	61.448	13.69	7.66	92.34
	3100100P2	00.02	14.200	01.440	10.00	7.00	32.04
5	s13b14ep1	97.952	10.192	53.157	15.02	20.5	79.55
5							
	s13b15bp1	98.245	6.352	56.474	19.39	21.1	78.88
6	s13b12ep2	94.145	18.031	53.121	12.69	13.9	86.13
	s13b13bp2	99.194	23.538	74.855	14.03	1.46	98.54
7	s13b15ep2	99.737	4.341	66.729	17.94	8.45	91.55
	s13b16bp2	98.764	12.61	65.549	14.75	5.81	94.19
8	s13b14ep2	95.894	17.03	55.965	12.87	11.1	88.93
	s13b15bp2	95.815	5.519	63.634	14.45	6.64	93.36
				_			
Location	Section-14	Max	Min	Avg	Std	0-40%	0-100%
1	s14b14bcp1	95.458	11.291	57.842	16.47	15.8	84.22
	s14b14ecp1	84.35	1.016	40.869	17.07	39	60.99
		0 1100					
2	s14b16bcp1	99.997	27.854	78.269	14.1	1.23	98.77
_	s14b16ecp1	93.425	2.64	48.825	16.93	25.5	74.55
	314b10ecp1	33.423	2.04	40.023	10.33	20.0	74.55
3	s14b10bcp2	99.609	13.718	74.519	16.21	3.5	96.5
3	s14b10bcp2		1.12	43.006		38.7	
	\$14b10ecp2	97.176	1.12	43.000	20.14	30.1	61.33
4	-4.45.4450	00 000	47 700	F7 470	40.55	7.07	00.00
4	s14b11bcp2	96.288	17.799	57.472	12.55	7.97	92.03
	s14b11ecp2	87.766	8.922	46.492	13.3	30.8	69.24
_							
5	s14b8ep2	98.248	3.223	55.72	16.95	17.4	82.61
	s14b9bp2	99.179	3.681	66.466	19.21	9.83	90.17
6	s14b10ep2	97.326	5.696	59.67	16.86	12.2	87.76
	s14b11bp2	99.035	7.848	61.543	20.46	15.9	84.15
7	s14b12ep3	97.503	0.366	53.049	23.17	25.4	74.56
	s14b13bp3	99.081	2.698	63.074	16.7	9.44	90.56
8	s14b16ep1	95.772	18.538	57.552	11.37	6.92	93.08
	s14b17bp1	99.524	11.129	65.68	14.5	4.23	95.77
	- 1			20.00	10	0	
				_	_		
Location	Section-15	Max	Min	Avg	Std	0-40%	0-100%
1	s15b8ep1	89.603	8.852	45.253	10.61	29.4	70.64
	s15b9bp1	85.76	1.963	51.074	12.56	16.2	83.75
	310000P1	00.70	1.500	01.074	12.00	10.2	00.70
2	s15b10ep1	98.877	9.017	64.423	15.57	6.24	93.76
	s15b11bp1	99.863	18.303	69.256	15.1	2.92	97.08

3	s15b12ep2	92.711	1.7	53.573	15.85	16.6	83.41
3	s15b12ep2	100	23.162	76.349	13.51	0.81	99.19
	\$130130p2	100	23.102	70.349	13.31	0.01	99.19
4	s15b13ep1	98.632	10.034	48.638	14.18	29.1	70.94
•	s15b14bp1	94.338	1.2	51.554	17.53	23.9	76.13
5	s15b15ep2	98.968	6.258	67.618	18.39	8.69	91.32
	s15b16bp2	99.38	4.142	67.538	18.46	9.33	90.67
6	s15b16ep1	93.922	7.598	54.72	13.77	12.9	87.15
	s15b17bp1	98.675	6.52	59.971	17.41	13.2	86.76
7	s15b16ecp1	95.925	2.118	53.329	17.52	18.6	81.4
	s15b17bcp1	97.579	19.225	64.768	12.28	2.59	97.41
8	s15b12bcp1	100	2.018	68.272	20.69	11.2	88.81
	s15b12bcp1	98.278	9.078	51.632	15.07	20.8	79.17
Location	Section-16	Max	Min	Avg	Std	0-40%	0-100%
1	s16b05ep3	97.824	20.427	54.413	13.28	12.2	87.84
	s16b06bp3	98.755	1.856	61.483	21.14	15.8	84.25
2	s16b08ep1	95.385	12.631	59.462	13.36	6.97	93.03
	s16b09bp1	99.359	2.882	62.856	18.52	9.97	90.03
3	s16b10bcp2	99.118	1.413	56.755	24.6	21.6	78.35
	s16b10ecp2	92.305	13.547	54.434	12.55	12.7	87.33
4	s16b09ep3	99.447	8.489	63.353	14.59	4.69	95.31
	s16b10bp3	99.142	9.154	66.83	16.53	6.93	93.07
	.40.44 **	00.00=	7.1-	F7 400	40.00	0.40	00.07
5	s16b11ep2	98.837	7.17	57.132	13.68	9.13	90.87
	s16b12bp2	97.527	13.312	66.142	14.52	5.32	94.68
6	016612054	00.650	12.06	67 450	14 70	2.0	06.4
6	s16b13ep1 s16b14bp1	99.652	12.86 16.392	67.453 72.718	14.78	3.9 3.57	96.1
	9100140P1	99.78	10.392	12.110	15.72	3.3 <i>1</i>	96.44
7	s16b15ep2	94.338	5.195	49.808	12.21	18.8	81.2
1	s16b15ep2	95.629	10.369	62.598	12.44	4.94	95.07
	310010002	33.023	10.003	02.000	12.77	7.37	55.01
8	s16b17bcp1	99.161	12.54	69.604	17.31	6.75	93.25
-	s16b17ecp1	98.919	2.985	59.29	22.28	20.3	79.72
		22.2.3					
		I			+		1
Location	Section-17	Max	Min	Avg	Std	0-40%	0-100%
Location 1	Section-17 s17b05ep2	Max 99.084	Min 3.669	Avg 57.325	Std 13.35	0-40% 8.54	0-100% 91.46

2	s17b09bcp1	99.991	31.474	87.864	11.73	0.21	99.79
	s17b09ecp1	99.921	19.664	72.39	15.74	4.46	95.54
3	s17b08ep1	99.148	3.81	67.691	17.7	6.07	93.93
	s17b09bp1	99.991	8.718	80.251	15.22	1.64	98.36
4	s17b11ep2	98.126	9.847	60.778	15.64	8.36	91.64
	s17b12bp2	100	4.017	68.71	20.2	10.2	89.82
5	s17b13ep2	99.985	9.447	67.586	16.28	5.81	94.19
	s17b14bp2	99.963	10.14	77.807	16.95	4.43	95.57
6	s17b17ep1	99.542	17.732	63.676	14.11	5.33	94.67
	s17b18bp1	99.808	13.669	71.196	16.95	5.44	94.56
7	s17b19ep2	99.151	3.632	60.557	16.5	9.99	90.01
	s17b20bp2	100	14.231	79.422	16.59	1.81	98.19
8	s17b16bcp2	99.872	36.612	84.617	11.13	0.03	99.97
	s17b16ecp2	99.933	26.532	72.838	14.15	1.37	98.63

Middle Tier

Location	Section-1	Max	Min	Avg	Std	0-40%	0-100%
1	ms01lsbp1	100	25.699	76.523	14.71	1.55	98.45
	ms01lsep1	99.515	23.019	74.306	13.42	1.15	98.85
2	ms01bkbp4	100	25.424	74.811	13.43	1.47	98.53
	ms01bkep4	99.014	29.411	79.877	11.56	0.28	99.72
3	ms01bkbp3	99.777	9.554	80.28	14.39	2.25	97.76
	ms01bkep3	99.493	14.966	78.13	12.64	1.1	98.9
4	ms01bkbp2	99.618	13.074	74.649	15.55	3.43	96.57
	ms01bkep2	98.596	15.253	72.257	13.51	2.5	97.5
Location	Section-14	Max	Min	Avg	Std	0-40%	0-100%
Location 1	Section-14 ms14bkbp3	Max 99.994	Min 1.563	Avg 71.259	Std 19.94	0-40% 7.45	0-100% 92.55
)			
1	ms14bkbp3	99.994	1.563	71.259	19.94 16.84	7.45	92.55
	ms14bkbp3	99.994	1.563	71.259	19.94	7.45	92.55
1	ms14bkbp3 ms14bkep3	99.994	1.563 3.223	71.259 49.607	19.94 16.84	7.45 29.5	92.55 70.53
2	ms14bkbp3 ms14bkep3 ms14bkbp2 ms14bkep2	99.994 98.004 97.176 97.717	1.563 3.223 1.508 13.339	71.259 49.607 55.297 67.201	19.94 16.84 17.5 14.54	7.45 29.5 19.3 4.47	92.55 70.53 80.66 95.53
1	ms14bkbp3 ms14bkep3 ms14bkbp2 ms14bkep2 ms14bkbp1	99.994 98.004 97.176 97.717	1.563 3.223 1.508 13.339	71.259 49.607 55.297 67.201 54.515	19.94 16.84 17.5 14.54	7.45 29.5 19.3 4.47 21.9	92.55 70.53 80.66 95.53 78.12
2	ms14bkbp3 ms14bkep3 ms14bkbp2 ms14bkep2	99.994 98.004 97.176 97.717	1.563 3.223 1.508 13.339	71.259 49.607 55.297 67.201	19.94 16.84 17.5 14.54	7.45 29.5 19.3 4.47	92.55 70.53 80.66 95.53
2	ms14bkbp3 ms14bkep3 ms14bkbp2 ms14bkep2 ms14bkbp1 ms14bkep1	99.994 98.004 97.176 97.717 99.64 94.487	1.563 3.223 1.508 13.339 1.526 1.709	71.259 49.607 55.297 67.201 54.515 49.041	19.94 16.84 17.5 14.54 20.83 16.99	7.45 29.5 19.3 4.47 21.9 25.4	92.55 70.53 80.66 95.53 78.12 74.62
2	ms14bkbp3 ms14bkep3 ms14bkbp2 ms14bkep2 ms14bkbp1	99.994 98.004 97.176 97.717	1.563 3.223 1.508 13.339	71.259 49.607 55.297 67.201 54.515	19.94 16.84 17.5 14.54	7.45 29.5 19.3 4.47 21.9	92.55 70.53 80.66 95.53 78.12

5	ms14ftbp1	99.863	11.346	65.764	16.99	8.78	91.22
	ms14ftep1	99.585	7.091	66.401	15.28	4.92	95.08
Location	Section-15	Max	Min	Avg	Std	0-40%	0-100%
1	ms15bkbp1	99.811	2.393	66.541	15.24	4.31	95.7
	ms15bkep1	99.973	13.748	67.349	13.87	2.92	97.08
2	ms15bkbp2	98.535	23.178	68.685	11.72	1.25	98.75
	ms15bkep2	95.052	4.933	58.621	15.92	12.4	87.57
3	ms15bkbp3	98.202	18.4	66.279	15.22	5.05	94.95
	ms15bkep3	98.526	5.079	59.979	14.5	9.35	90.65
Location	Section-16	Max	Min	Avg	Std	0-40%	0-100%
1	ms16ftbp2	99.927	20.354	67.874	14.16	2.62	97.39
	ms16ftep2	99.136	12.454	66.391	14.65	3.75	96.25
2	ms16ftbp1	99.866	3.901	63.907	17.46	10.4	89.55
	ms16ftep1	99.246	3.523	62.342	17.86	9.92	90.08
3	ms16bkbp3	99.585	11.645	68.937	16.39	5.24	94.76
	ms16bkep3	99.087	7.995	58.3	15.2	11.9	88.15
4	ms16bkbp2	98.275	15.143	66.397	14.5	4.89	95.12
	ms16bkep2	98.199	7.485	68.111	15.75	4.74	95.26
5	man of Childhan f	05 400	0.050	C4 00C	40.0	F 04	04.7
5	ms16bkbp1 ms16bkep1	95.409 98.129	9.359 5.198	64.986 66.33	13.9 17.76	5.31 9.56	94.7 90.44
	шеторкерт	90.129	5.190	00.33	17.70	9.50	90.44
Location	Section-17	Max	Min	Avg	Std	0-40%	0-100%
1	ms17rsbp1	99.93	7.234	74.628	14.27	1.49	98.51
	ms17rsep1	98.834	8.993	70.209	15.9	4.74	95.26
2	ms17bkbp1	98.611	2.451	53.292	17.3	20.9	79.11
	ms17bkep1	93.538	10.852	53.458	13.35	15.1	84.95
3	ms17bkbp2	99.148	7.735	58.477	14.96	11.5	88.54
	ms17bkep2	92.195	4.289	50.727	14.87	22.2	77.81
	47111	00.000	7.540	74.004	44.40	4.0.4	00.00
4	ms17bkbp3	99.396	7.518	74.661	14.43	1.94	98.06
	ms17bkep3	99.527	10.391	72.725	15.16	2.6	97.4

Upper Tier

Location	Section-1	Max	Min	Avg	Std	0-40%	0-100%
1	us1b16ep2	98.944	6.371	61.558	14.33	7.65	92.35
	us117bp2	95.543	8.306	67.334	13.21	3.22	96.78
2	us1b16ep1	99.289	14.634	62.969	13.82	4.55	95.45
	usb17bp1	99.957	9.219	71.35	15.9	3.96	96.04
3	us1b17ep2	100	10.885	71.294	15.87	4.11	95.89
	us1b18bp2	93.602	20.815	63.79	11.64	3.23	96.77
4	us1b17ep1	99.161	20.073	72.199	16.21	4.38	95.62
	us1b18bp1	98.223	14.341	70.906	14.93	2.9	97.1
5	us1b15ep2	96.712	3.046	60.051	14.13	7.83	92.17
	us1b16bp2	99.719	19.478	62.381	13.15	4.87	95.13
6	us1b15ep1	99.988	19.02	70.18	14.96	2.65	97.35
O	us1b16bp1	96.23	18.544	66.028	12.94	3.13	96.87
Location	Section-2	Max	Min	Avg	Std	0-40%	0-100%
1	us2b15ep2	99.194	33.837	68.344	10.08	0.25	99.75
	us2b16bp2	99.402	18.864	66.201	12.72	1.83	98.17
2	us2b16ep2	100	23.709	74.49	14.61	1.35	98.66
	us2b17bp2	99.921	27.256	78.806	13.3	0.26	99.74
3	us2b17ep2	99.713	15.629	68.713	15.6	3.78	96.23
	us2b18bp2	98.535	17.43	72.265	13.51	3.21	96.79
4	us2b15ep1	99.976	34.811	77.302	12.24	0.1	99.9
	us2b16bp1	97.259	25.852	65.545	13.37	1.9	98.1
5	us2b16ep1	100	30.736	72.34	13.21	0.57	99.43
Ü	us2b17bp1	99.53	25.101	76.615	12.77	0.31	99.69
6	ue0b17ep1	00.051	22.202	77 155	12.01	0.00	00.11
6	us2b17ep1 us2b18bp1	99.951 99.557	22.292 21.013	77.155 73.62	13.01 13.27	0.89 1.25	99.11 98.75
Location	Section-3	Max	Min	Avg	Std	0-40%	0-100%
1	us3b15ep2	99.979	27.005	82.018	14.44	0.51	99.49
	us3b16bp2	99.921	25.971	78.628	16.01	1.32	98.68
2	us3b16ep2	98.941	15.22	72.959	15.63	3.12	96.88
	us3b17bp2	99.609	10.47	74.406	18.29	5.47	94.54

0	05470	400	40.000	00.000	40.70	0.40	00.04
3	us3b17ep2	100	13.999	60.999	13.78	6.19	93.81
	us3b18bp2	99.353	21.438	63.295	12.44	2.01	97.99
4	-01-454	00.40	40.404	54.450	40.00	40.0	00.07
4	us3b15ep1	98.12	10.491	54.156	12.33	10.9	89.07
	us3b16bp1	95.629	16.227	58.322	12.82	6.98	93.02
5	us3b16ep1	95.125	9.38	56.888	13.23	10.7	89.26
5	us3b10ep1	99.997	21.575	59.78	13.4	5.33	94.67
	ussbirbpi	33.331	21.373	39.70	13.4	3.33	34.07
6	us3b17ep1	95.842	20.055	61.79	11.65	4.24	95.76
	us3b18bp1	97.821	22.292	64.011	12.26	1.75	98.25
Location	Section-4	Max	Min	Avg	Std	0-40%	0-100%
1	us4b15ep2*	99.924	17.366	80.162	16.63	2.52	97.48
	us4b16bp2*	100	25.098	82.091	12.84	0.56	99.45
2	us4b16ep2*	99.744	10.91	73.386	18.49	6.27	93.73
	us4b17bp2*	99.335	17.753	68.167	13.06	1.72	98.29
3	us4b18bp2 [*]	97.186	32.366	66.229	12.24	0.89	99.11
	us4b17ep2*	99.982	12.833	73.172	16.3	3.48	96.52
4	us4b15ep1 ²	96.905	20.015	64.942	12.63	3.78	96.23
	us4b16bp1	99.985	21.569	64.56	13.78	3.54	96.46
		00.00	4.000	00.070	45.07	2.0	00.4
5	us4b16ep1	99.89	4.096	68.279	15.87	3.9	96.1
	us4b17bp1	99.386	4.1	66.245	16.03	5.21	94.79
6	us4b17ep1	99.814	6.001	65.976	19.58	11.3	88.71
O	us4b18bp1*	99.759	11.99	69.284	13.82	1.18	98.82
	do 15 100p 1	00.700	11.00	00.201	10.02	1.10	00.02
Location	Section-5	Max	Min	Avg	Std	0-40%	0-100%
1	us5b15ep2	99.918	15.891	76.534	15.25	1.46	98.54
	us5b16bp2	100	16.34	76.401	15.08	2.18	97.82
2	us5b16ep2	100	13.669	70.728	16.33	5.02	94.98
	us5b17bp2	99.747	34.463	68.953	11.97	0.68	99.32
3	us5b17ep2	100	31.163	80.896	15.08	0.36	99.64
-	us5b18bp2	99.728	28.455	81.807	11.53	0.2	99.8
	20021000	55.7.25		5007		~· -	55.0
4	us5b15ep1	97.332	12.497	56.205	14.3	12.7	87.27
	us5b16bp1	99.817	9.393	63.096	16.08	5.92	94.08
	·						
5	us5b16ep1	98.376	15.211	56.182	14.97	14.6	85.41

-

^{*} Associated C-scan result with digital photograph not provided

Í		0.4.0.40		00.004	40 = 4	4 = 4	0= 00
	us5b17bp1	94.048	5.44	62.334	12.54	4.71	95.29
6	us5b17ep1	97.689	9.106	61.08	14.84	9.47	90.53
Ü	us5b18bp1	99.237	27.1	74.782	11.4	0.47	99.53
	шесь геор :	00.20.		02		0	00.00
Location	Section-6	Max	Min	Avg	Std	0-40%	0-100%
1	us6b15ep3	100	3.889	68.103	20.08	9.09	90.91
	us6b16bp3	99.789	17.885	74.628	15.62	1.47	98.53
2	us6b16ep3	100	10.085	64.519	15.13	5.56	94.44
	us6b17bp3	99.881	28.855	77.581	14.04	0.46	99.54
		00.774	40.00	70.005	40.00	0.47	07.00
3	us6b17ep3	99.771	18.98	70.085	12.38	2.17	97.83
	us6b18bp3	99.85	9.466	73.235	16.19	4.07	95.93
4	us6b15ep1	99.64	20.604	63.595	14.48	5.44	94.56
⊤ T	us6b16bp1	100	16.001	70.138	15.85	2.22	97.78
	doop roop r	100	10.001	70.100	10.00	_,	01.10
5	us6b16ep1	91.67	11.493	55.739	12.44	11.5	88.53
	us6b17bp1	94.774	11.566	57.152	13.18	9.47	90.53
6	us6b17ep1	100	13.495	68.629	16.64	4.84	95.16
	us6b18bp1	98.834	3.764	69.639	15.55	4.21	95.79
Location	Section-7	Max	Min	Avg	Std	0-40%	0-100%
1	us7b16ep3	99.664	16.242	81.9	14.32	1.27	98.73
	us7b17bp3	99.707	21.3	84.523	11.7	0.32	99.68
					10.01		22.24
2	us7b17ep3	99.863	14.753	71.679	12.84	1.16	98.84
	us7b18bp3	99.869	27.036	76.067	13.66	0.57	99.43
3	us7b16ep2	97.833	8.962	63.67	14.22	5.39	94.61
3	us7b10ep2 us7b17bp2	99.963	13.352	74.439	15.54	1.65	98.35
	do / b / r bp2	00.000	10.002	7 1. 100	10.01	1.00	00.00
4	us7b16ep1	97.802	7.146	54.657	15.64	16.1	83.86
	us7b17bp1	98.016	20.391	64.126	13.3	3.47	96.53
	·						
5	us7b17ep2	99.817	14.06	74.05	14.99	2.06	97.94
	us7b18bp2	99.429	28.501	72.129	12.75	0.75	99.25
6	us7b17ep1	99.56	21.044	71.708	14.28	1.48	98.52
	us7b18bp1	99.945	16.627	77.877	13.61	0.64	99.36
	1				1		
Location	Section-8	Max	Min	Avg	Std	0-40%	0-100%
Location 1	Section-8	Max 100	Min 21.419	Avg 76.823	Std 16.93	0-40% 2.37	0-100% 97.63

2	us8b17ep2	100	4.597	62.88	18.81	11.7	88.34
_	us8b18bp2	99.719	26.383	68.749	12.79	0.42	99.58
3	us8b17ep1	99.24	5.171	62.543	16.4	7.54	92.46
	us8b18bp1	99.521	21.364	73.509	15.29	2.27	97.73
					10.20		
4	us8b16ep3	99.927	9.014	75.785	17.73	3.59	96.41
	us8b17bp3	99.973	24.939	83.22	13.62	0.57	99.43
5	us8b16ep2	97.65	19.954	61.916	14.48	6.79	93.22
	us8b17bp2	99.985	16.071	73.389	14.69	2.05	97.95
6	us8b16ep1	99.536	1.557	64.88	18.18	9.3	90.7
	us8b17bp1	99.786	17.43	73.786	14.15	1.07	98.93
7	us8b18ep3	100	6.001	81.172	16.85	2.34	97.66
	us8b19bp3	99.823	22.796	75.469	14.18	1.96	98.04
8	us8b18ep2	94.212	7.821	51.008	15.16	23	77.01
	us8b19bp2	90.046	9.438	48.57	13.61	28.3	71.66
9	us8b18ep1	98.147	5.159	64.881	16.27	7.6	92.4
	us8b19bp1	96.502	5.22	51.572	17.1	27.5	72.45
10	us8b19ep3	99.753	7.335	69.283	17.47	5.63	94.38
	us8b20bp3	100	13.935	75.212	14.88	1.42	98.58
4.4	-01.404	00.454	00.454	74.000	40.50		00
11	us8b19ep1	99.454	29.451	74.262	13.58	1 5 40	99
	us8b20bp1	95.006	10.47	62.596	13.41	5.18	94.82
Location	Section-9	Max	Min	Avg	Std	0-40%	0-100%
1	us9b16ep3	99.295	16.227	69.847	14.22	2.32	97.68
	us9b17bp3	99.658	14.56	67.07	16.48	4.57	95.44
2	us9b16ep2	99.954	9.612	73.642	17.88	5.54	94.46
	us9b17bp2	100	30.977	84.56	11.99	0.37	99.63
3	us9b16ep1	100	21.197	74.984	14.75	2.2	97.8
	us9b17bp1	100	35.275	86.106	12.59	0.05	99.95
4	us9b17ep3	100	5.379	75.552	18.87	5.34	94.66
	us9b18bp3	100	10.794	83.977	16.09	2.17	97.83
5	us9b17ep2	99.728	17.991	75.998	13.67	0.72	99.28
	us9b18bp2	99.792	9.035	77.468	15.88	2.55	97.45
	01.17	00.005	40.000	74000	45.01	0.0=	07.00
6	us9b17ep1	99.866	10.962	74.396	15.81	2.97	97.03
	us9b18bp1	99.905	18.959	78.507	14.06	0.88	99.12

7	us9b19ep1	94.014	2.018	51.954	16.82	21.7	78.33
,	us9b20bp1	96.658	15.211	56.025	14.71	14.4	85.63
	u590200p1	90.000	13.211	30.023	14.71	14.4	05.05
Location	Section-10	Max	Min	Avg	Std	0-40%	0-100%
1	us10b17ep3	100	32.121	80.721	13.77	0.43	99.57
•	us10b18bp3	99.783	2.326	72.368	23.43	11	89.01
2	us10b17ep2	100	34.606	80.566	14.06	0.33	99.67
	us10b18bp2	100	19.185	80.429	13.3	0.9	99.1
3	us10b17ep1	100	16.871	82.913	15.01	1.57	98.43
	us10b18bp1	99.985	10.256	88.88	11.09	0.41	99.59
4	ua10b16an2	100	10 747	00.710	14.07	1 70	00.00
4	us10b16ep3	100	12.747	80.712 79.14	14.07	1.72	98.29
	us10b17bp3	99.841	12.128	79.14	13.98	0.74	99.26
5	us10b16ep2	100	3.37	78.495	20.31	5.32	94.68
J	us10b17bp2	100	10.259	87	11.57	0.77	99.24
	d0100170P2	100	10.200	0,	11.01	0.77	00.21
6	us10b16ep1	99.957	15.443	83.216	16.82	3.32	96.68
	us10b17bp1	99.933	17.21	84.023	13.6	0.9	99.1
7	us10b18ep1	95.321	6.862	53.055	14.99	18.2	81.77
	us10b19bp1	97.701	7.759	56.071	14.29	12.3	87.69
	. 401. 40 0	400	00.000	70.004	40.00	0.0	00.4
8	us10b18ep2	100	23.269	79.001	12.08	0.6	99.4
	us10b19b p2	97.872	7.805	64.74	16.27	8.19	91.81
9	us10b19ep1	99.56	8.318	60.603	18.04	14	86.02
J	us10b13cp1	98.864	0.47	58.69	20.17	15.3	84.72
	G5100200P1	30.00	0.47	00.00	20.17	10.0	04.72
10	us10b19ep2	99.789	10.803	56.353	15.11	13.2	86.85
	us10b20bp2	99.414	5.4	50.68	17.64	26.5	73.5
Location	Section-11	Max	Min	Avg	Std	0-40%	0-100%
1	us11b16ep3	99.603	13.95	72.565	13.69	1.23	98.77
	us11b17bp3	99.432	6.667	67.98	15.66	4.69	95.31
2	us11b16ep2	98.214	3.52	58.955	12.41	6.5	93.5
	us11b17bp2	98.501	12.491	61.703	13.76	6.11	93.89
3	uc11h17on2	06.99	10 722	64 075	11 02	2.46	07.55
S	us11b17ep3 us11b18bp3	96.88 94.325	19.722 15.058	64.975 63.764	11.82 12.19	2.46 3.01	97.55 96.99
	as i in ionho	34.323	13.036	03.704	14.19	3.01	30.33
4	us11b16ep1	99.304	10.571	71.034	17.39	6.07	93.93
•	us11b17 bp1	92.927	1.459	50.339	14.23	23.9	76.07

5	us11b17ep1	85.192	11.148	52.303	11.7	14.5	85.53
3	us11b17ep1	95.577	12.005	61.011	12.36	5.45	94.55
	ustrotopi	33.311	12.003	01.011	12.30	3.43	34.33
6	us11b17ep2	97.357	2.61	66.249	16.5	7.24	92.76
O	us11b17ep2	99.365	11.99	69.987	11.85	1.2	98.8
	изттитоирг	99.303	11.99	09.901	11.00	1.2	90.0
7	us11b18ep2 [†]						
	us11b19bp2 [†]						
Location	Section-12	Max	Min	Avg	Std	0-40%	0-100%
1	us12b16ep3	90.403	8.739	45.531	12.19	32.3	67.68
	us12b17bp3	93.477	9.185	50.257	14.97	26.8	73.21
2	ua12b16ap2	96.233	11.294	58.167	15.14	11.2	88.8
2	us12b16ep2				13.14		
	us12b17bp2	93.541	14.167	57.259	13.93	12.1	87.94
3	us12b16ep1	95.687	20.446	63.876	13.36	3.65	96.35
_	us12b17bp1	89.56	10.198	49.64	13.86	25.4	74.61
4	us12b17ep3	96.719	8.52	60.606	13.17	5.85	94.15
	us12b18bp3	98.523	8.028	66.525	17.26	8.65	91.35
5	us12b17ep2	98.242	13.66	70.357	15.37	3.94	96.07
	us12b18bp2	99.023	3.12	68.798	14.01	3.66	96.34
6	us12b17ep1	98.327	14.035	66.82	15.41	4.57	95.44
	us12b18bp1	99.451	15.317	67.738	13.55	2.85	97.15
Location	Section-13	Max	Min	Avg	Std	0-40%	0-100%
1	us13b16ep1	95.51	6.795	50.51	15.69	24.1	75.93
	us13b17bp1	93.178	1.816	51.887	19.17	26.4	73.65
2	us13b17ep1	98.791	17.051	63.794	13.74	4.05	95.95
	us13b18bp1	99.765	22.756	64.685	13.91	3.68	96.32
3	us13b18ep1	90.891	9.902	47.006	11.3	27.9	72.12
	us13b19bp1	99.615	9.64	63.958	17.1	7.71	92.29
4	us13b19ep1	QQ 70A	6.02	30 201	12.01	62.2	37.75
4		88.724	6.02	38.281		62.3	37.75
	us13b20bp1	98.602	2.543	49.043	18	29.4	70.61
5	us13b16ep2	95.168	8.584	55.372	12.62	10.4	89.63
J	us13b17bp2	99.017	5.629	66.299	17.91	8.59	91.41
	us 13017042	99.017	J.UZ3	00.233	17.31	0.08	31.41

-

[†] Statistical analysis results not provided

6	us13b17ep2	99.359	9.295	55.896	14.08	10.8	89.19
O		99.359	14.911		12.57	6.81	93.19
	us13b18bp2	94.469	14.911	59.188	12.57	0.81	93.19
7		00.50	4.4	E4 E00	44.00	40.0	00.00
7	us13b18ep2	96.52	4.1	51.563	14.62	19.6	80.36
	us13b19bp2	95.668	6.218	56.328	16.2	15.9	84.12
o.t	101.10	00.050	40.550	50.740	4400	00.4	70.0
8 [‡]	us13b19ep2	92.659	10.556	50.749	14.92	26.1	73.9
	us13b20bp2	99.542	2.485	56.247	19.47	20.4	79.65
Location	Section-14	Max	Min	Avg	Std	0-40%	0-100%
1	us14b17ep2	85.543	3.886	37.287	10.5	62.8	37.16
·	us14b18bp2	93.697	2.726	49.625	14.66	23.6	76.39
	GG 1 15 1 GS P Z	00.001	220	10.020	1 1100	20.0	7 0.00
2	us14b16ep2	98.284	12.173	69.429	15.49	3.53	96.47
_	us14b17bp2	99.93	7.463	64.524	16	4.91	95.09
	do110170p2	00.00	7.100	01.021	10	1.01	00.00
3	us14b15ep2	75.397	8.639	36.629	10.97	64.3	35.74
Ü	us14b16bp2	76.236	4.261	35.403	10.52	69.7	30.27
	G0110100P2	7 0.200		00.100	10.02	00.7	00.27
4	us14b15ep1	96.282	26.917	62.932	12.83	2.96	97.04
•	us14b16bp1	99.997	4.154	68.759	20.18	10.8	89.22
	изт-втоврт	00.007	7.104	00.700	20.10	10.0	00.22
5	us14b16ep1	97.347	19.713	64.519	14.16	3.8	96.2
Ü	us14b17bp1	99.896	5.882	67.955	19.05	8.64	91.36
	de l'istropi	00.000	0.002	07.000	10.00	0.0 .	01100
6	us14b17ep1	74.203	7.009	28.631	9.366	89	11.04
•	us14b18bp1	76.856	3.132	36.484	11.29	63.1	36.94
	GG 1 15 1 GS p 1	7 0.000	0.102	00.101	11120	00.1	00.01
Location	Section-15	Max	Min	Avg	Std	0-40%	0-100%
1	us15b15ep1	95.647	31.044	66.295	11.39	0.72	99.28
	us15b16bp1	99.496	1.38	69.589	15.35	2.42	97.58
2	us15b16ep1	96.835	16.819	65.757	12.15	2.09	97.92
	us15b17bp1	98.172	12.476	69.728	13.23	1.52	98.48
3	us15b15ep2	99.728	19.246	69.067	15.61	3.91	96.09
	us15b16bp2	99.783	10.998	68.224	16.09	4.64	95.36
	1-					-	
4	us15b16ep2	98.037	26.926	67.069	13.35	2.73	97.27
	us15b17bp2	98.727	15.324	68.259	14.42	3.79	96.21
		· · <u>-</u> ·		22.20			
5	us15b17ep2	97.582	10.519	59.63	14.58	8.49	91.51
· ·	us15b18bp2	96.297	15.131	60.458	12.93	6.44	93.56

⁻

[‡] Location not indicated on Section Level Drawing

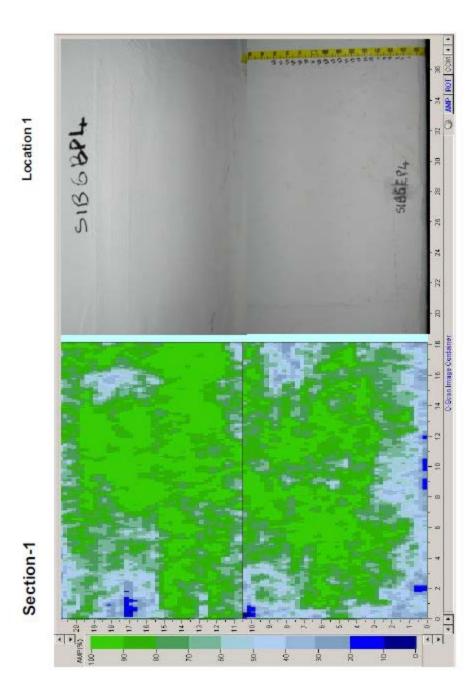
^{*} Associated C-scan result with digital photograph not provided

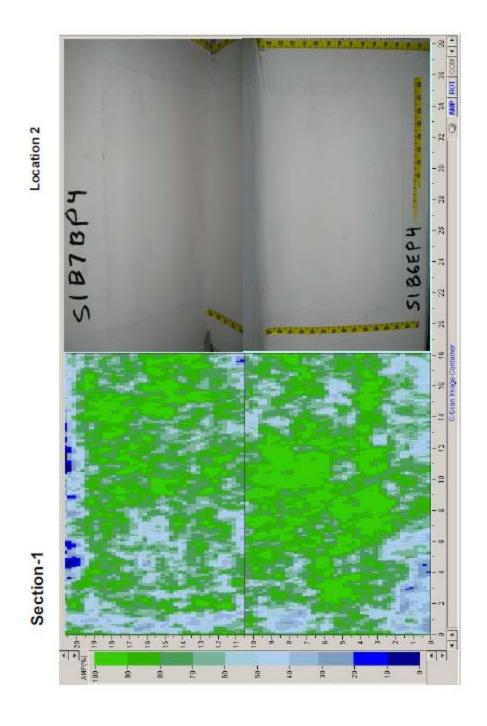
6	us15b17ep1	98.608	23.498	66.266	11.78	1.35	98.66
	us15b18bp1	98.907	27.921	76.583	13.33	0.78	99.22
Location	Section-16	Max	Min	Avg	Std	0-40%	0-100%
1	us16b16ep2	93.55	7.418	52.608	13.23	17.1	82.93
	us16b17bp2	98.574	6.395	50.715	15.25	24.8	75.18
2	us16b15ep1	99.179	20.717	61.229	13.7	4.6	95.4
	us16b16bp1	97.259	7.378	55.048	16.7	18.2	81.79
3	us16b15ep2	95.644	15.061	57.428	13.29	9.8	90.21
	us16b16bp2	91.557	5.553	49.703	14.99	25.7	74.27
4	us16b16ep1	93.846	8.727	56.938	13.48	10.5	89.47
	us16b17bp1	99.969	11.908	59.85	14.48	8.93	91.07
	401.47	00.000	40.000	00.550	40.00	0.50	00.44
5	us16b17ep2	96.838	12.082	66.558	13.96	3.59	96.41
	us16b18bp2	97.653	5.629	62.549	16.13	8.92	91.08
6	us16b17ep1	97.506	16.584	63.996	15.93	8.03	91.97
0	us16b17ep1	100	1.581	63.437	19.23	11	89.03
	us rob robp r	100	1.501	00.407	19.23	11	03.03
Location	Section-17	Max	Min	Avg	Std	0-40%	0-100%
1	us17b16ep1	95.852	16.166	55.043	13.47	13.9	86.15
•	us17b17bp1	99.881	4.744	56.033	17.36	16.6	83.43
	изти пирт	33.001	7.777	00.000	17.00	10.0	00.40
2	us17b15ep1	99.002	13.69	69.381	15.25	3.39	96.61
	us17b16bp1	98.892	3.388	52.022	17.04	21.9	78.12
	<u>'</u>						
3	us17b17ep1	92.662	19.902	57.757	12.85	9.07	90.93
	us17b18bp1	99.161	9.164	64.14	14.96	5.96	94.04
4	us17b15ep2	90.992	13.083	51.593	12.15	17.1	82.9
	us17b16bp2	96.02	10.934	48.973	14.88	28.2	71.81
5	us17b16ep2	95.272	5.742	48.297	14.4	27.4	72.64
	us17b17bp2	91.01	2.674	47.804	14.73	24.7	75.29
6	us17b17ep2	95.134	2.179	59.249	13.31	6.97	93.03
	us17b18bp2	98.697	7.726	55.547	17.63	19.4	80.62

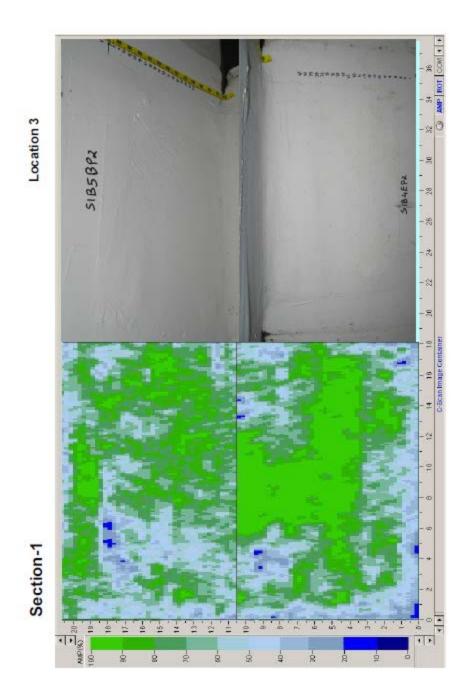
Appendix D: C-Scan Results With Digital Pictures

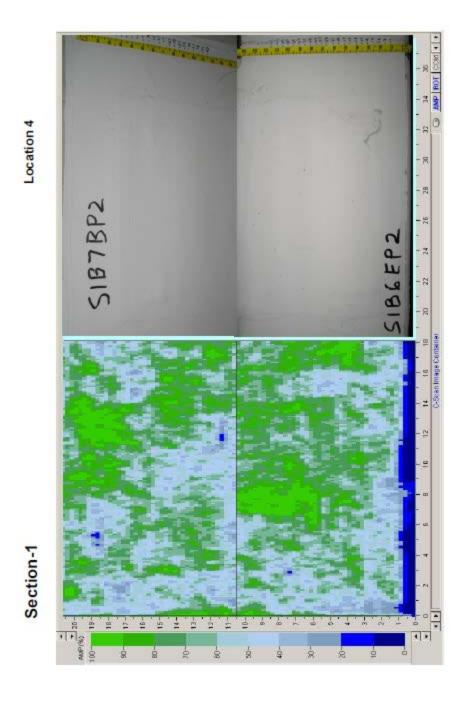
In Appendix D, the Middle Tier and Upper Tier data are labeled as such. However, due to an oversight in preparation of the original files, the Lower Tier data are not explicitly labeled. Therefore, pages not labeled as "Middle Tier" or "Upper Tier" present data gathered for the Lower Tier.

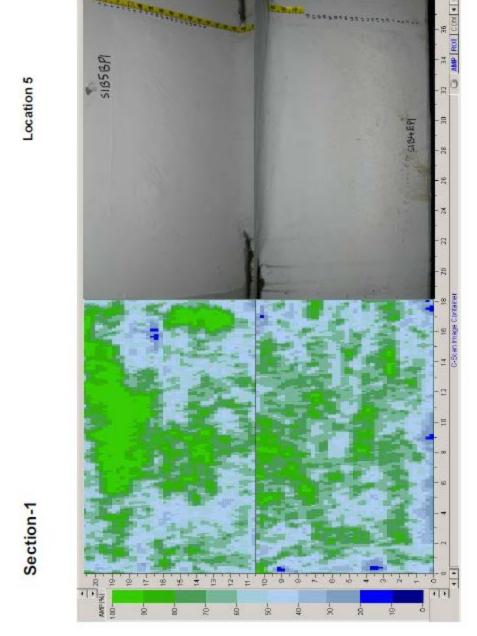
Also, during technical review, some labels on individual images were found to be inaccurate, and so those have been corrected by the authors.

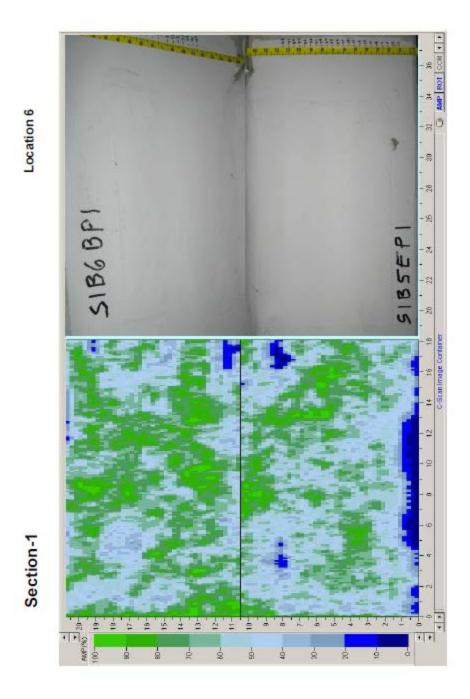


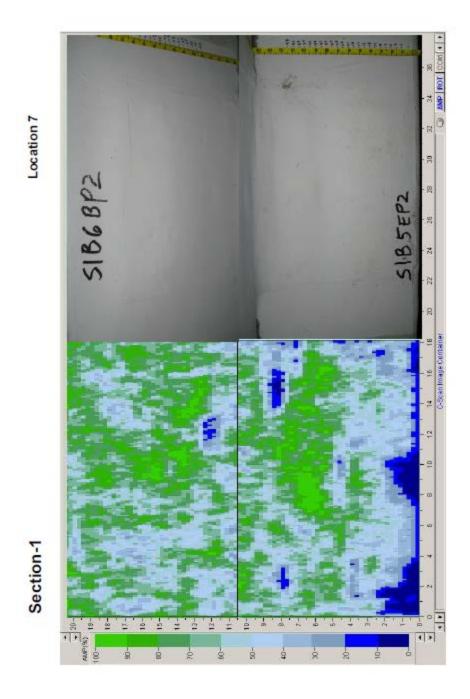


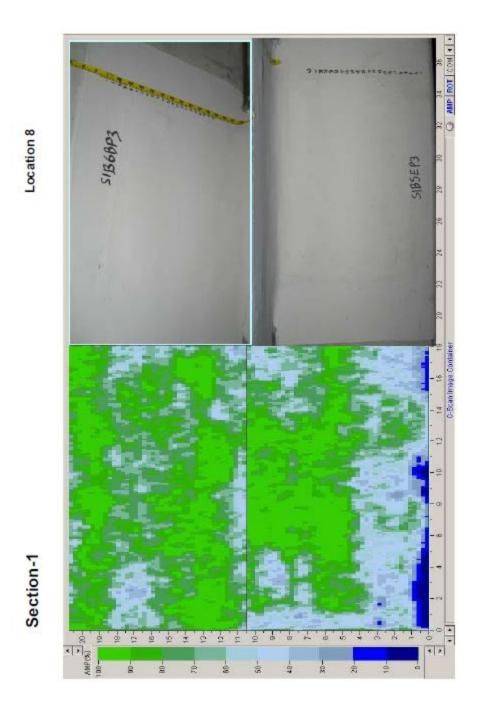


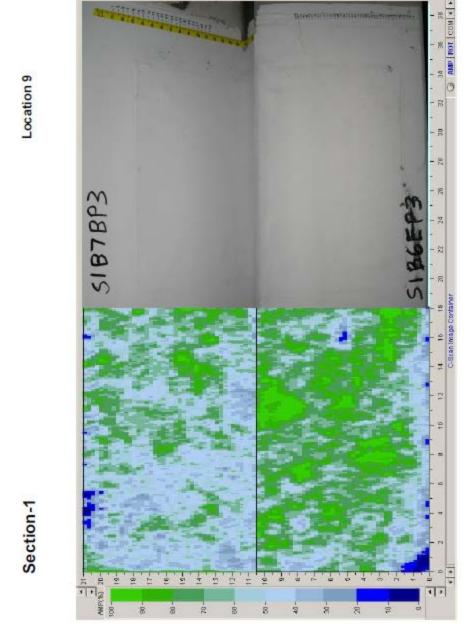




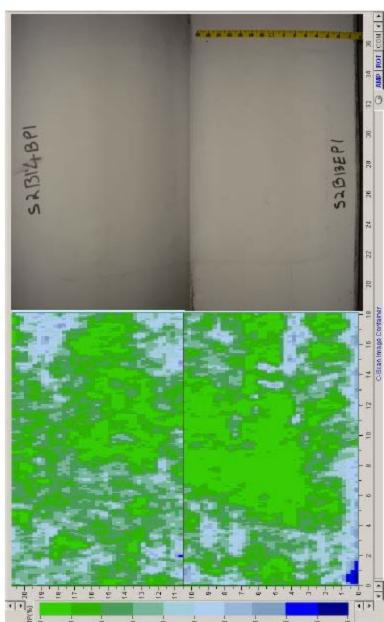


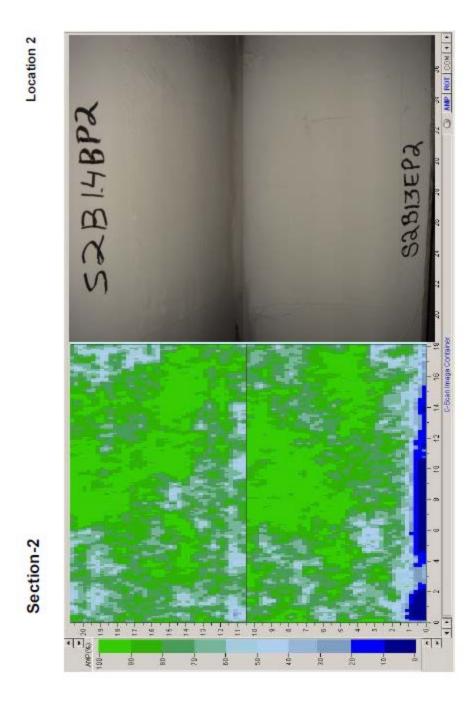








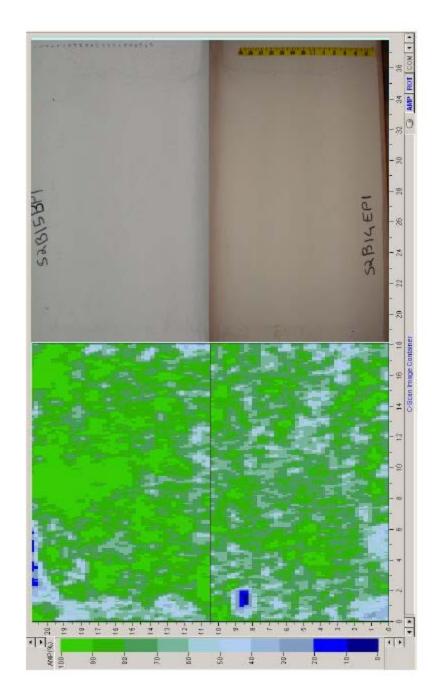


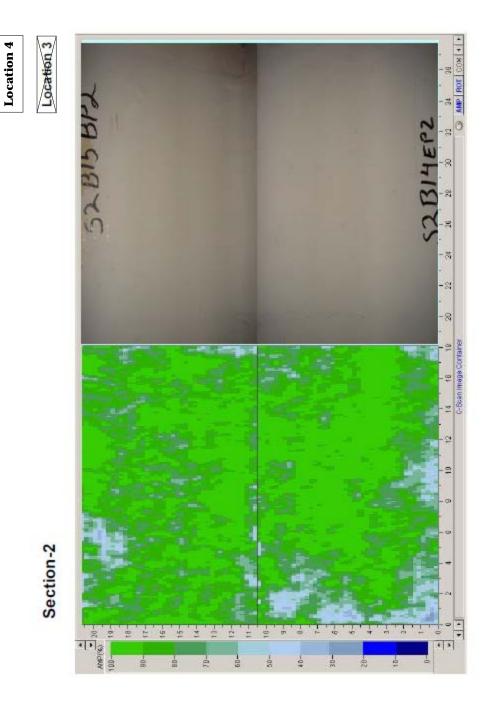


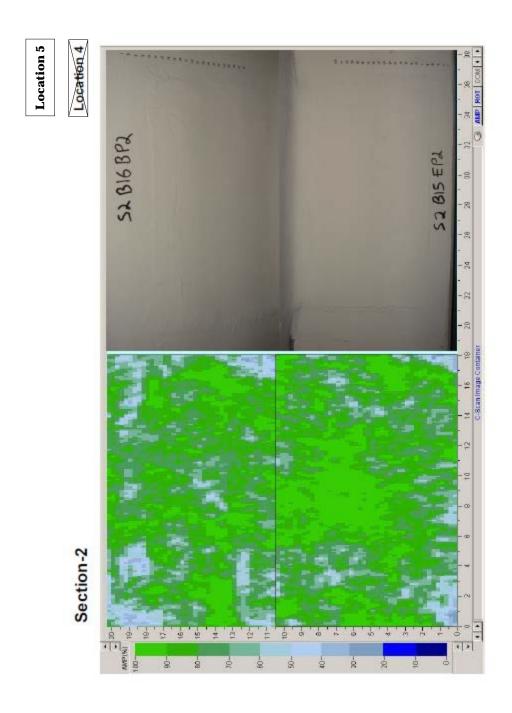
Location 3

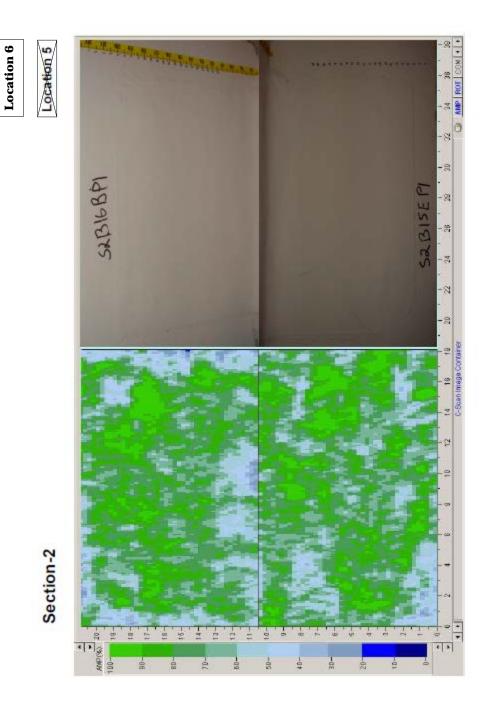
Location 8

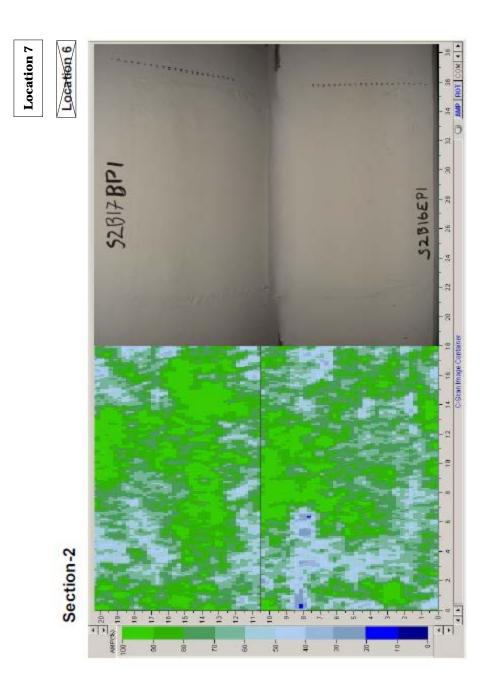
Section-2

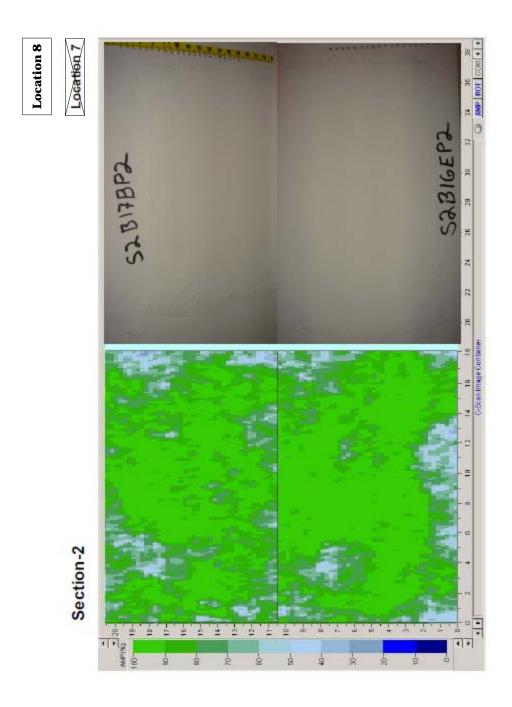


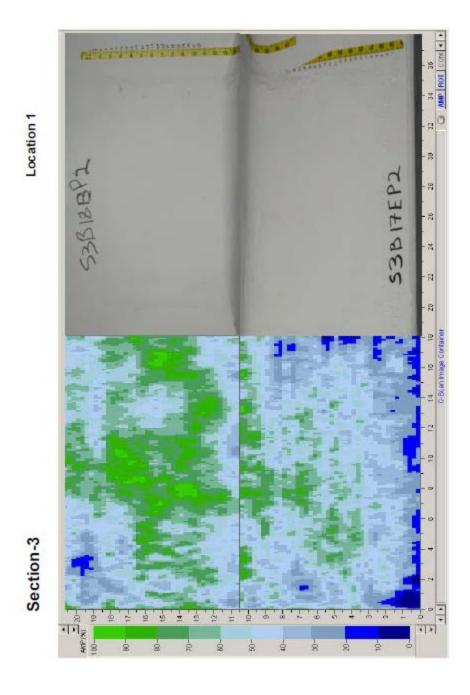


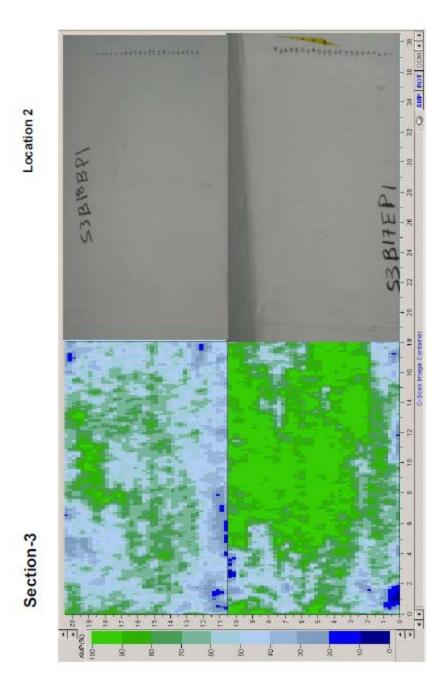


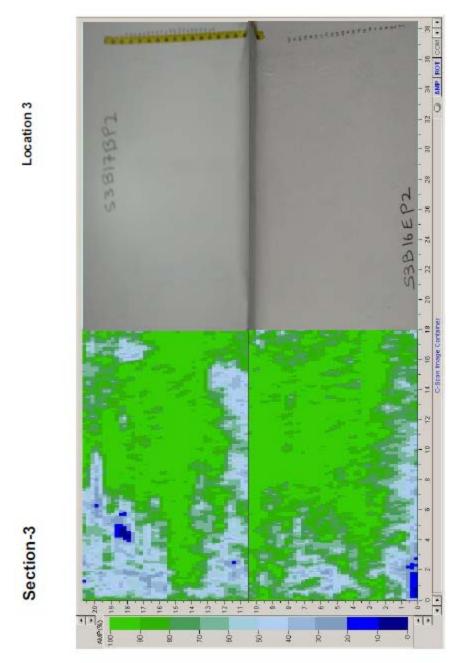


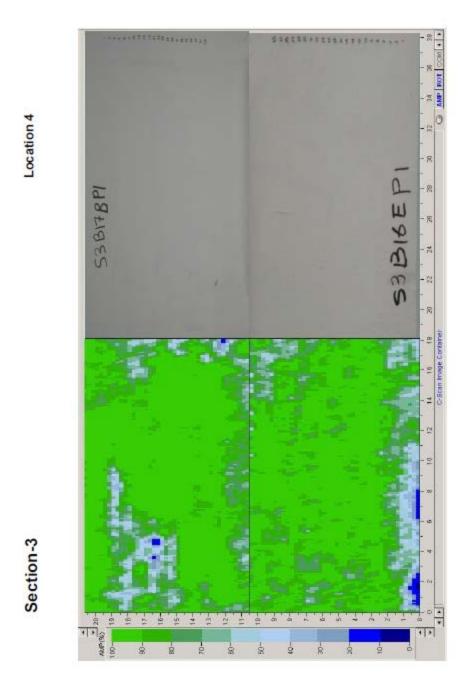


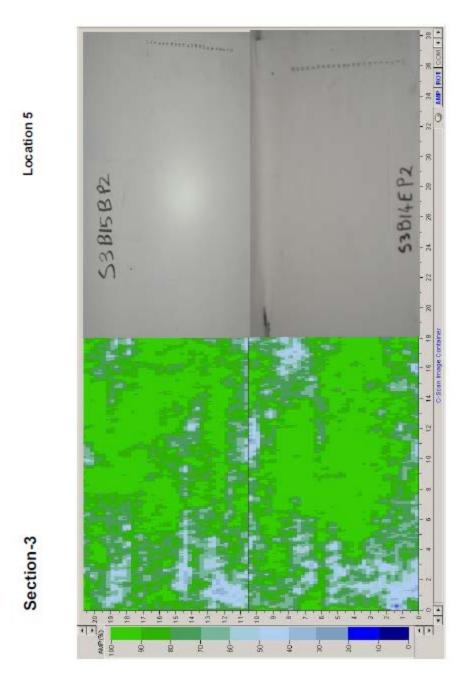


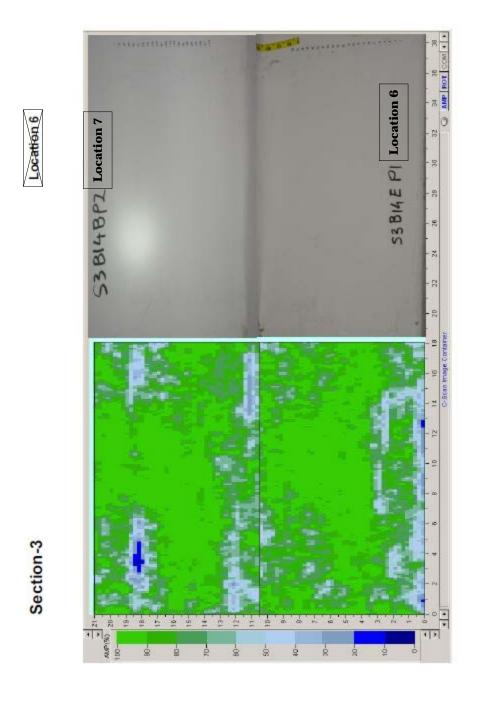






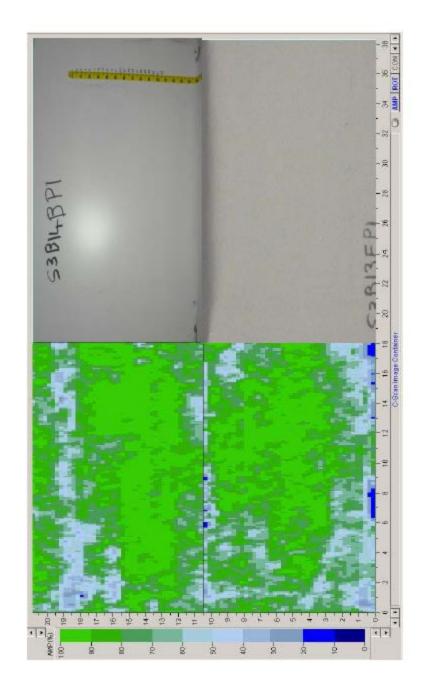




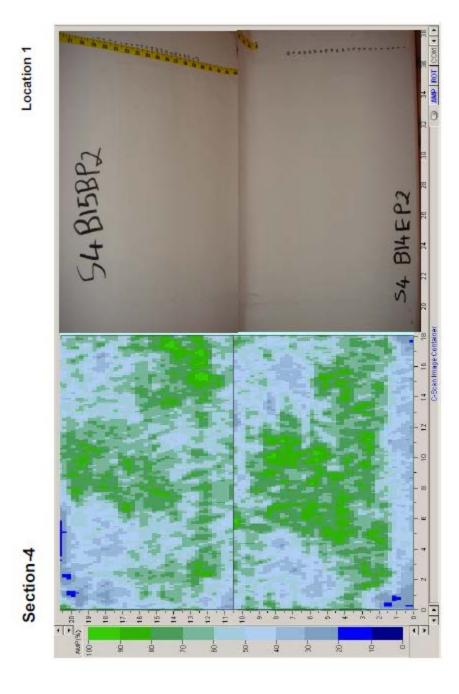


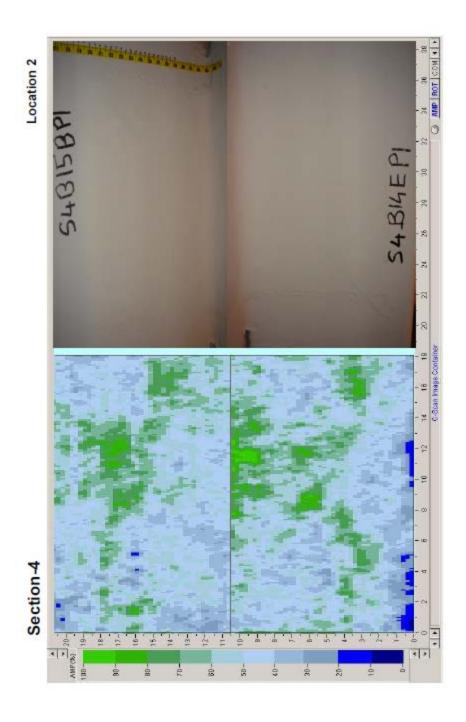
Location 8

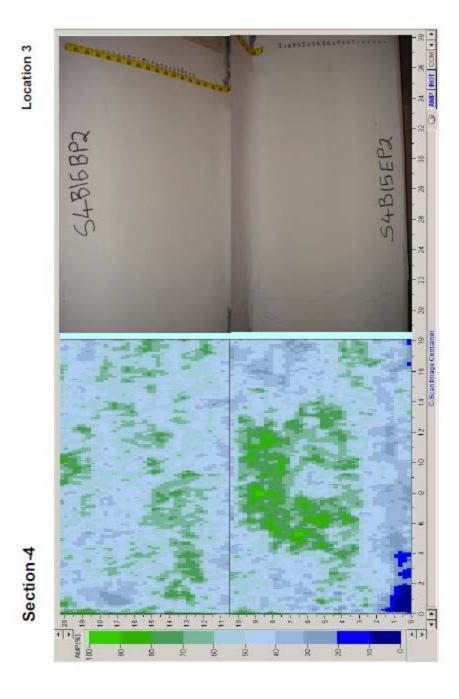
Location 7

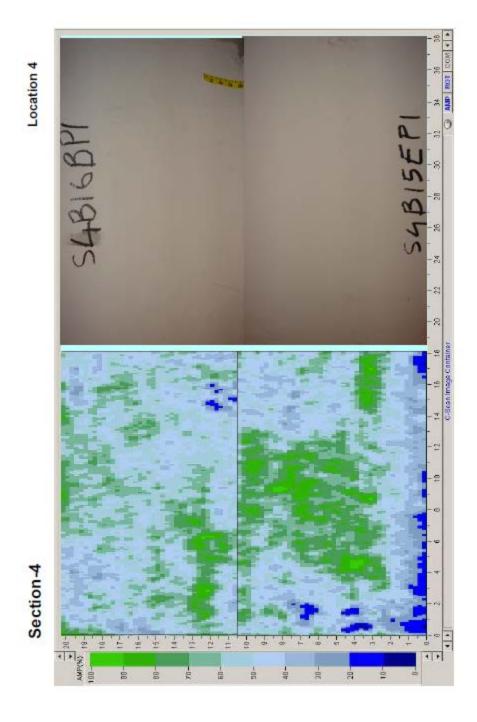


Section-3

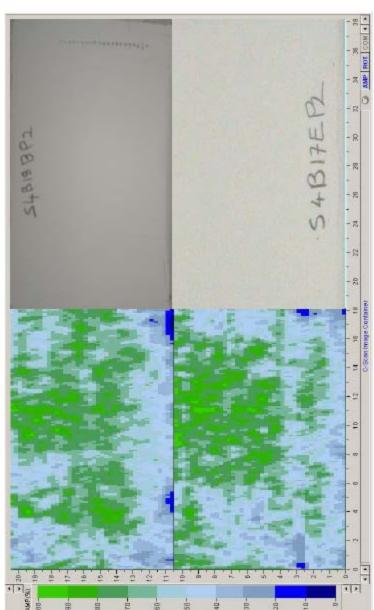


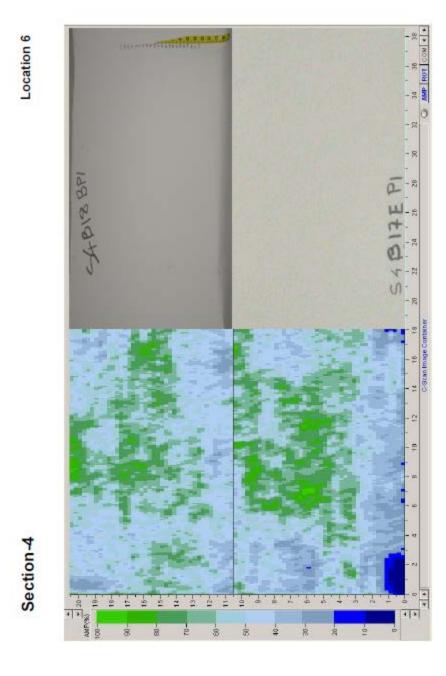


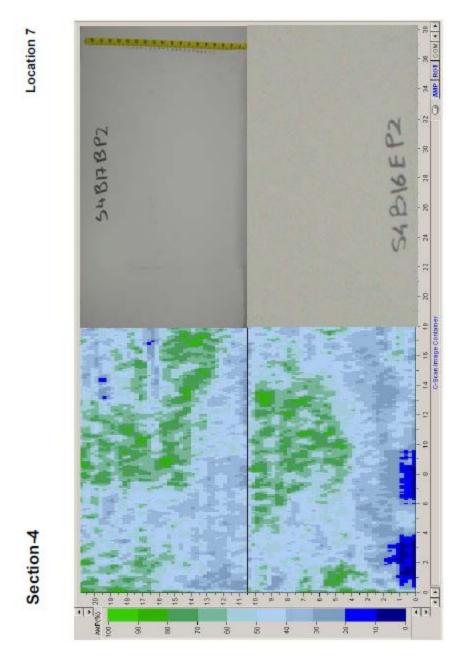




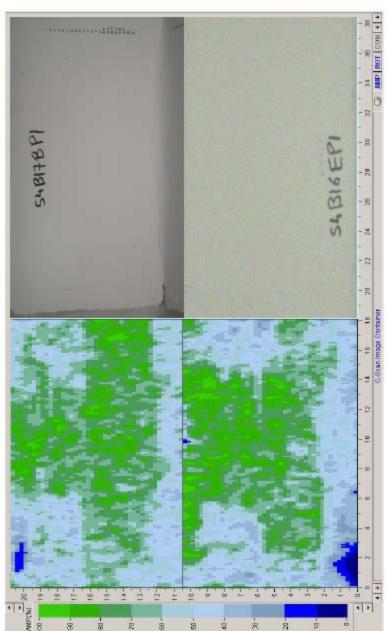


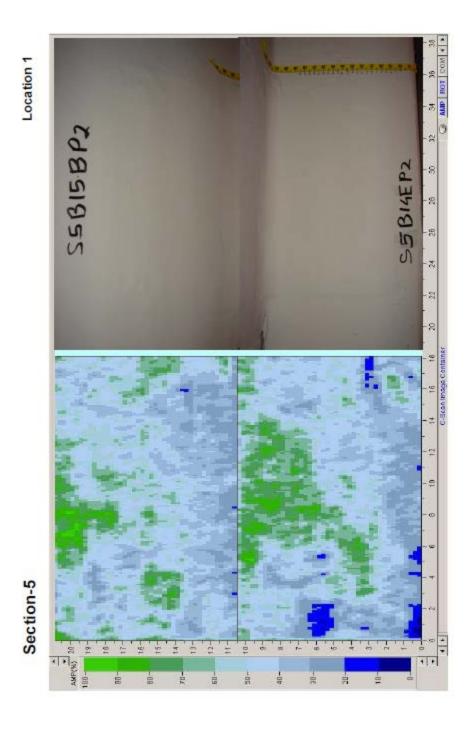


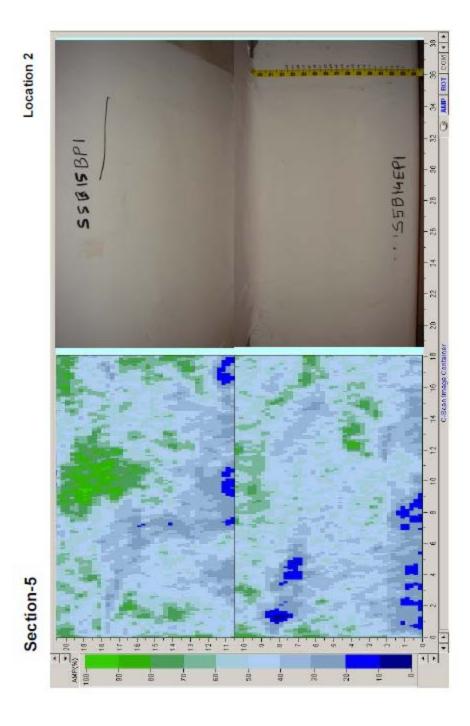


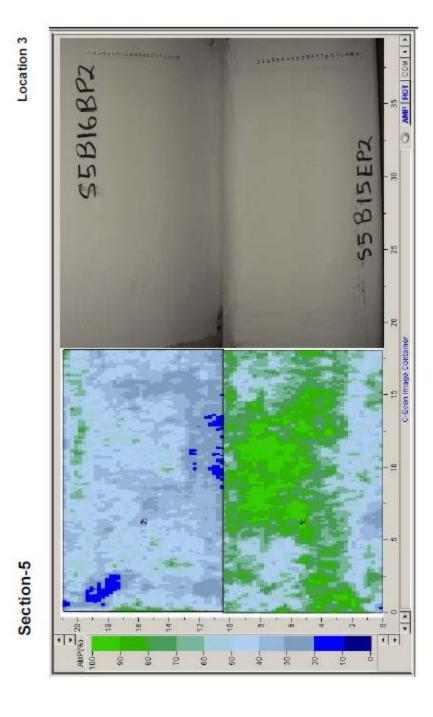


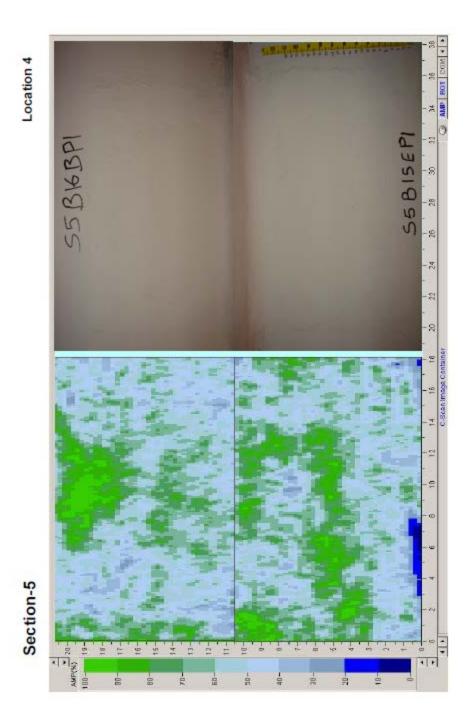


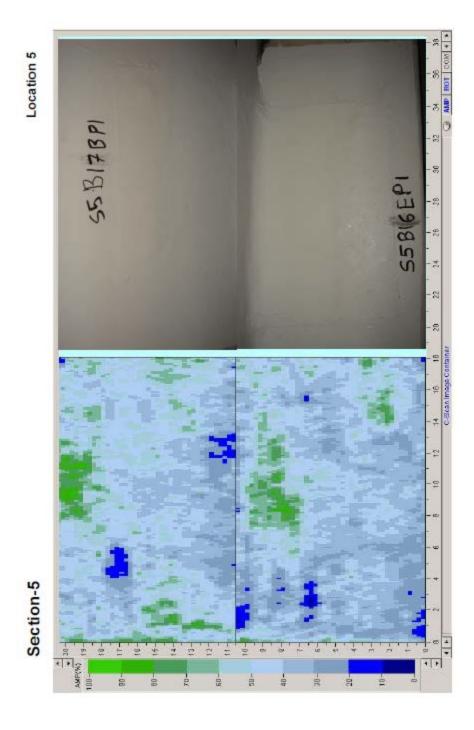


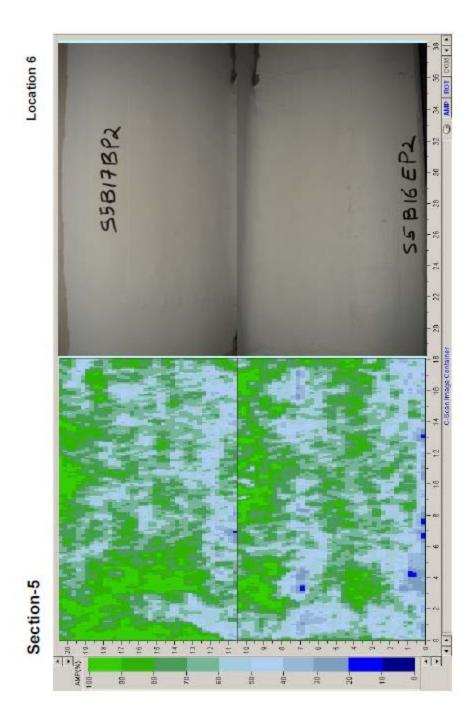


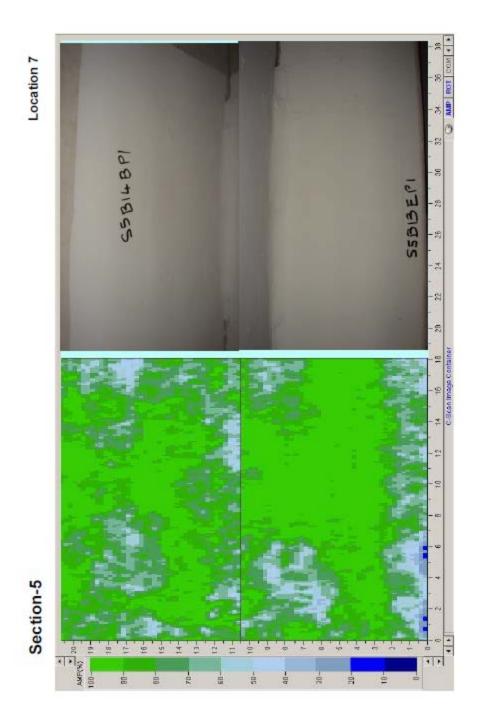


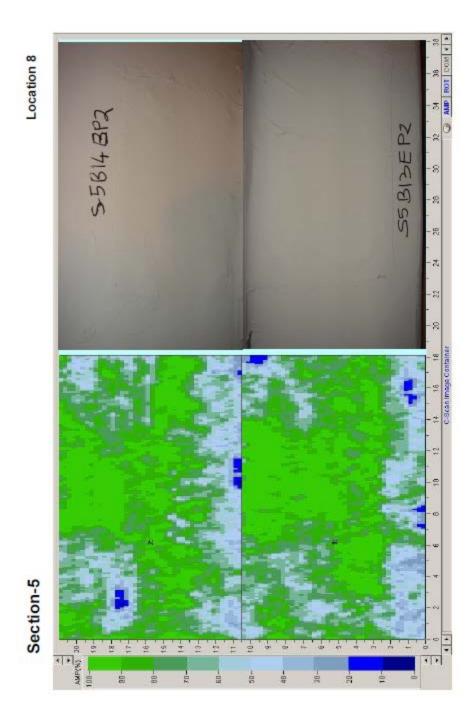


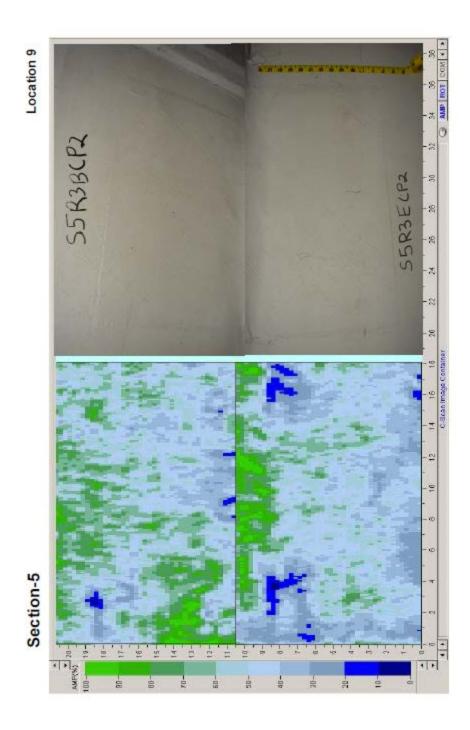


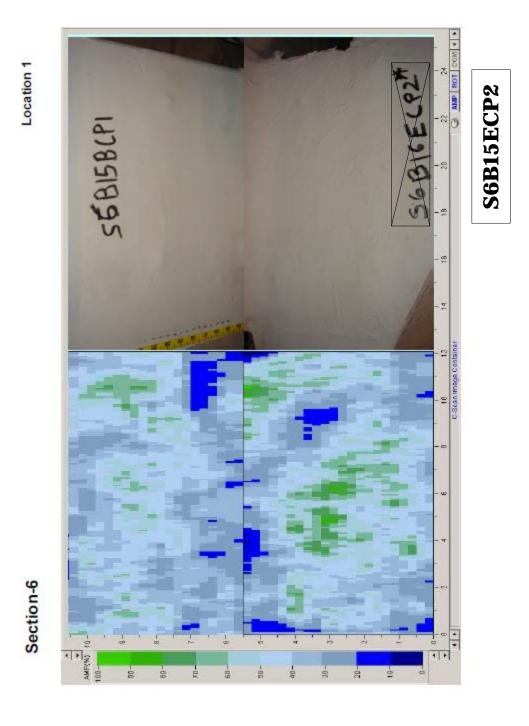


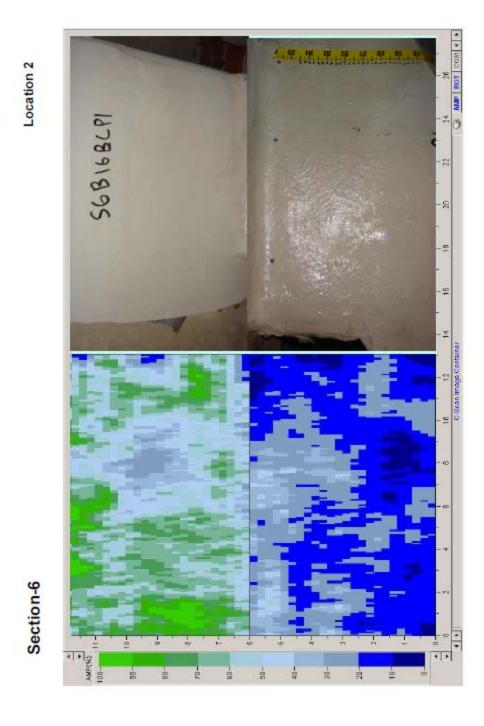


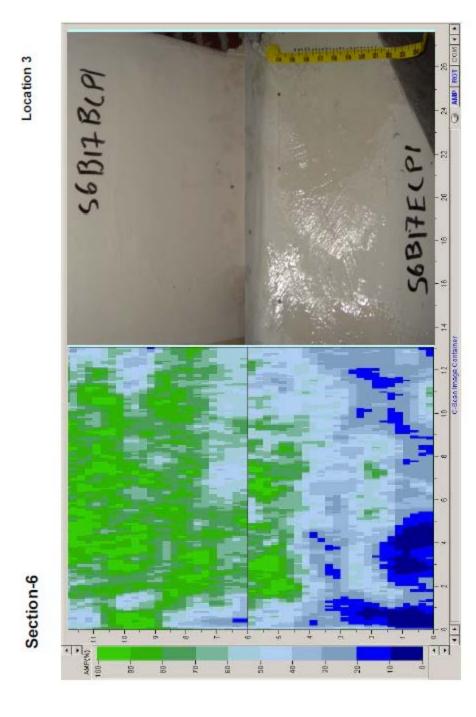


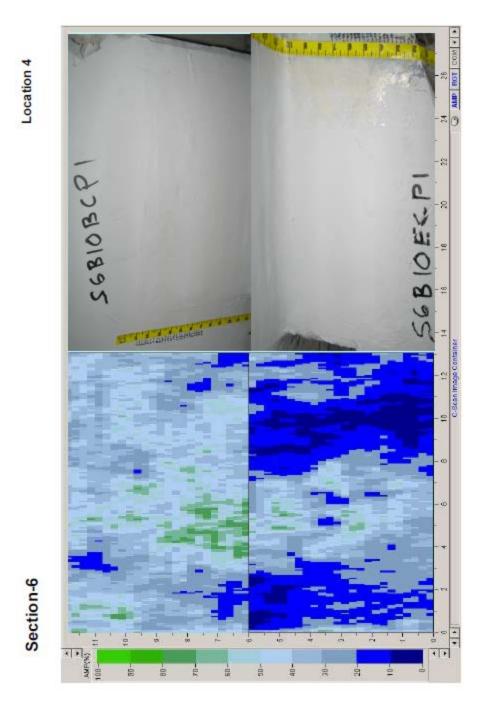


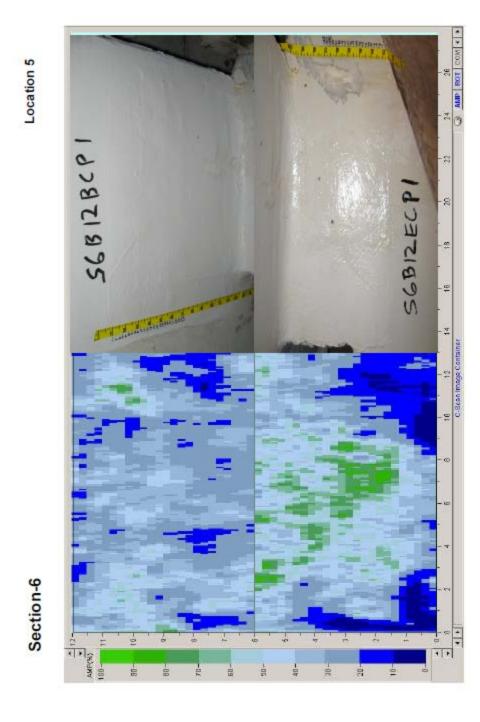


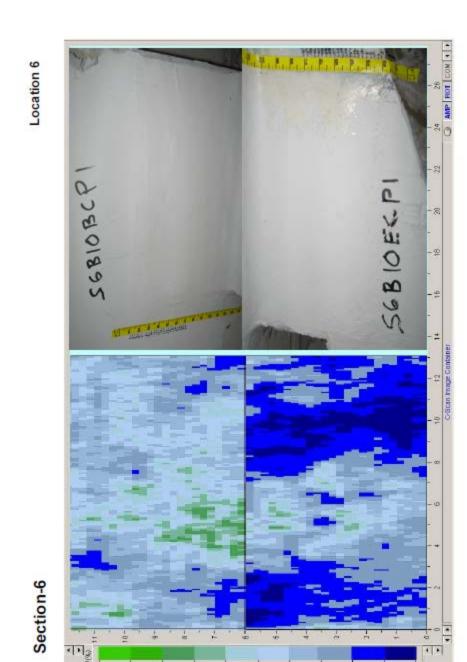


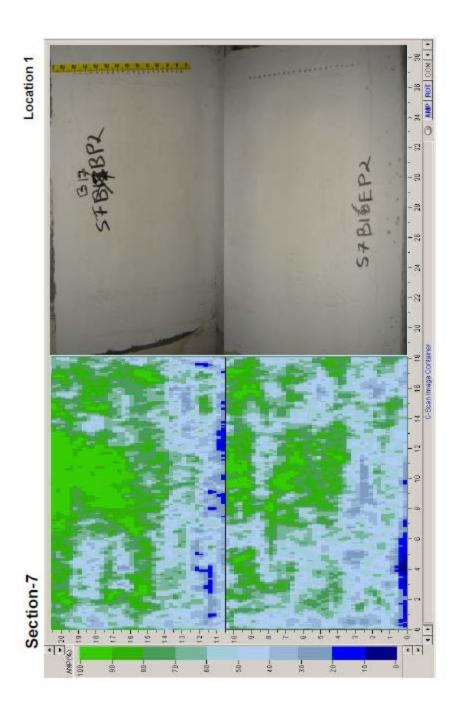


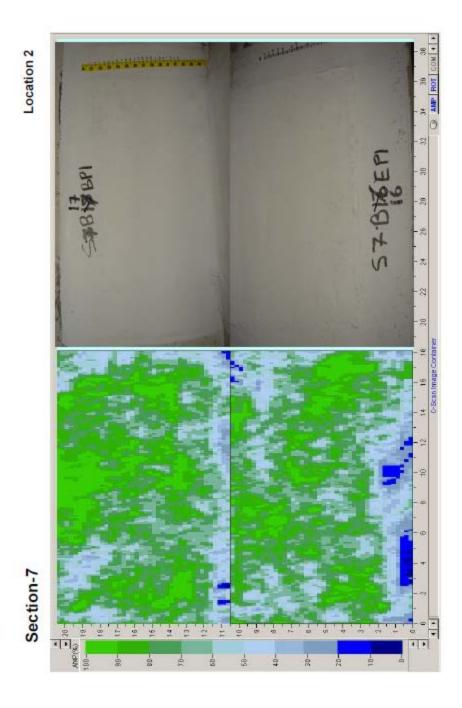


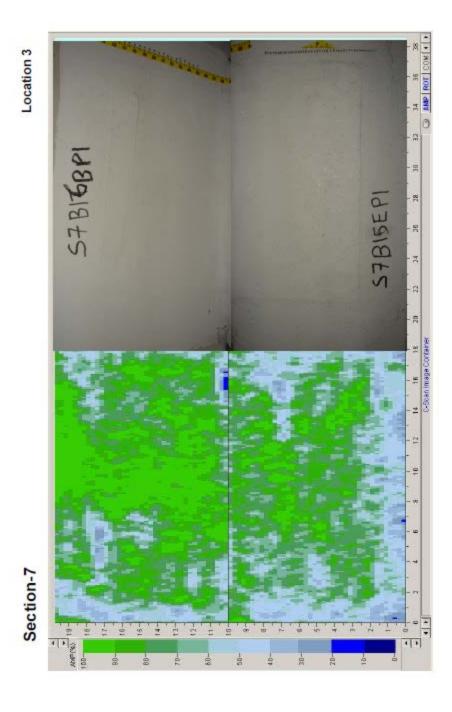


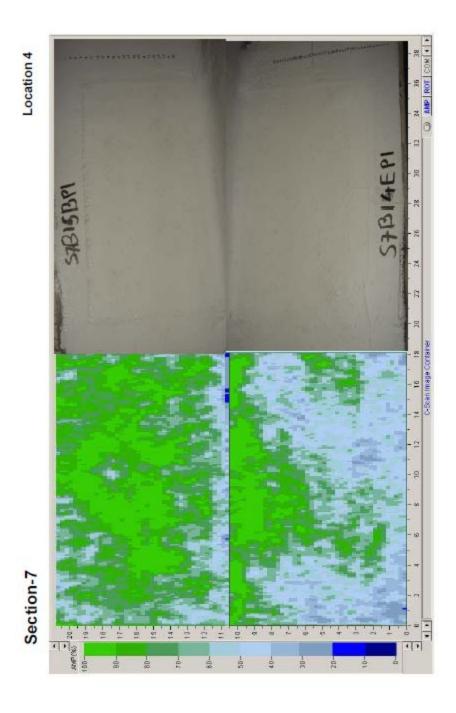


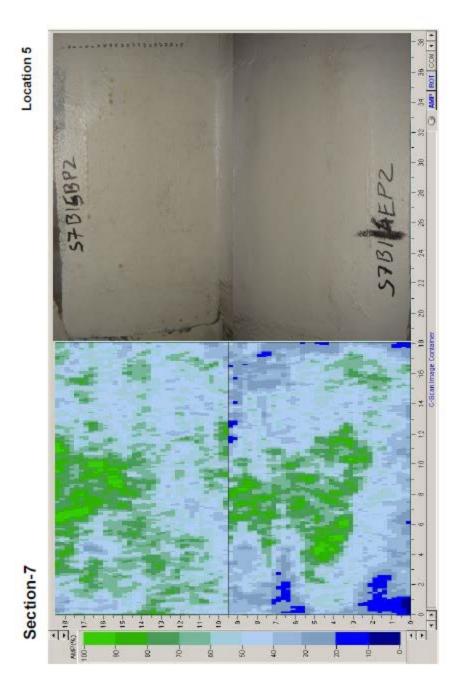


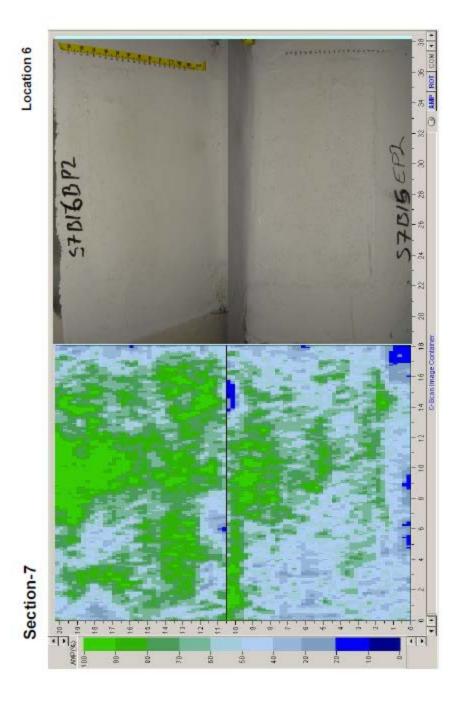


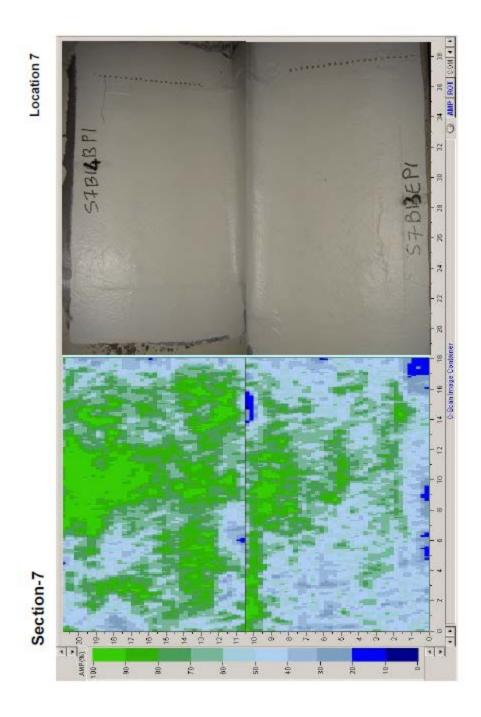


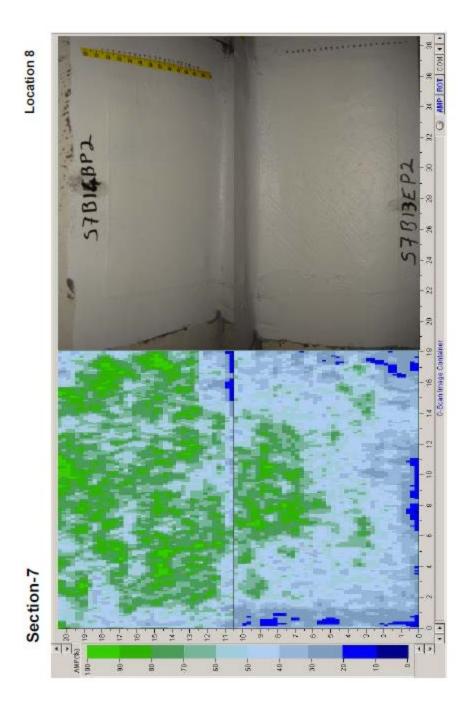


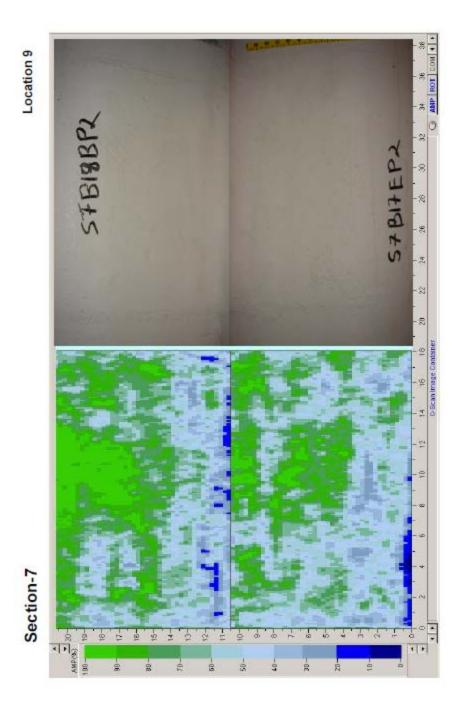


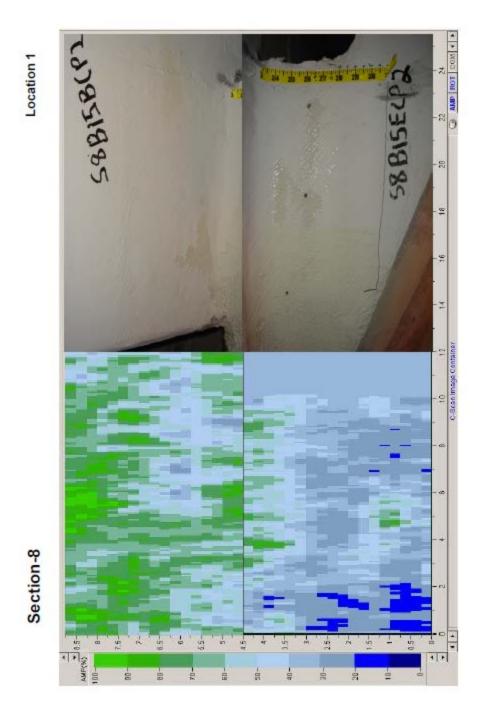


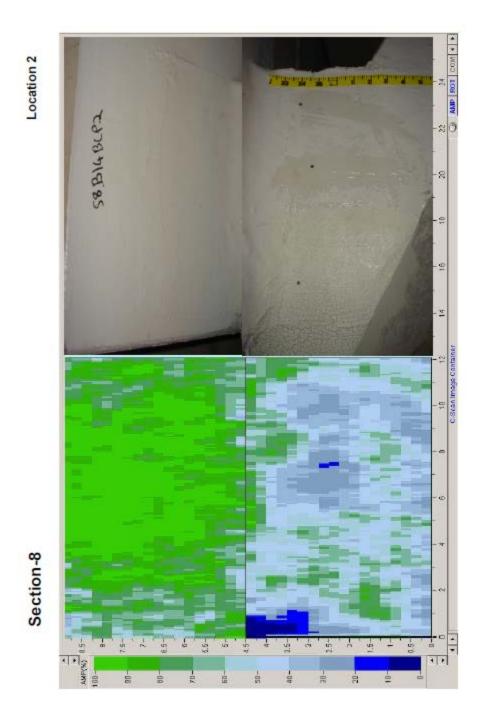


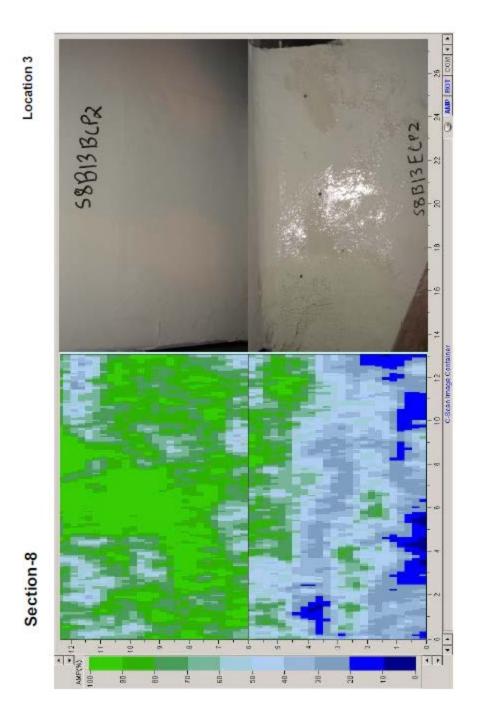


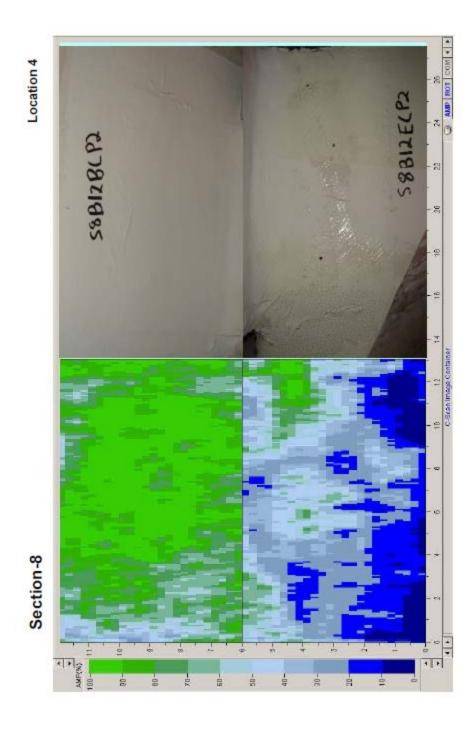


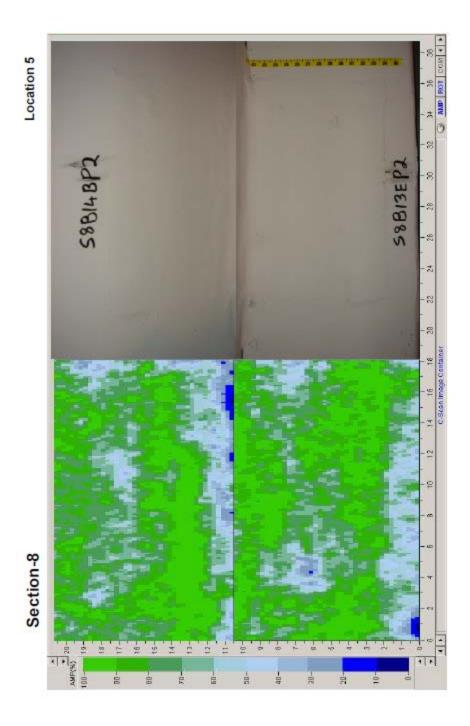


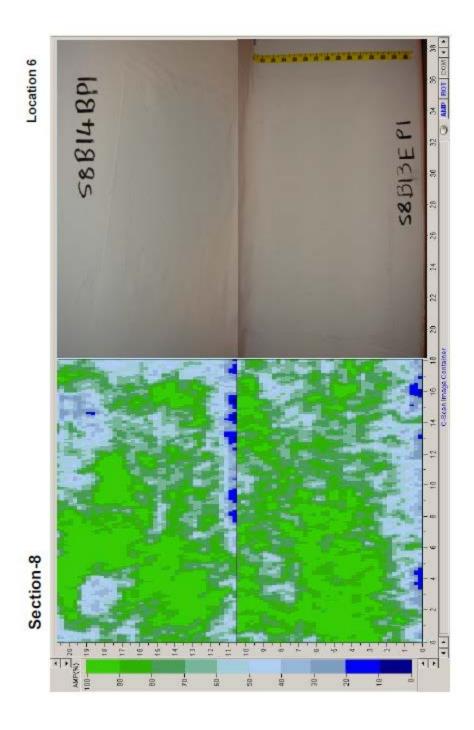


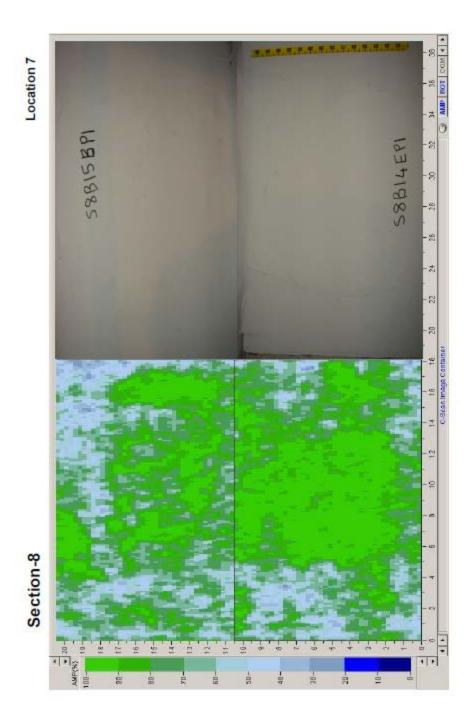


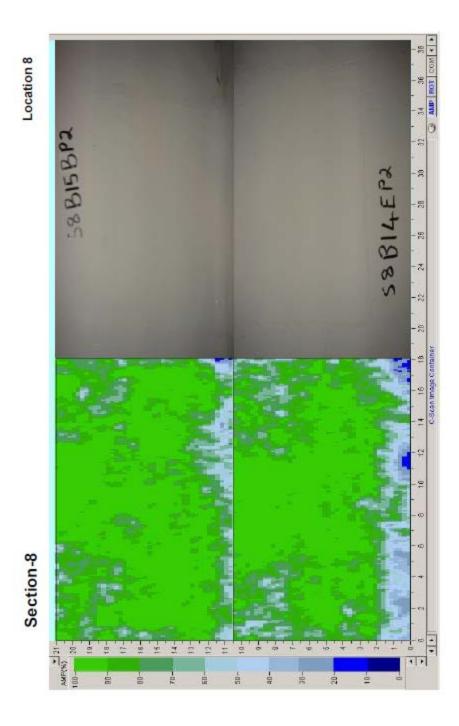


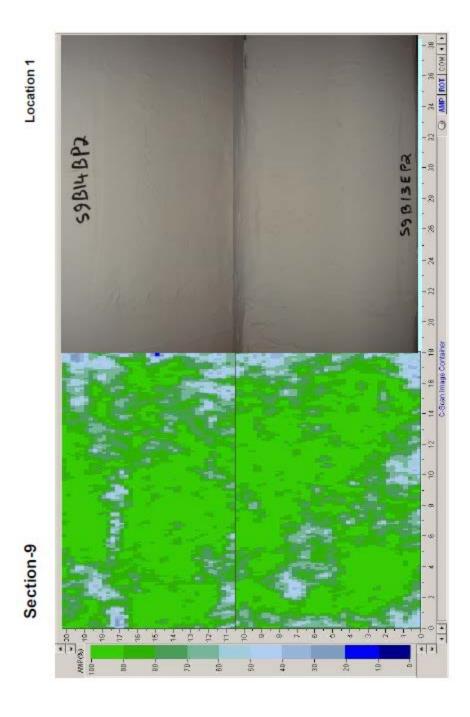


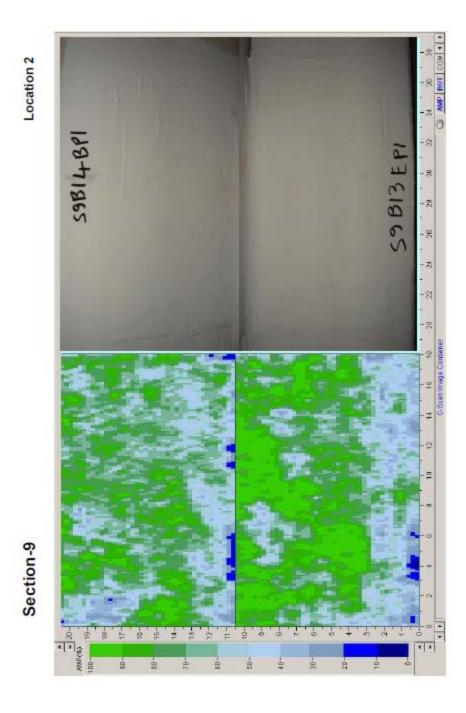


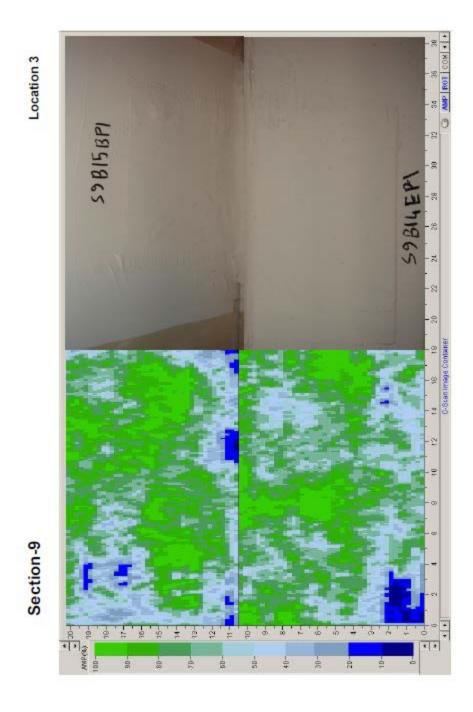


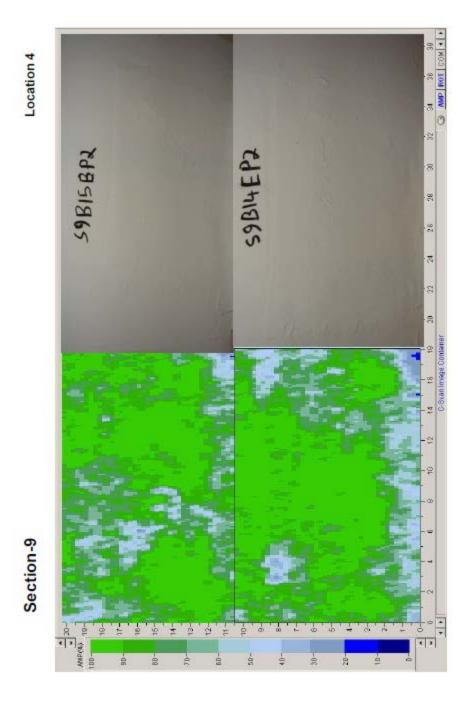


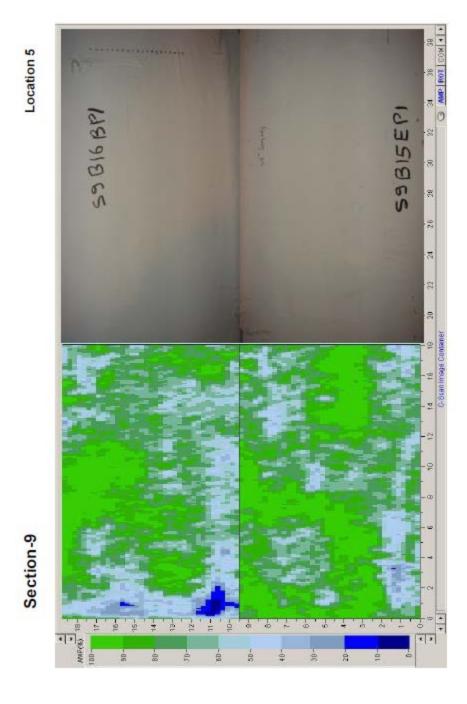


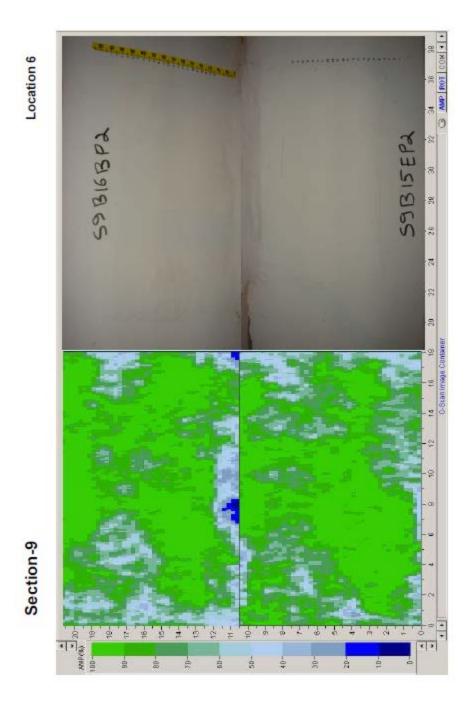


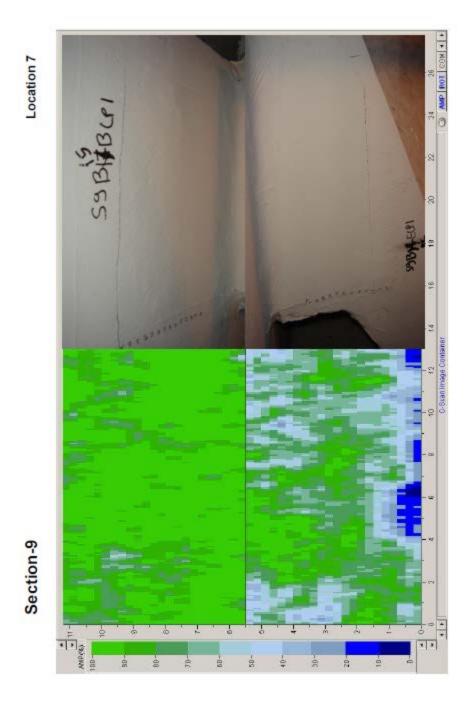


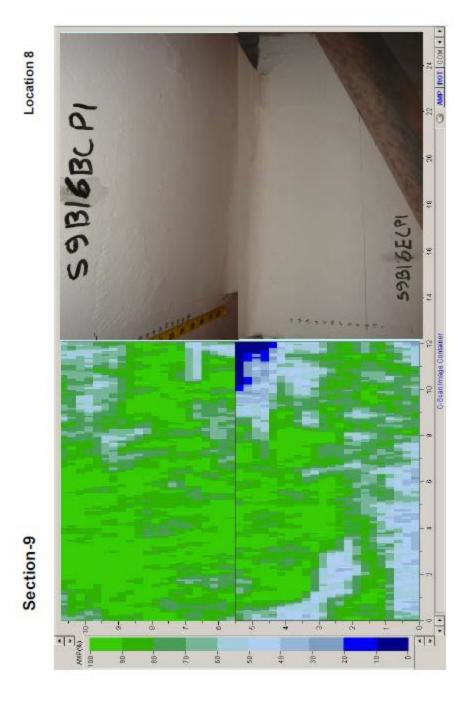


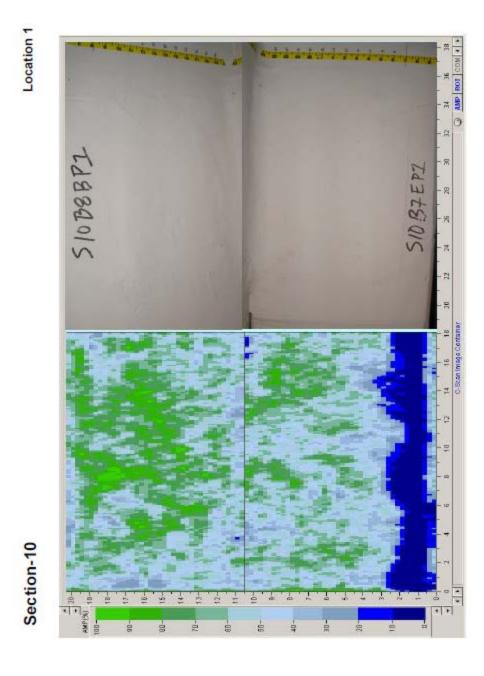




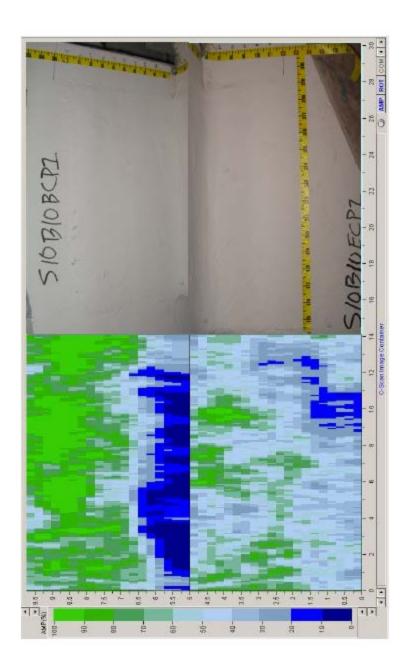






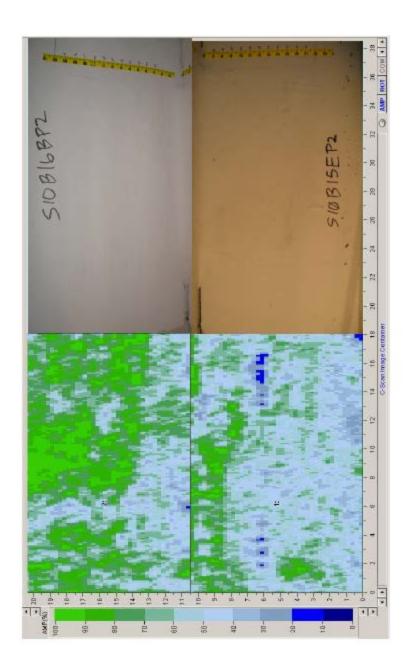






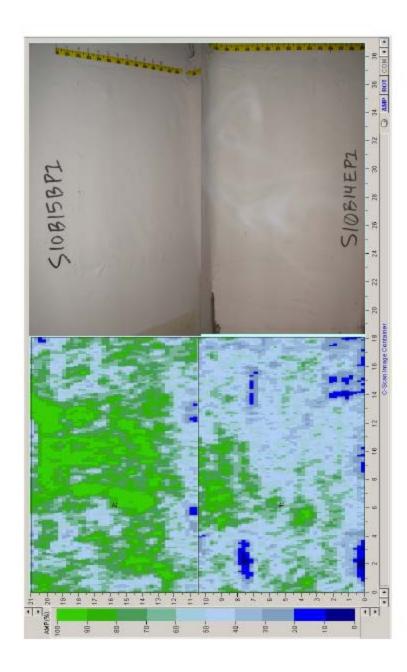
Section-10





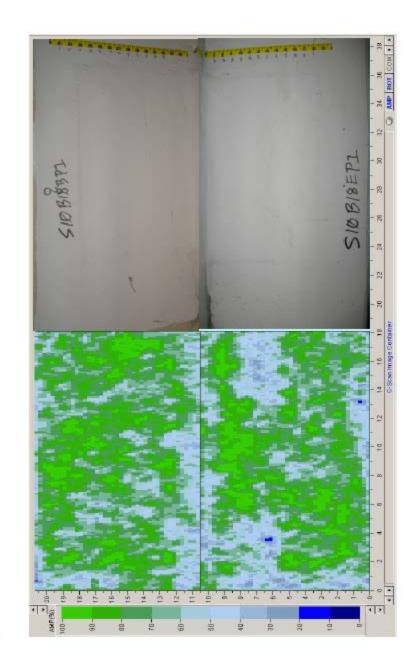
Section-10





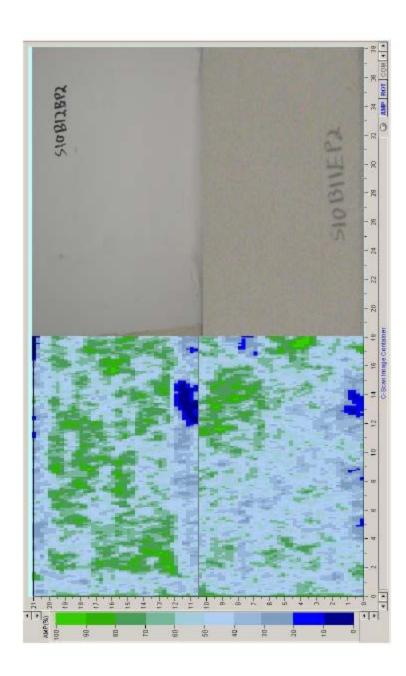
Section-10



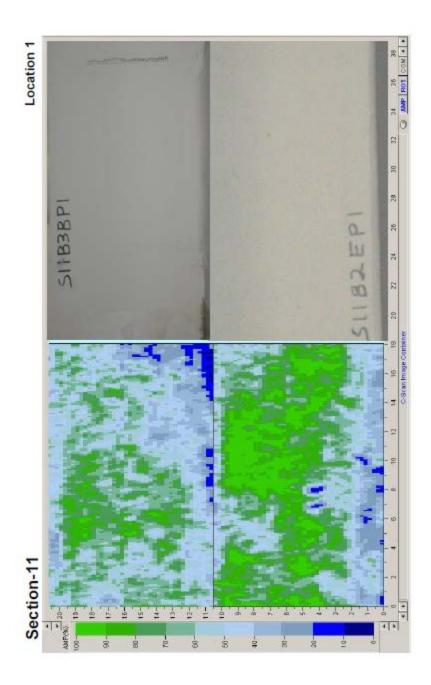


Section-10

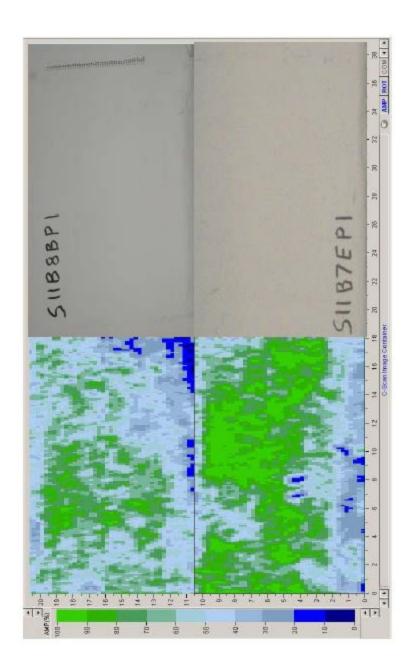




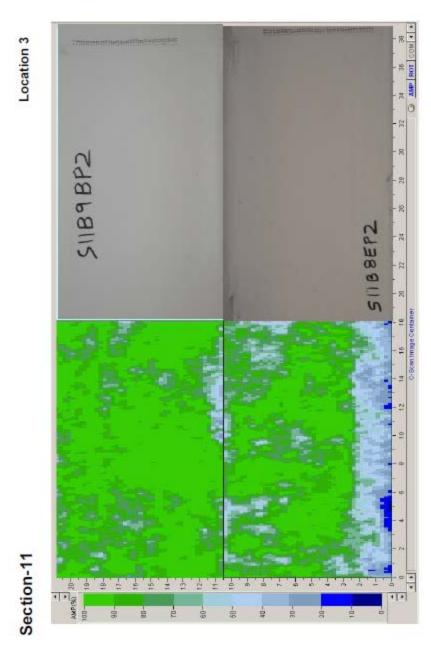
Section-10

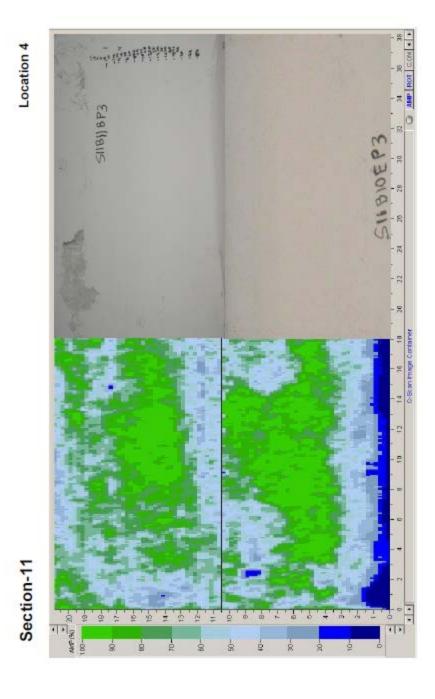






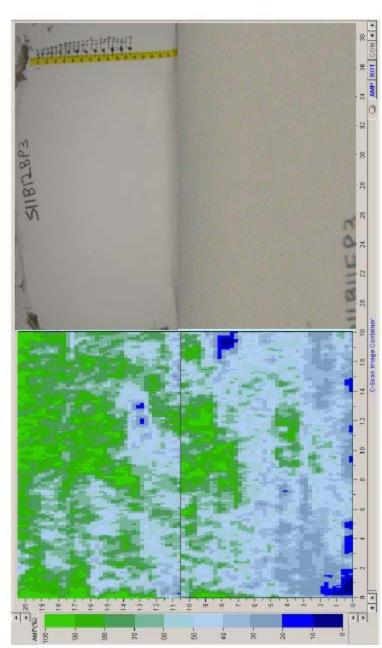
Section-11

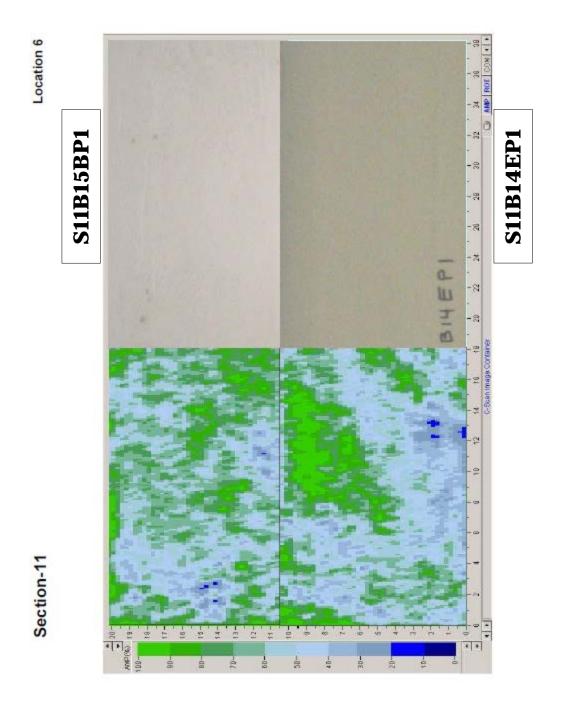


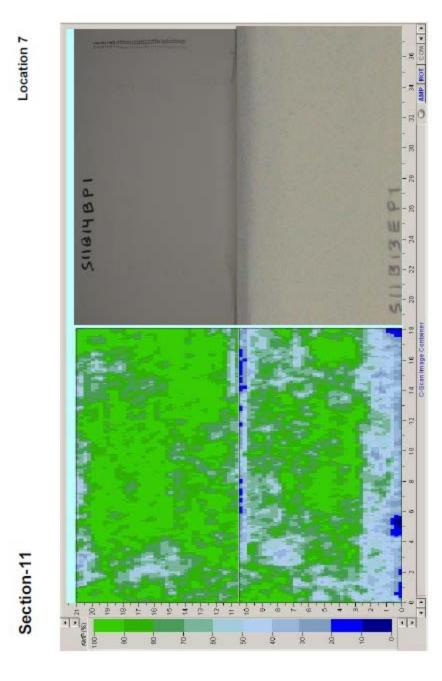


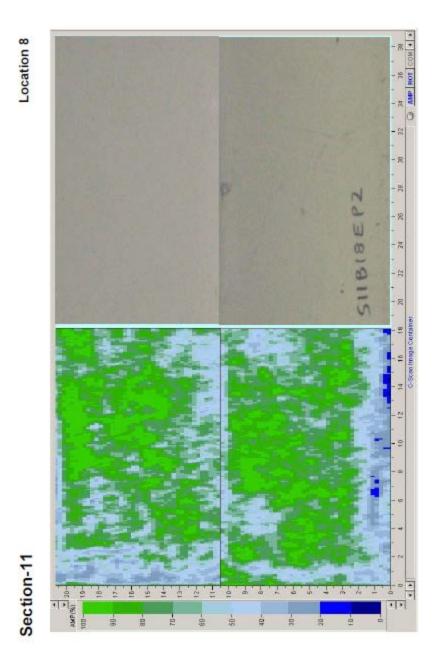


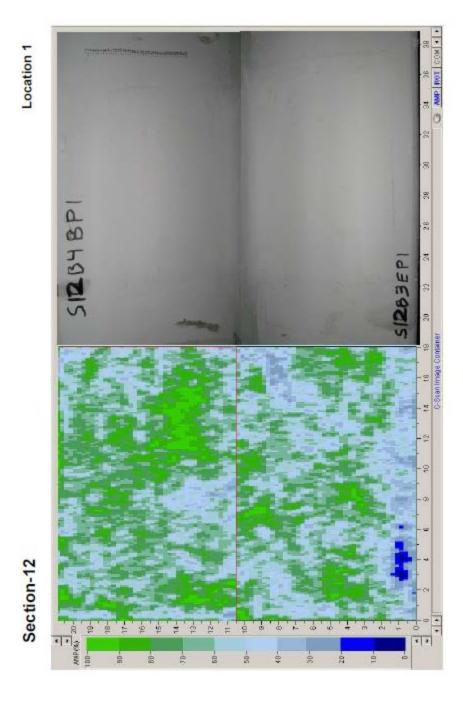
Section-11

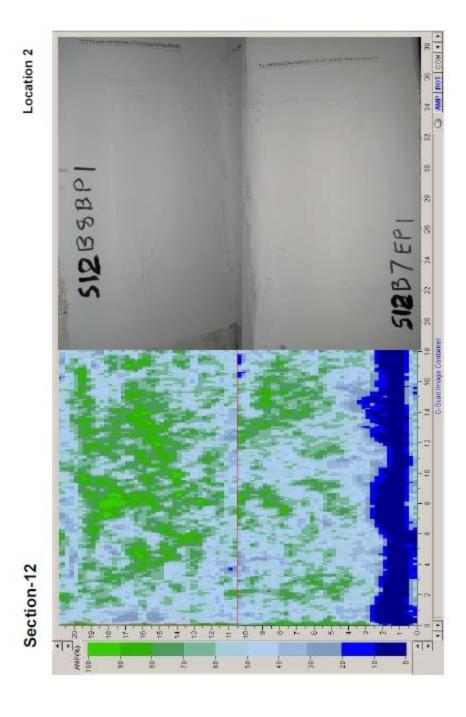


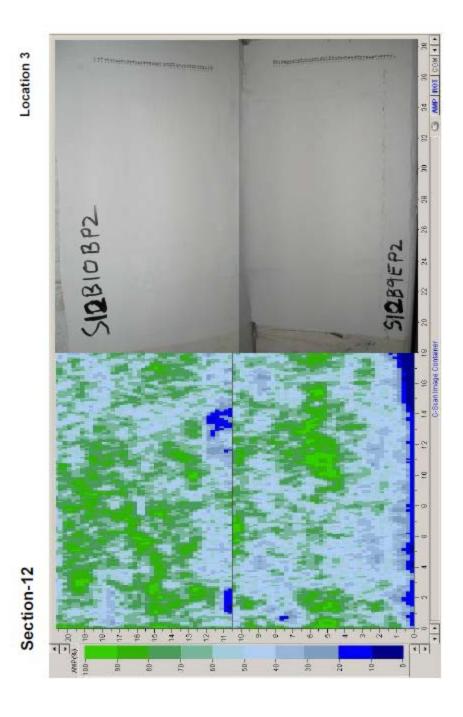


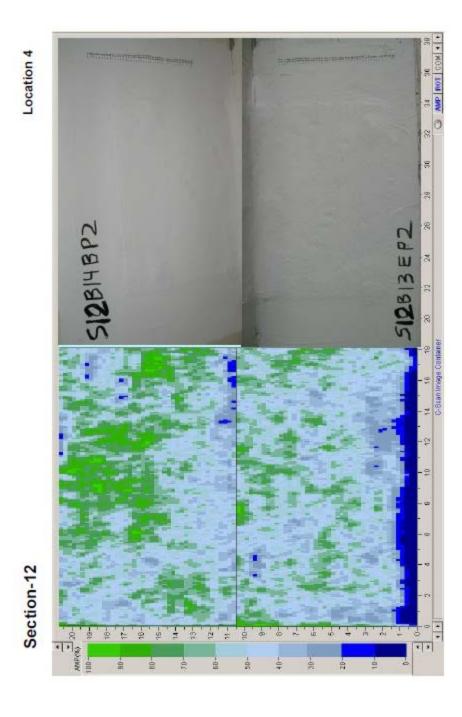


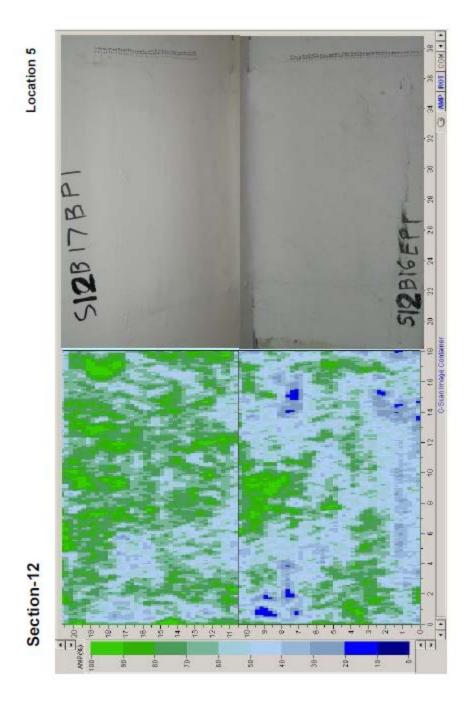


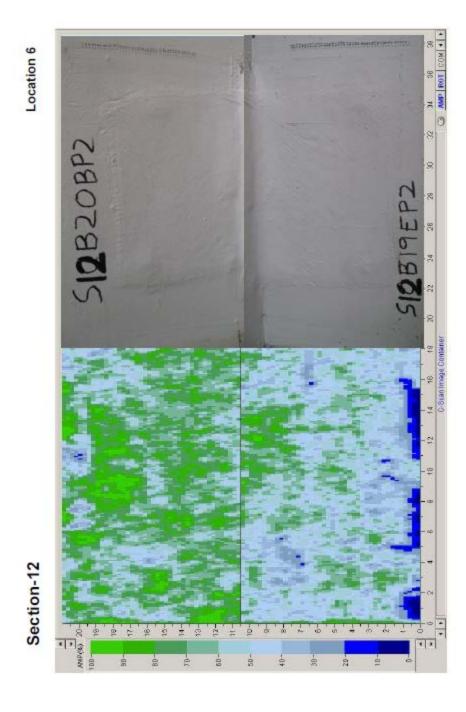


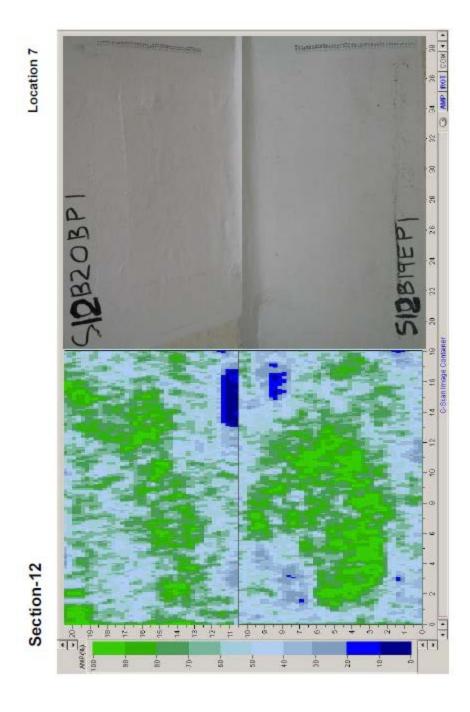


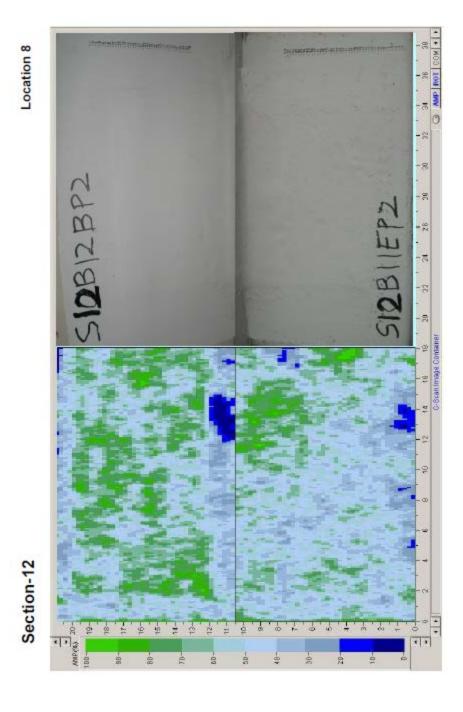


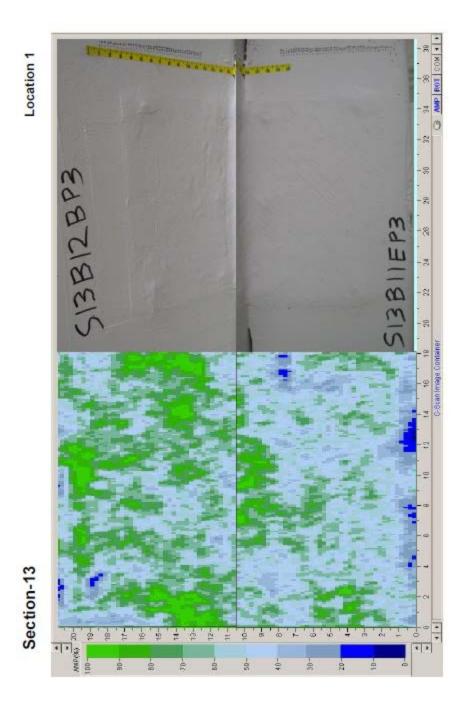


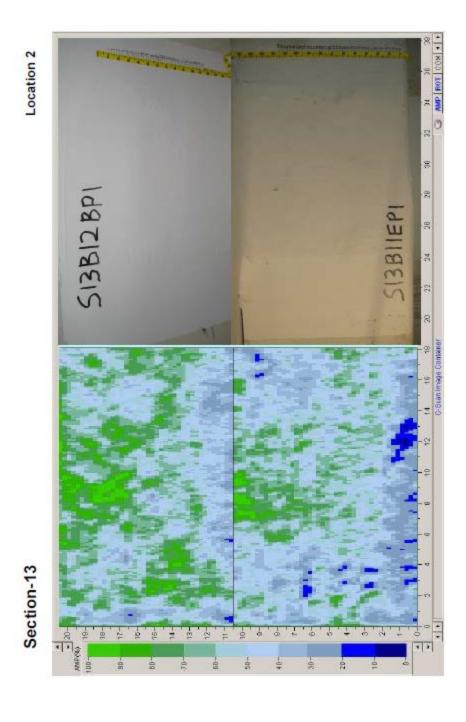


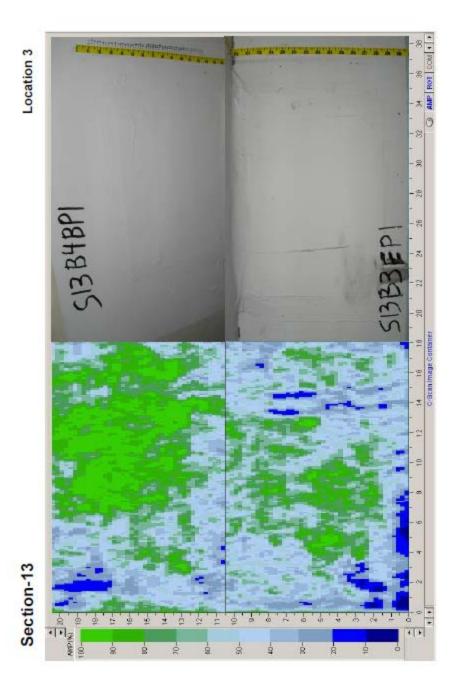


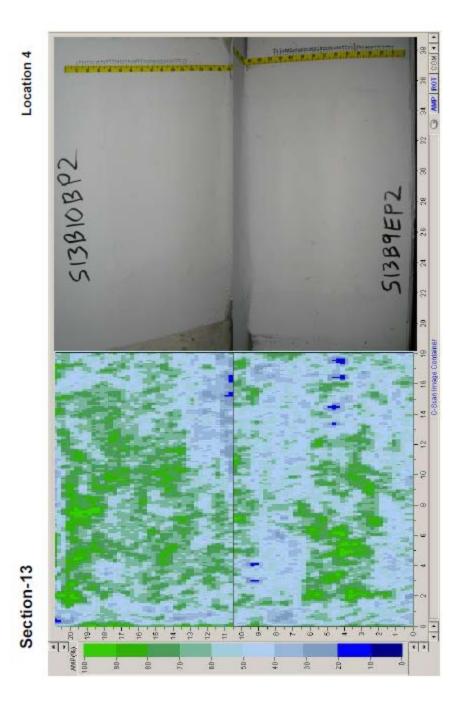


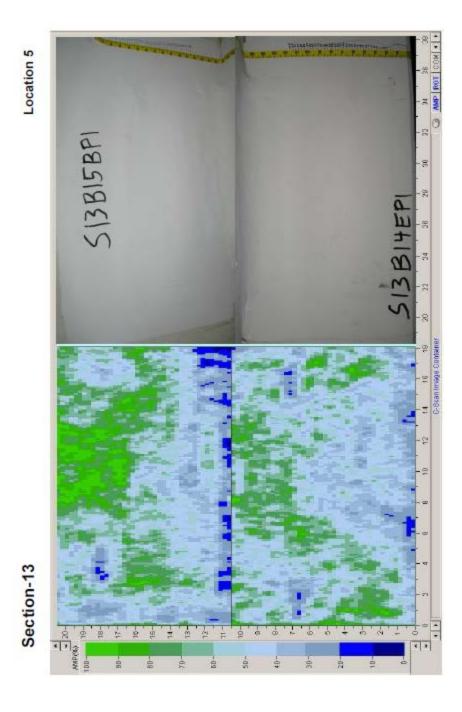


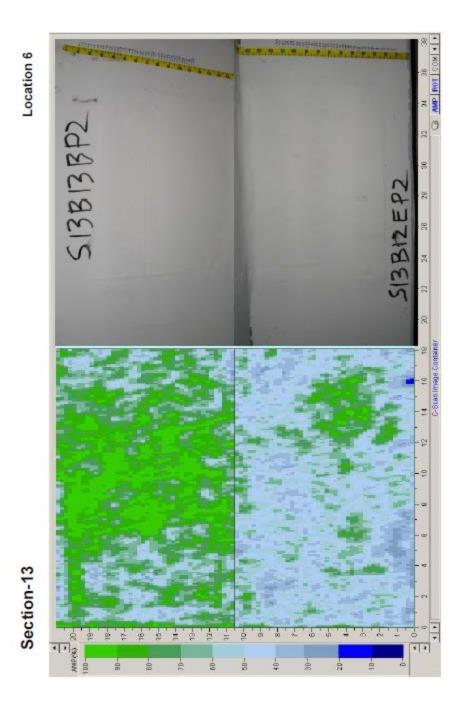


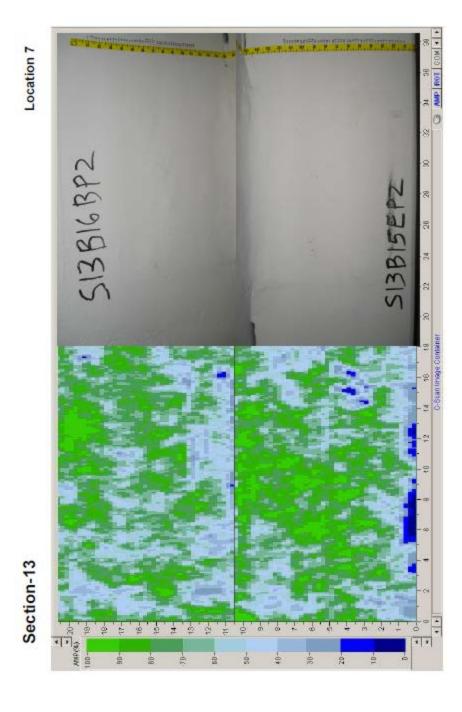


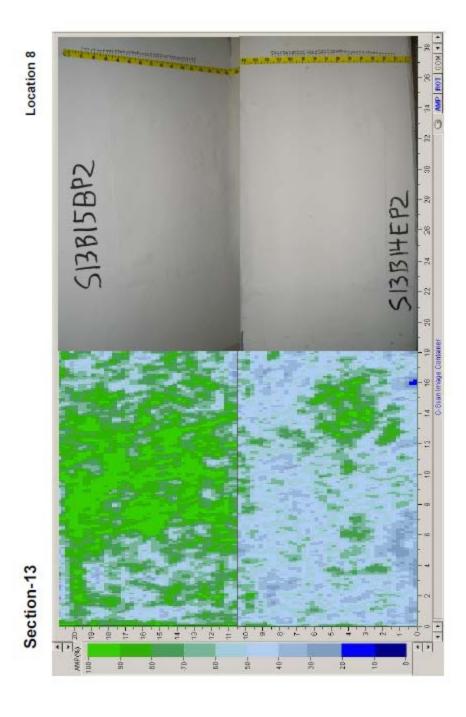


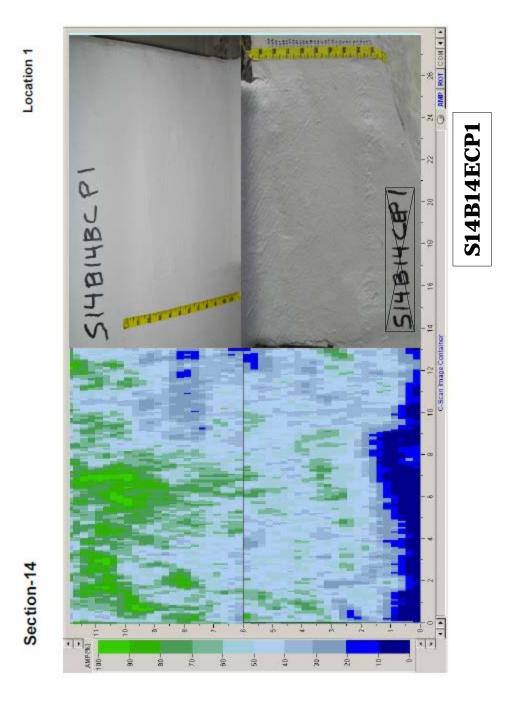




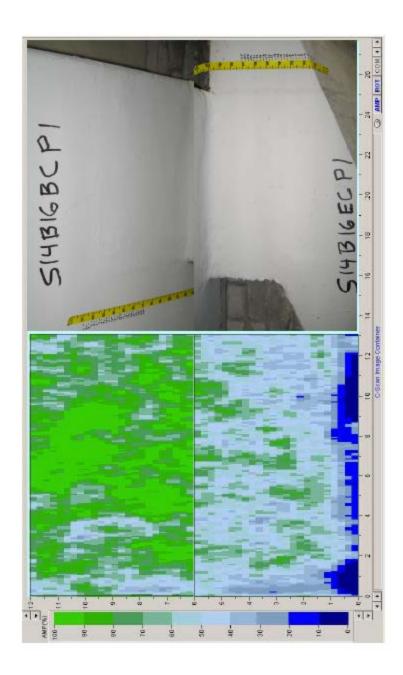




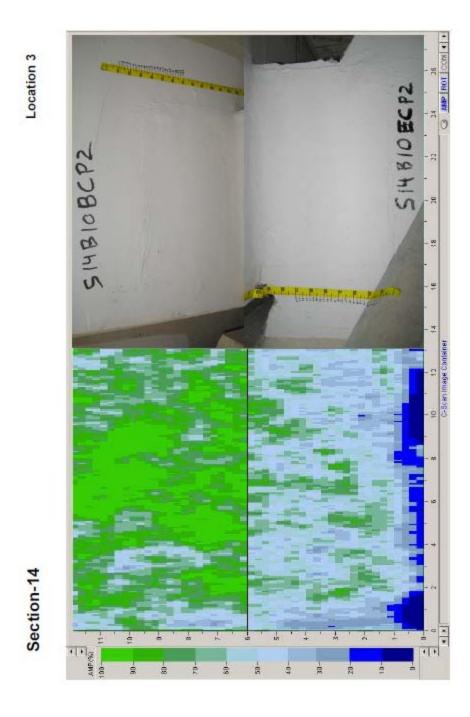




Location 2

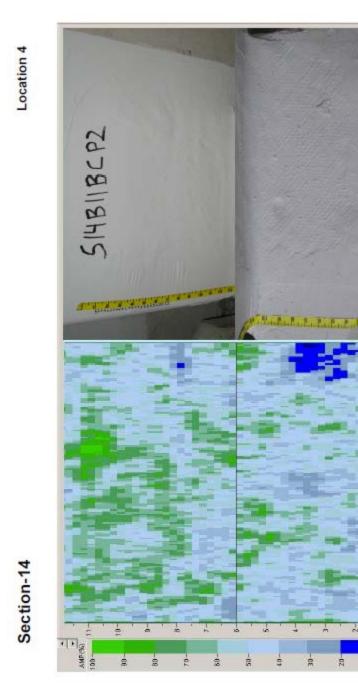


Section-14

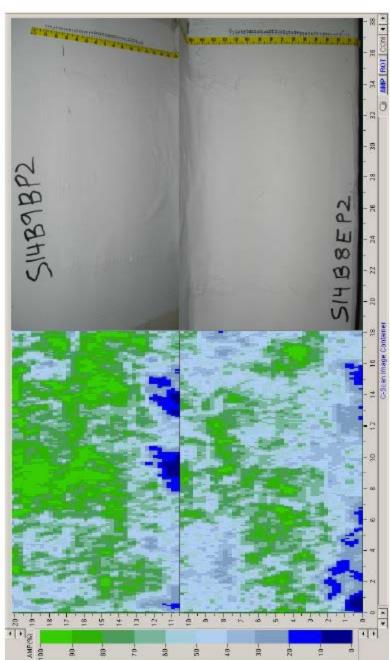


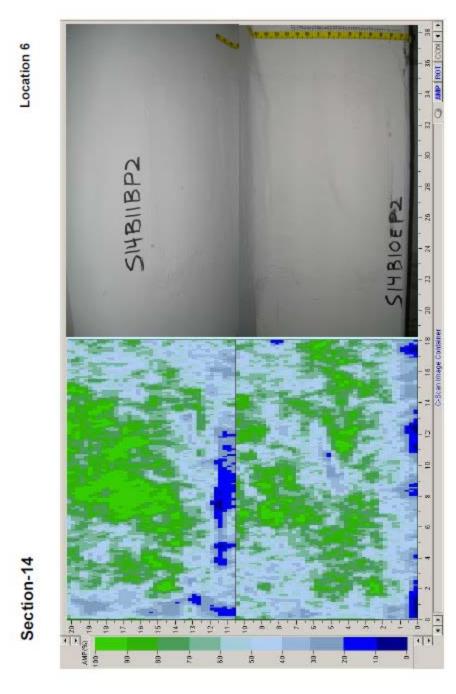
SHBIIECPZ

28

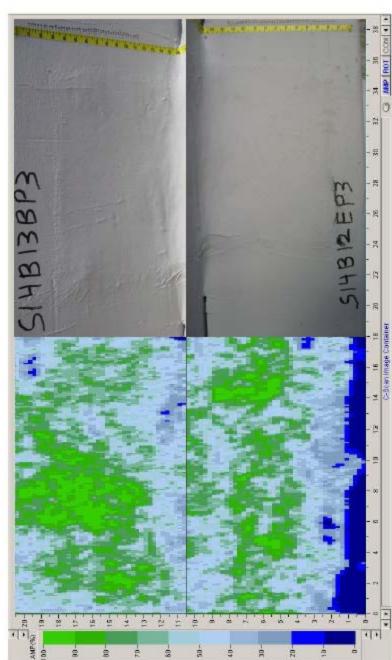




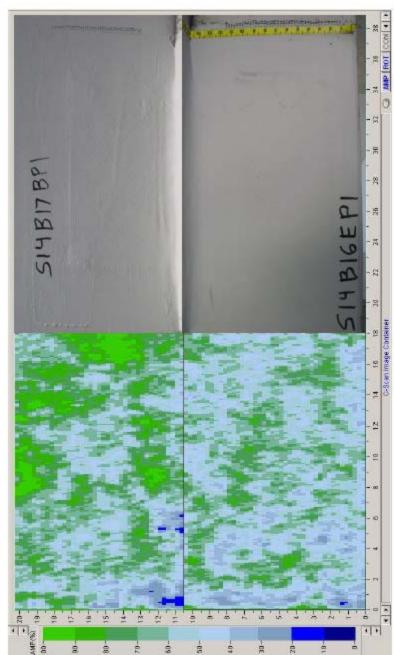


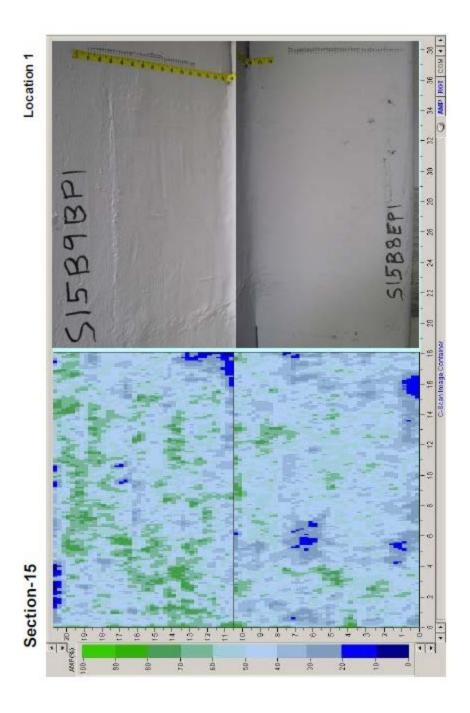




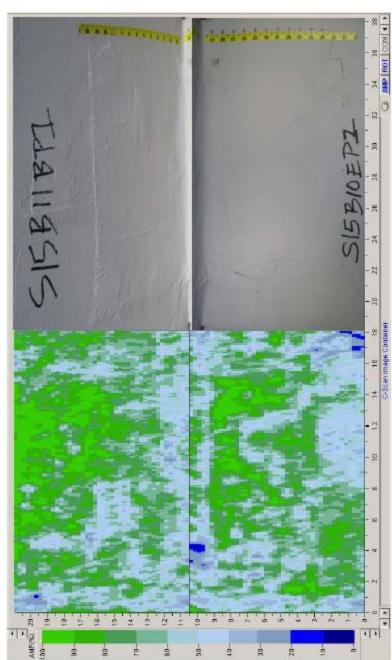


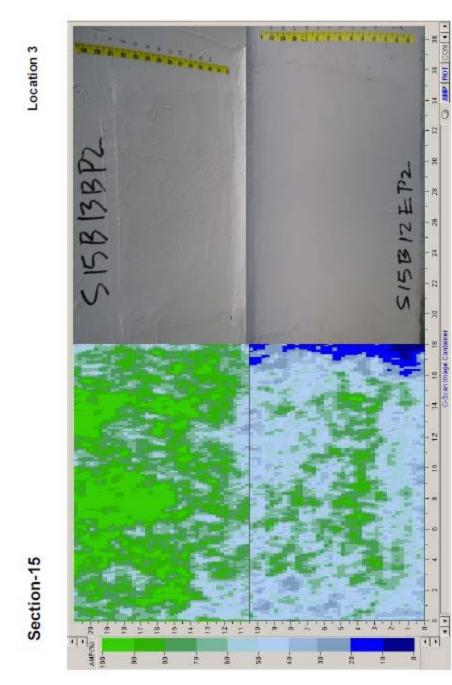




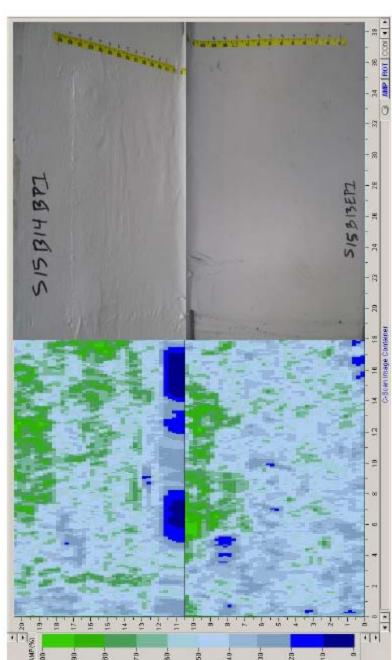




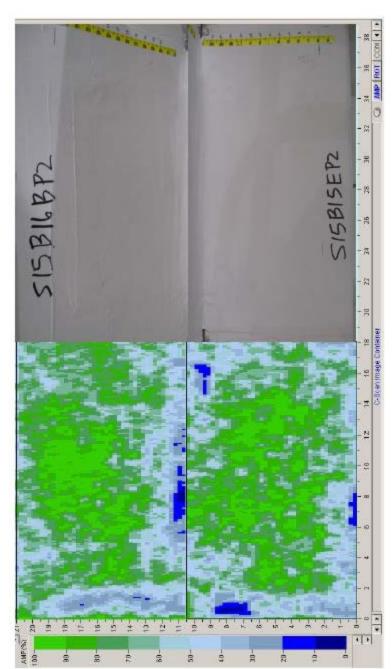


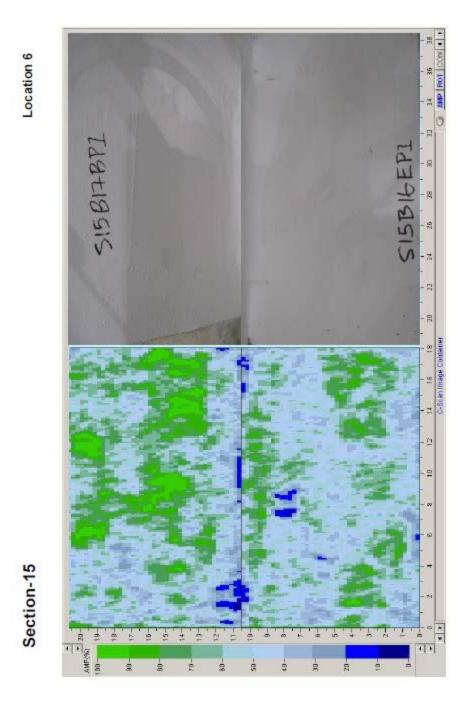




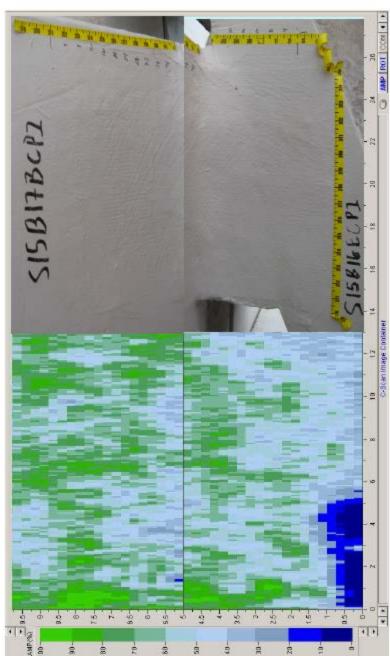




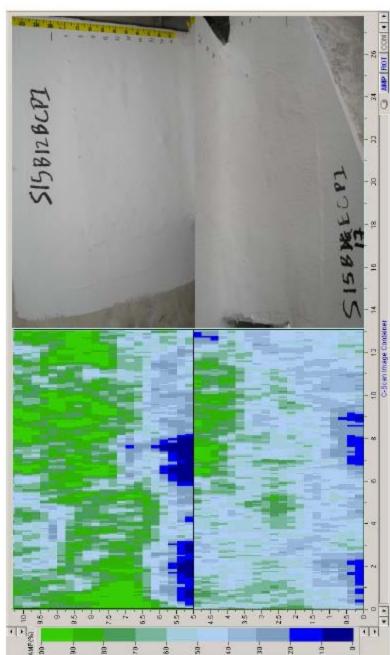




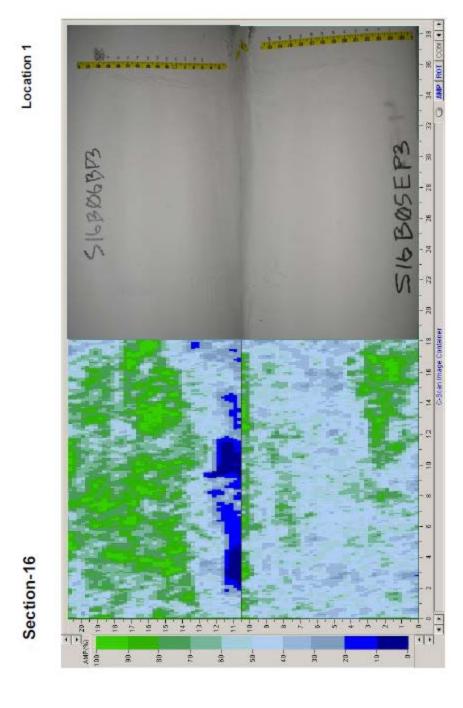




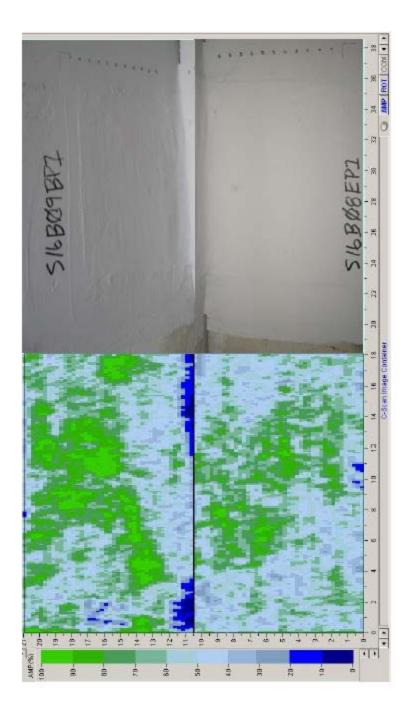




Section-15

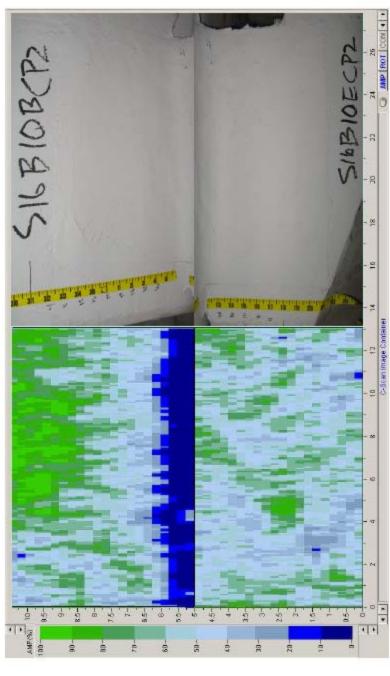


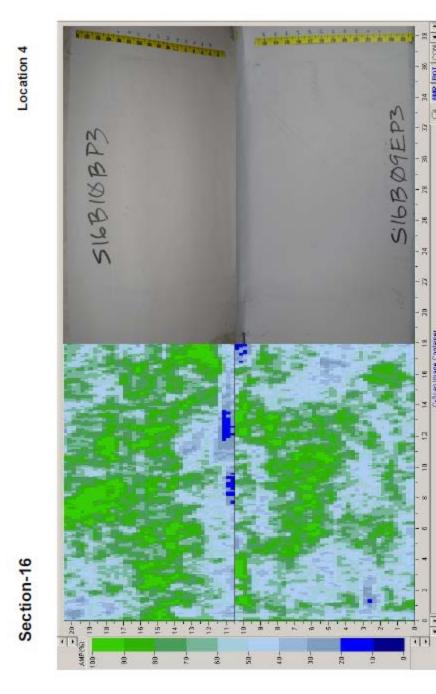




Section-16

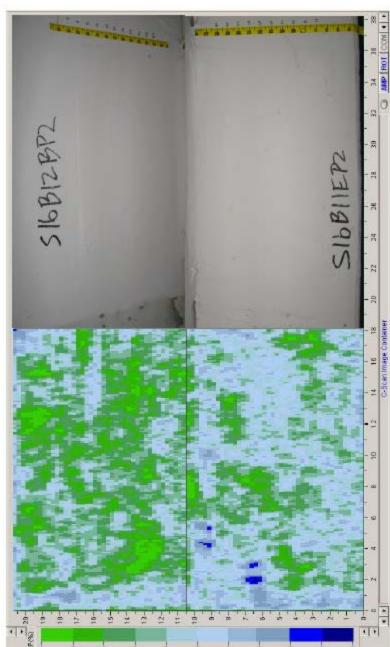


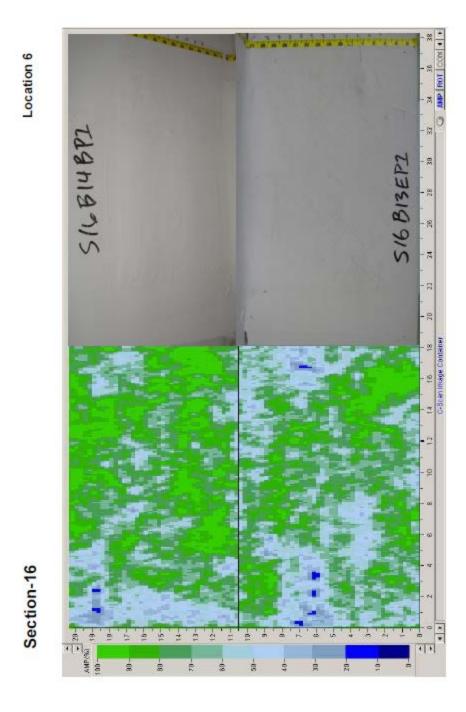


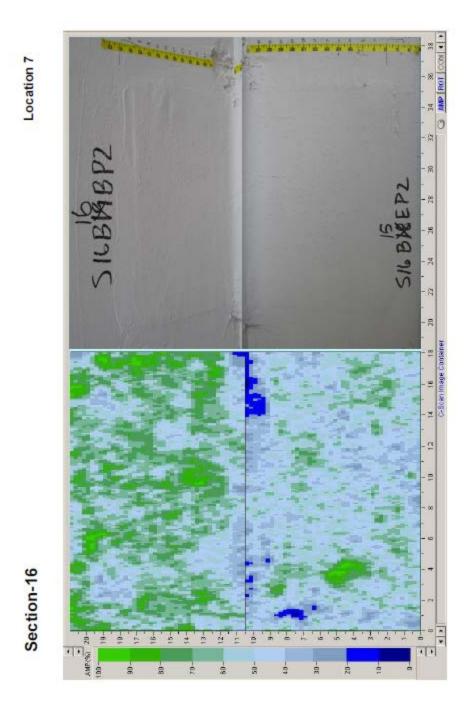




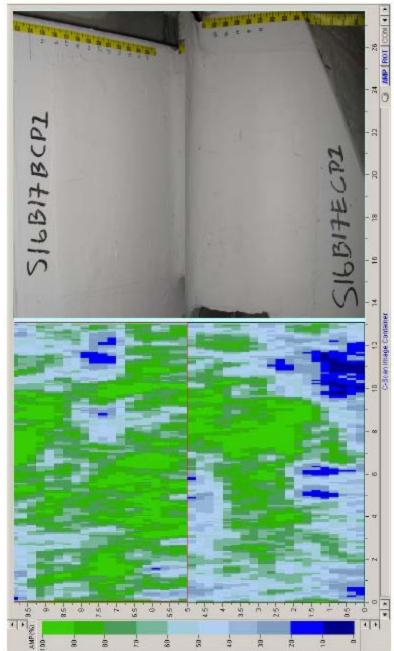
Section-16



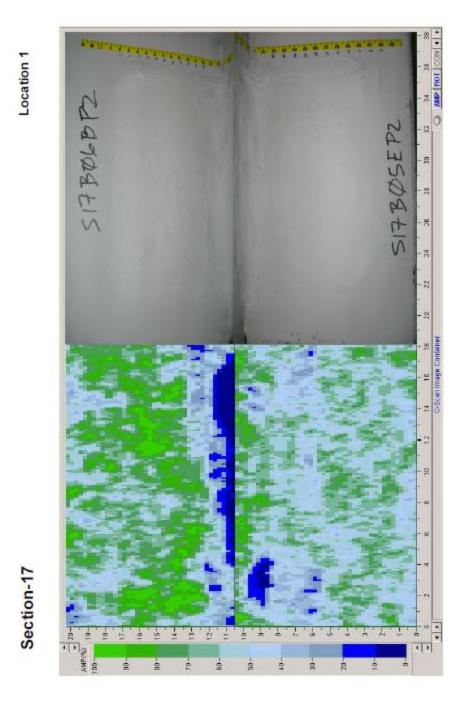




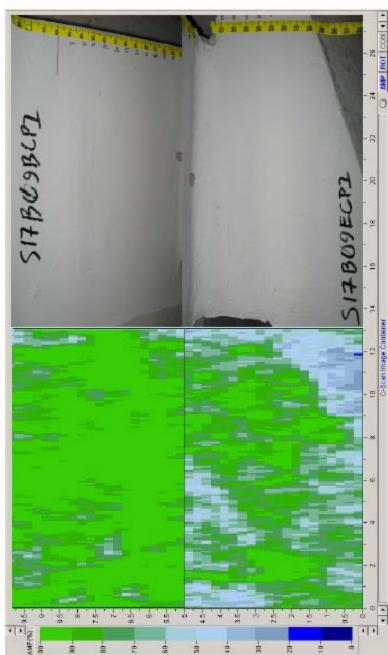


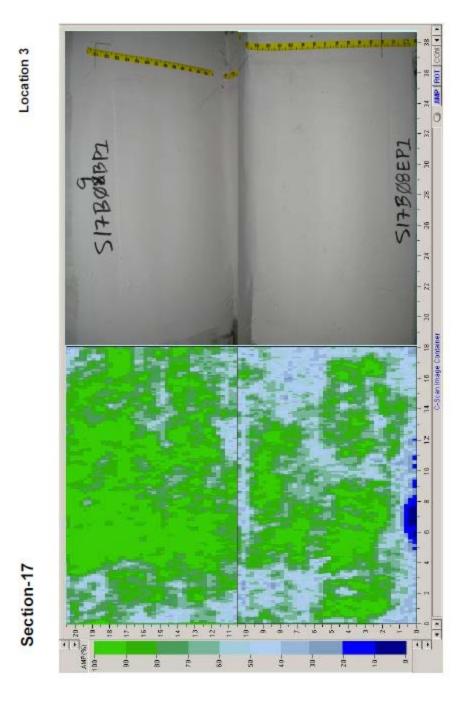


Section-16

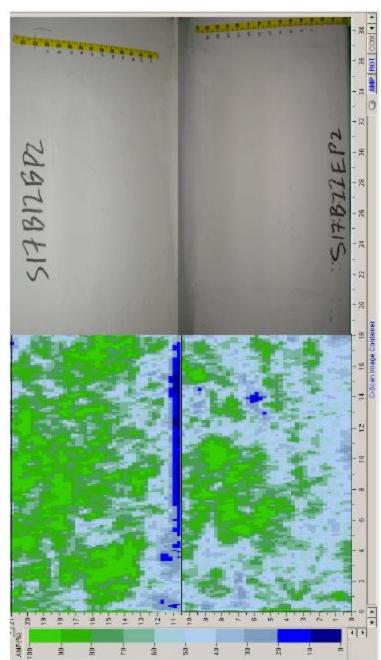


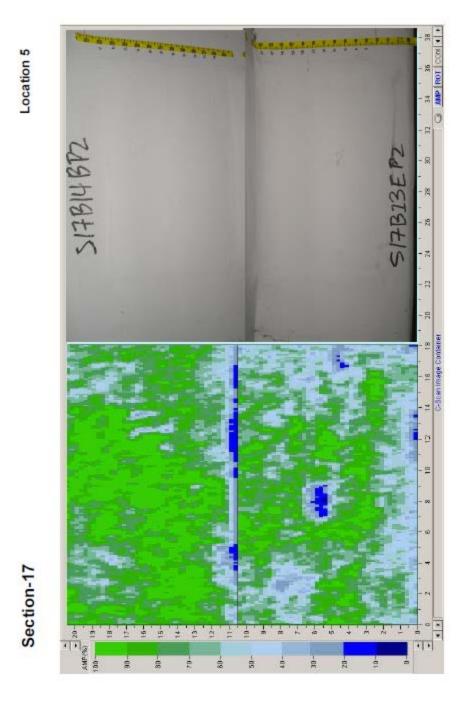


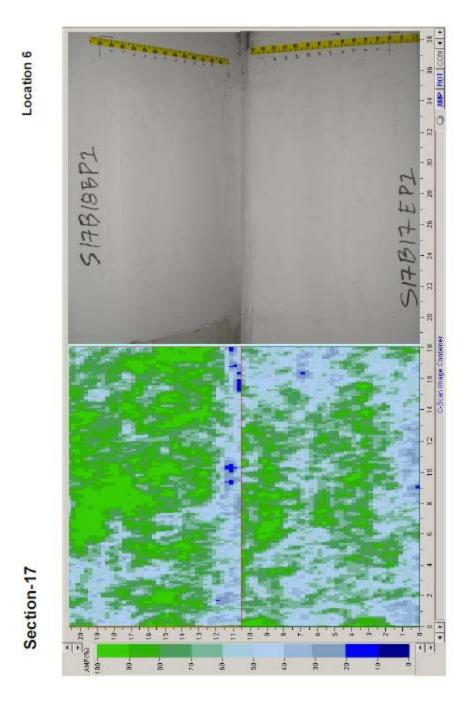


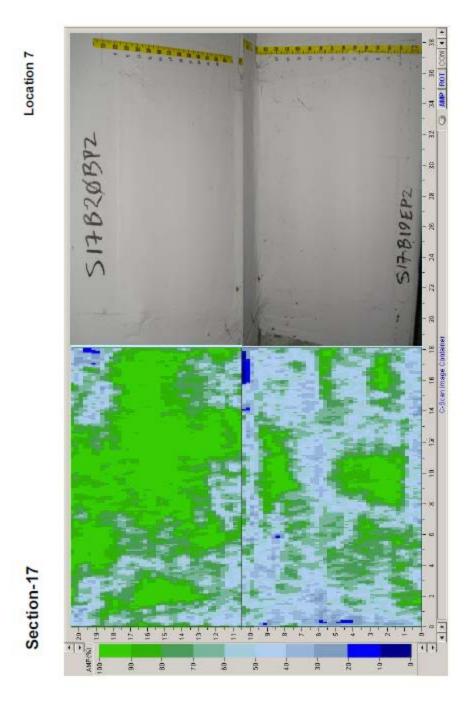


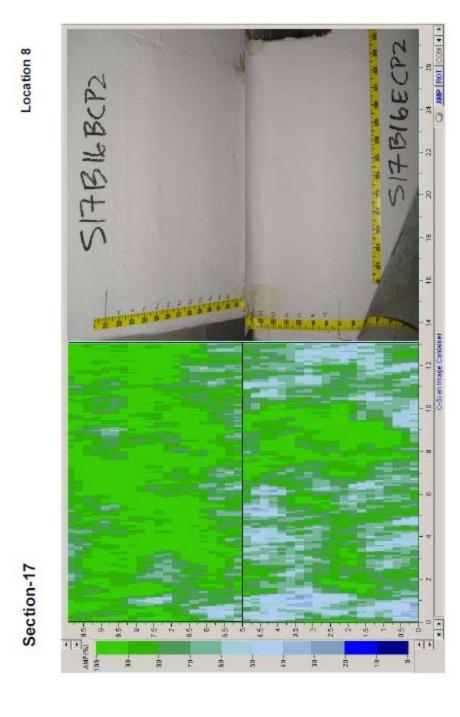


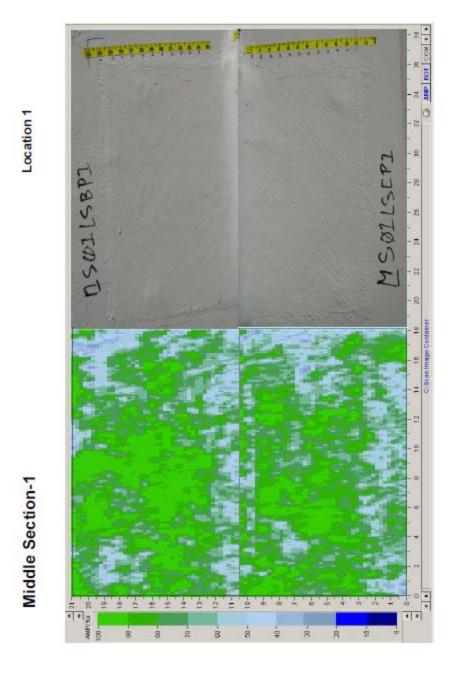




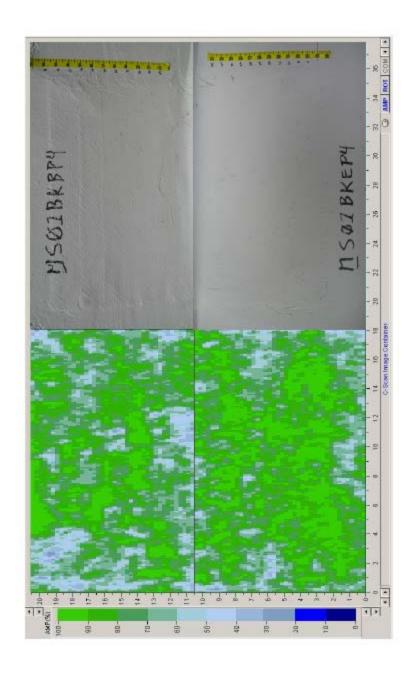


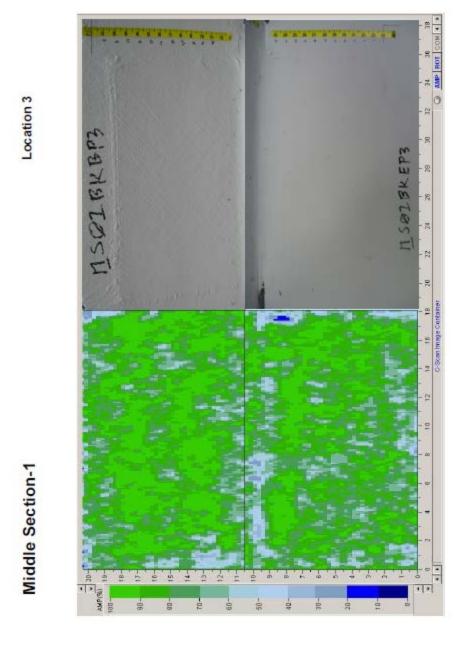


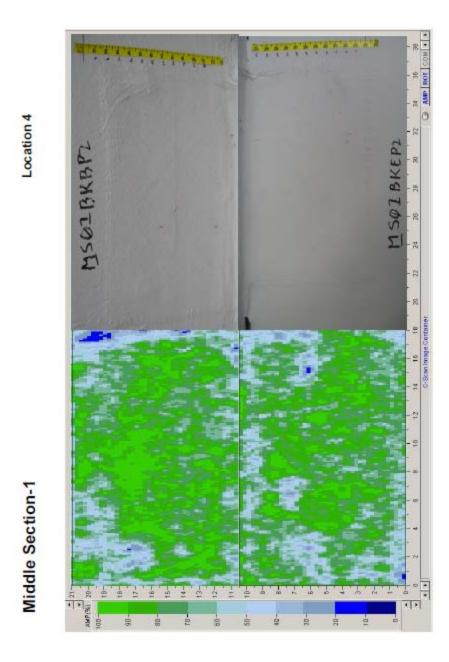


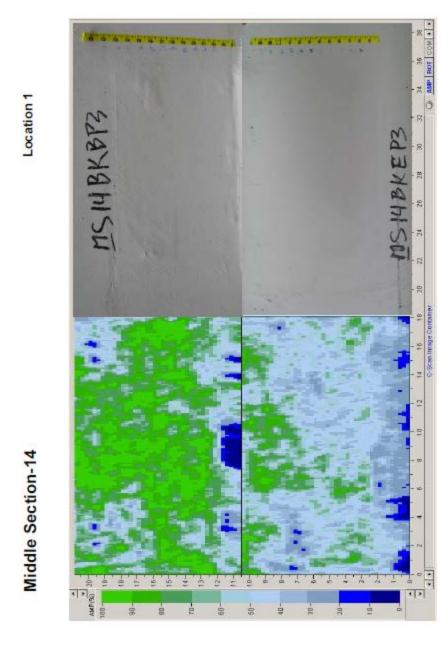


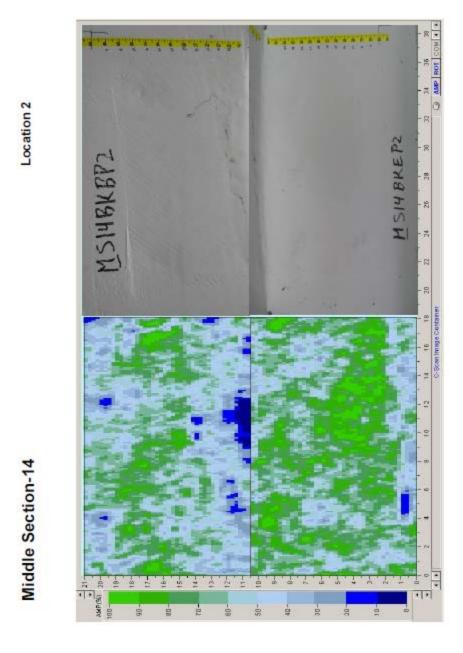


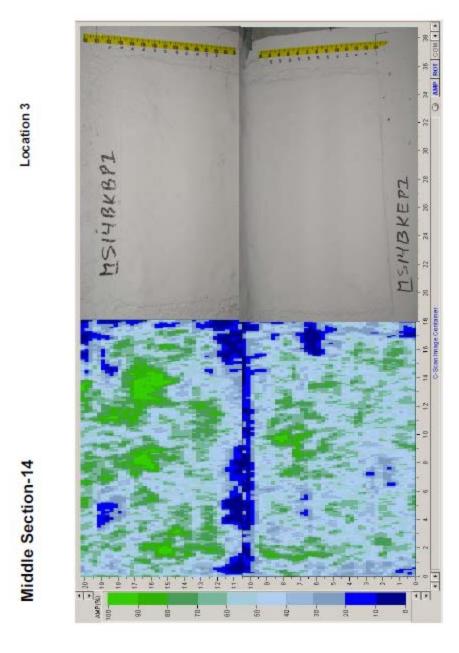




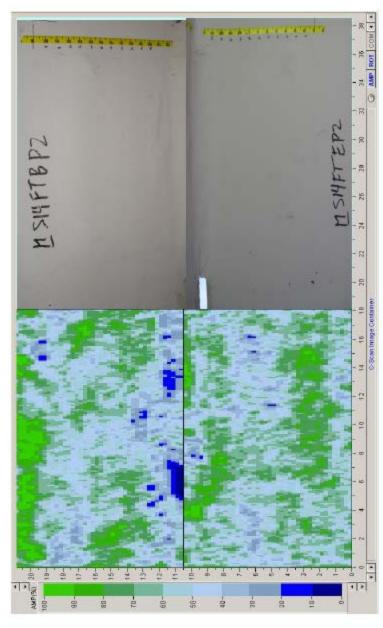






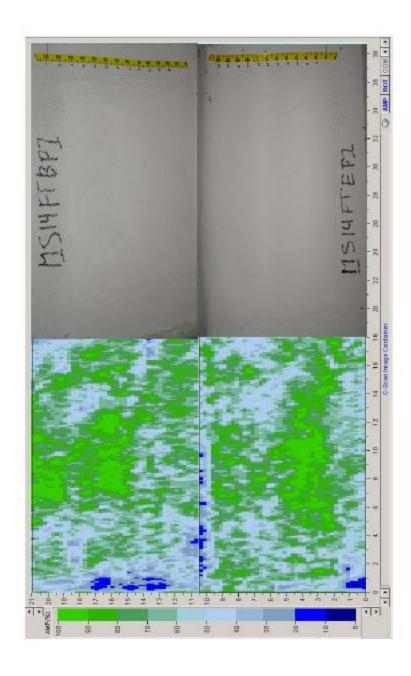


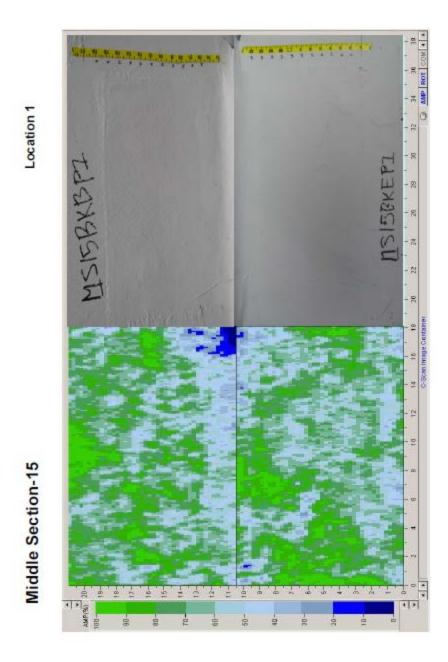


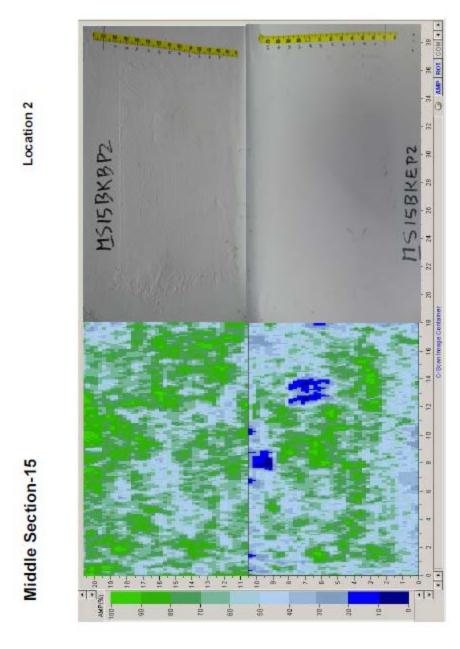


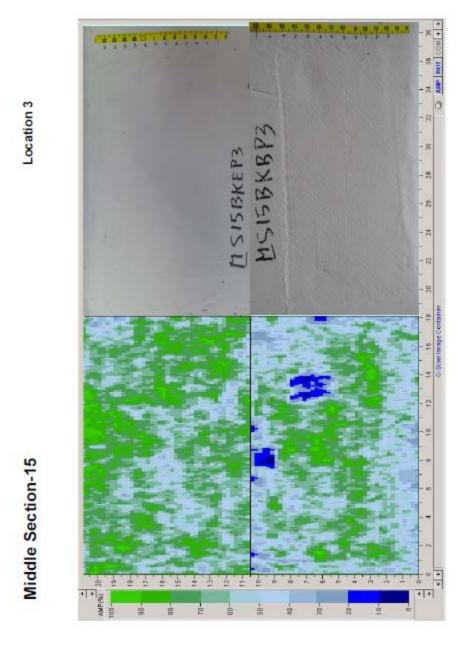


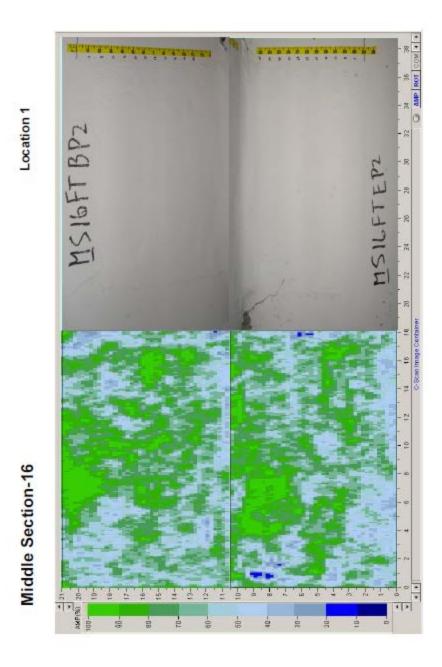
Location 5

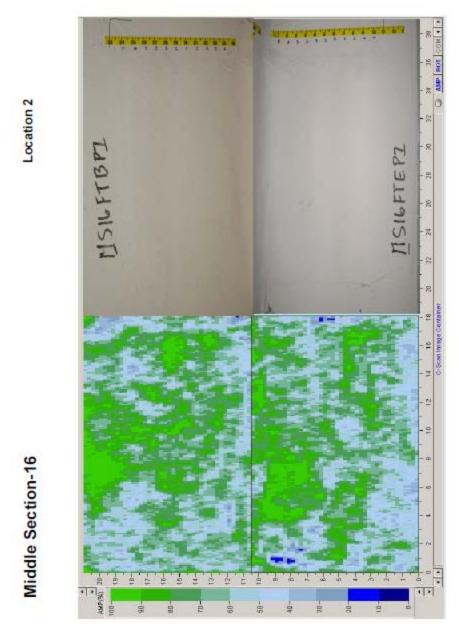


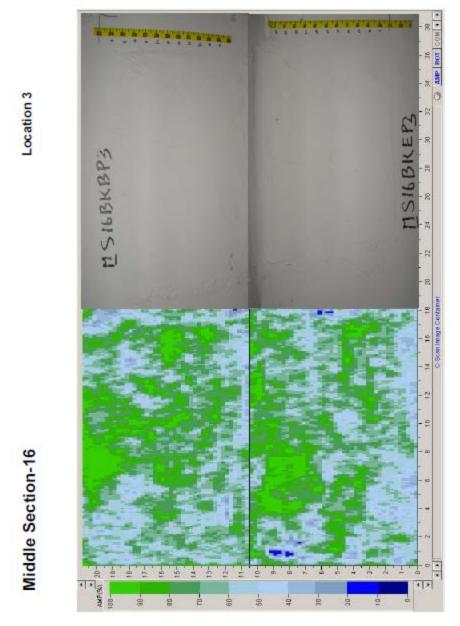


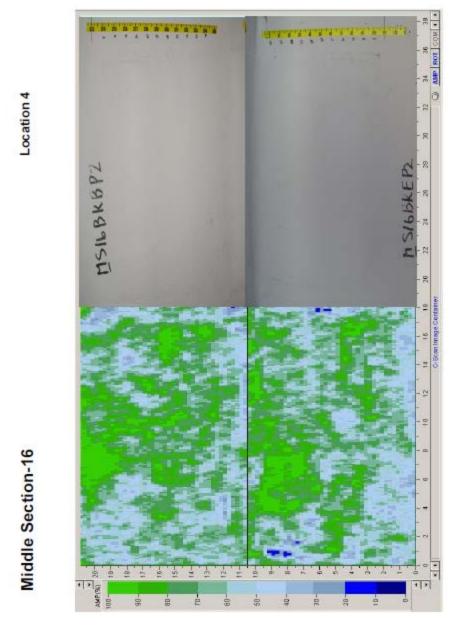




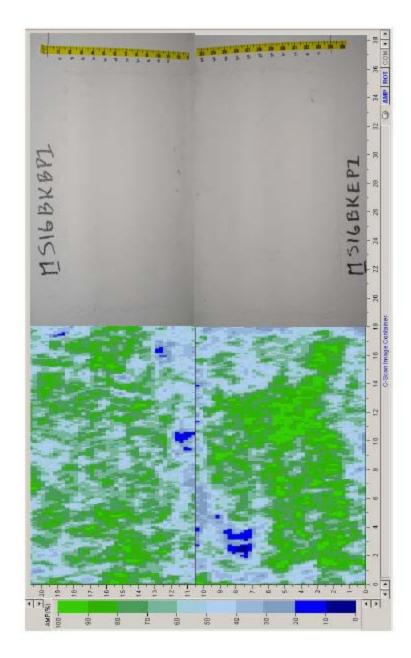






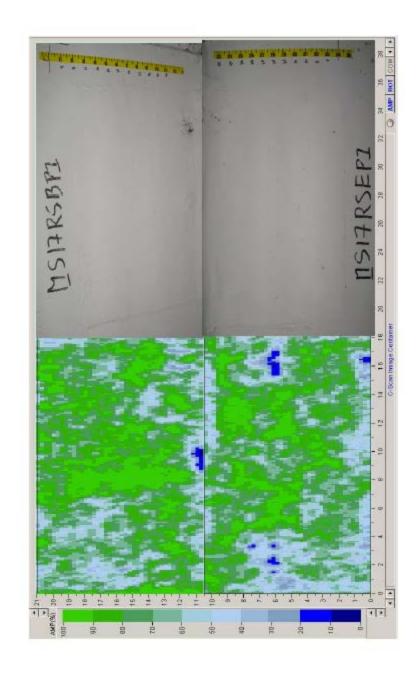


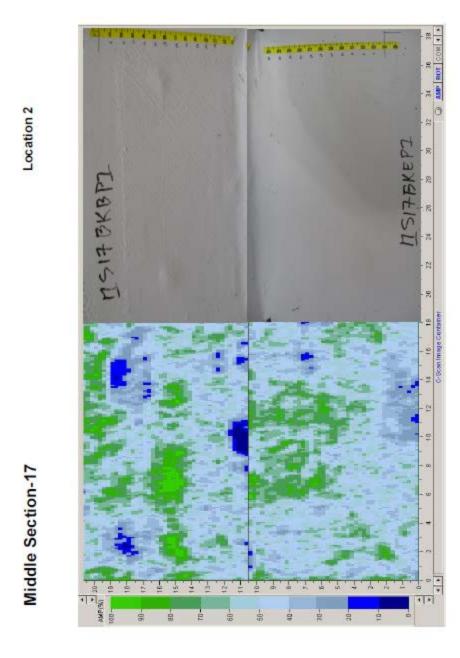


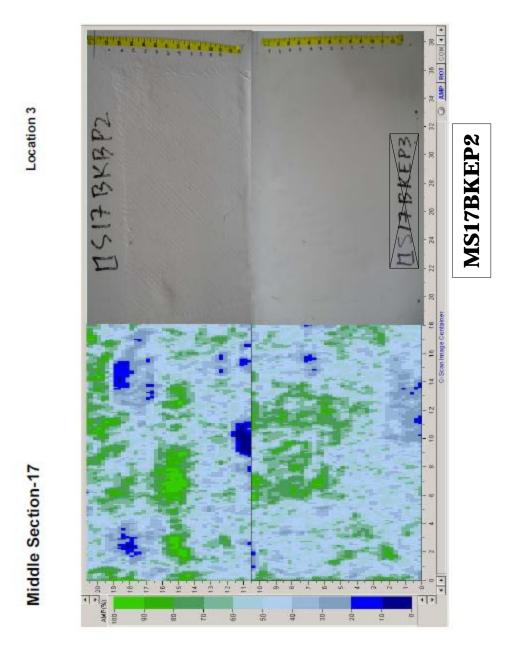


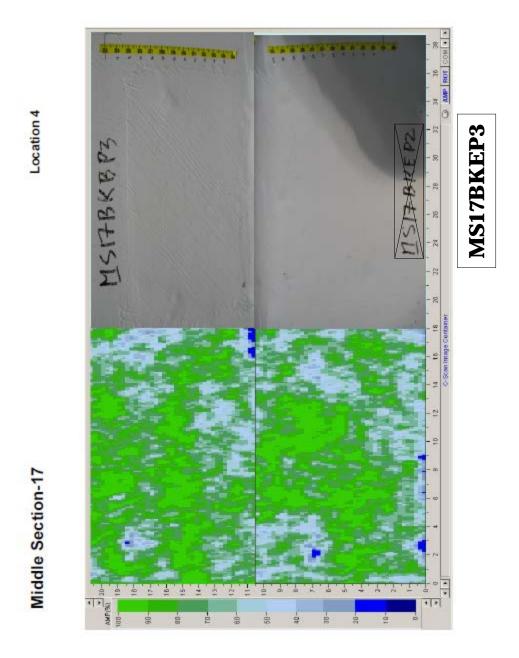


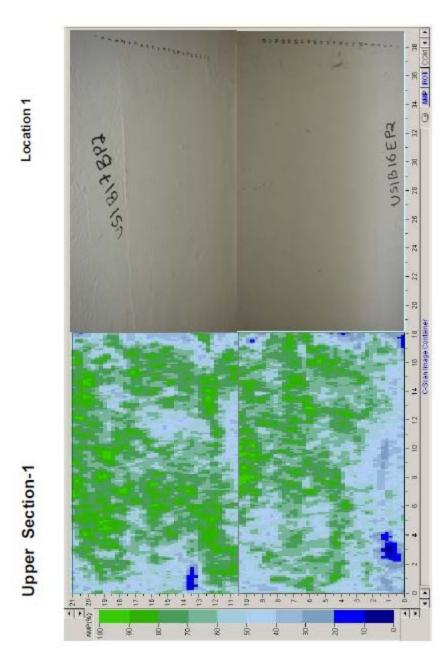
Location 1

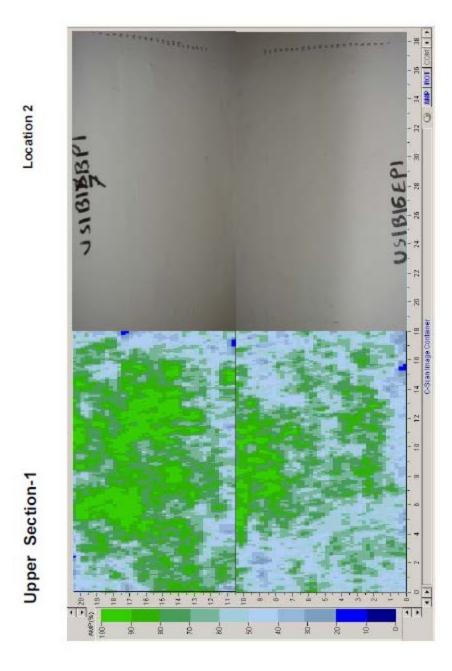


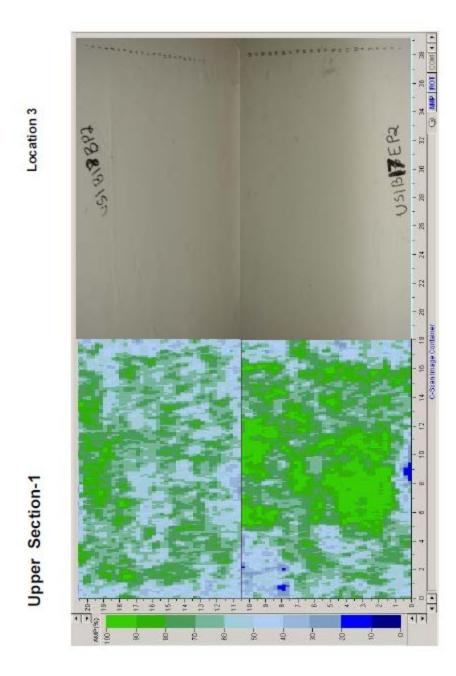


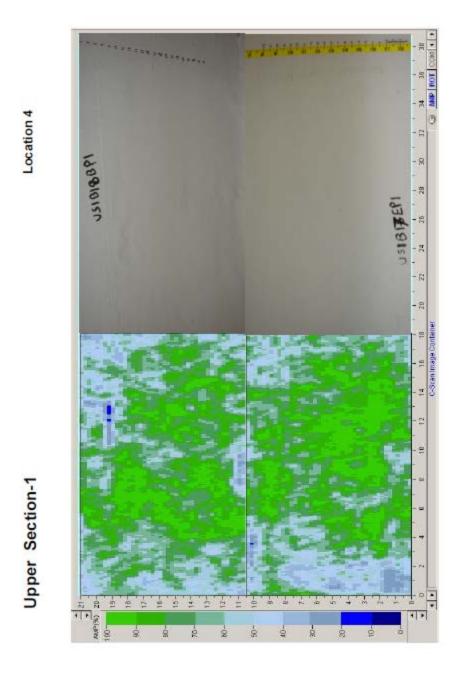


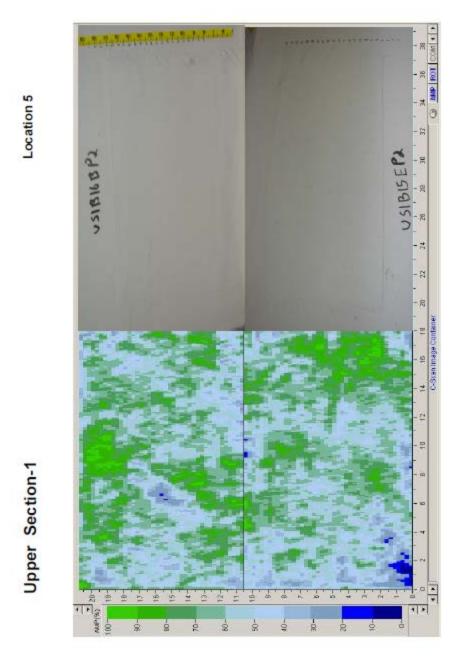


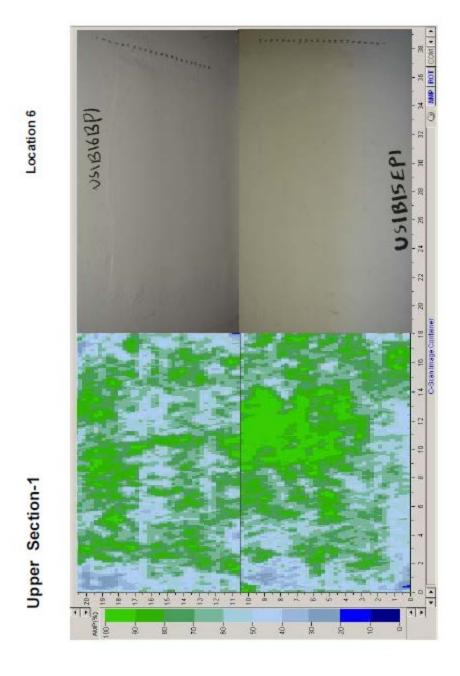


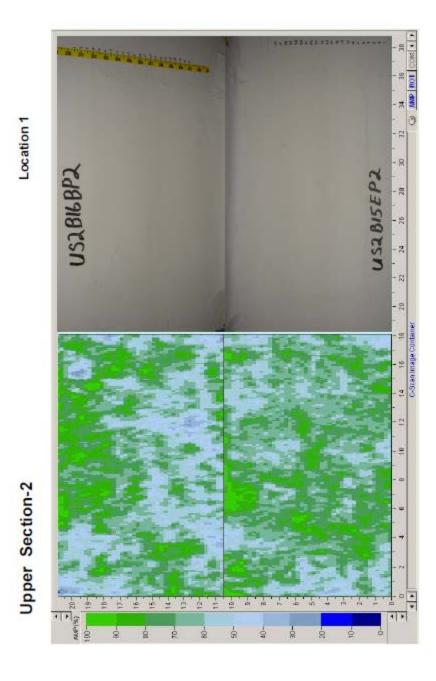


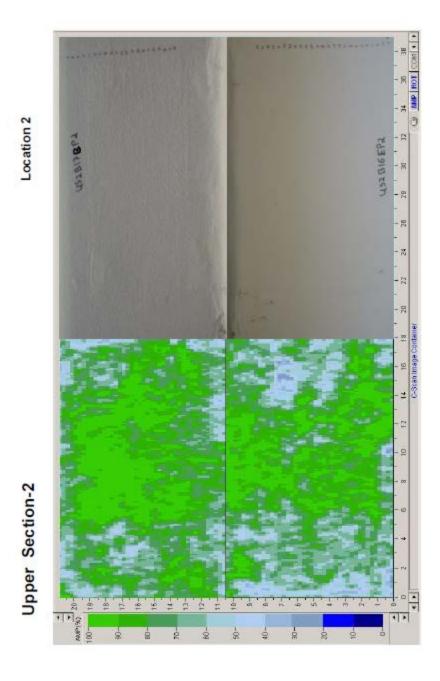


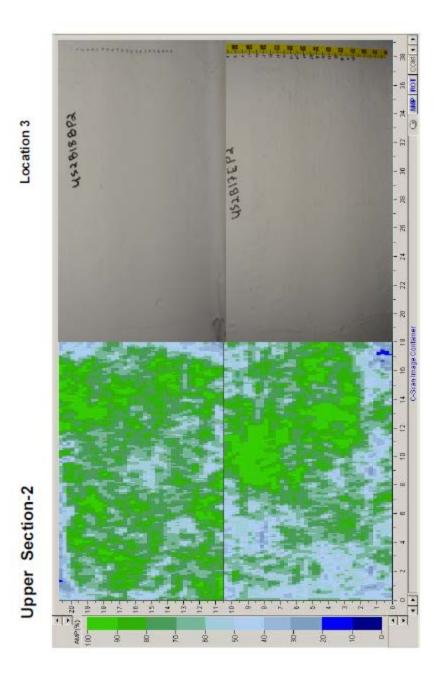


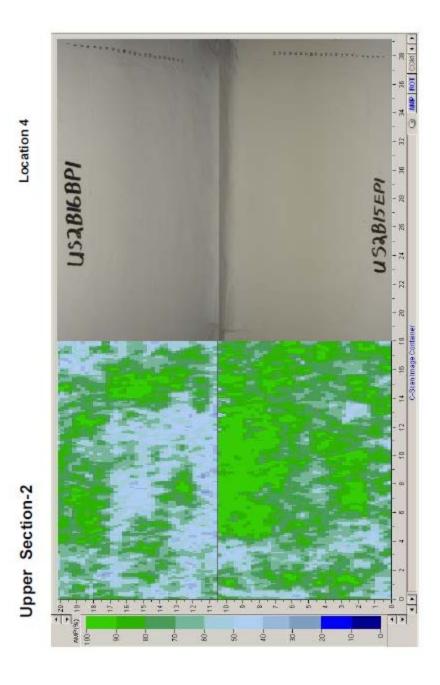


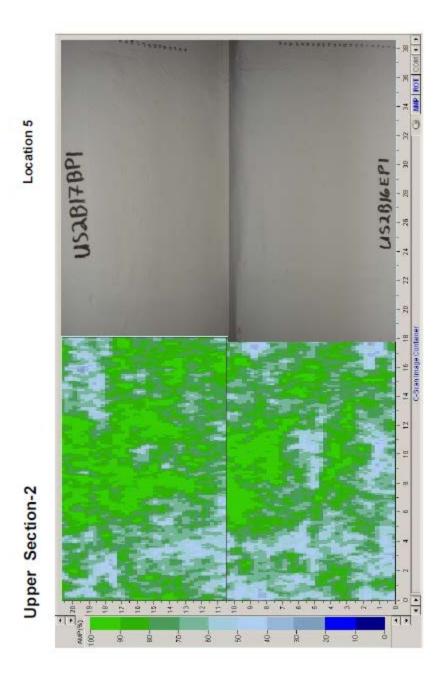


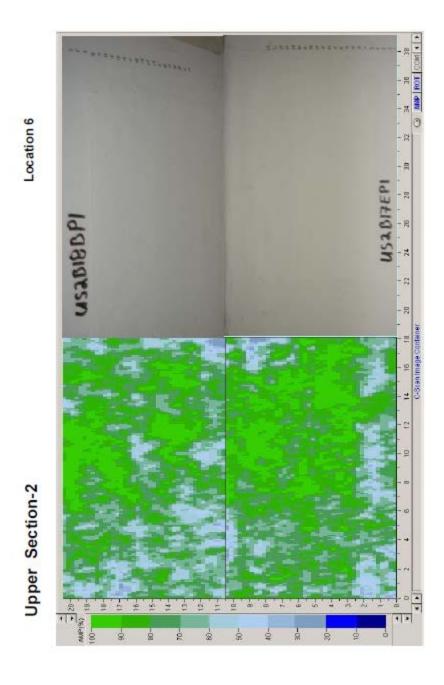


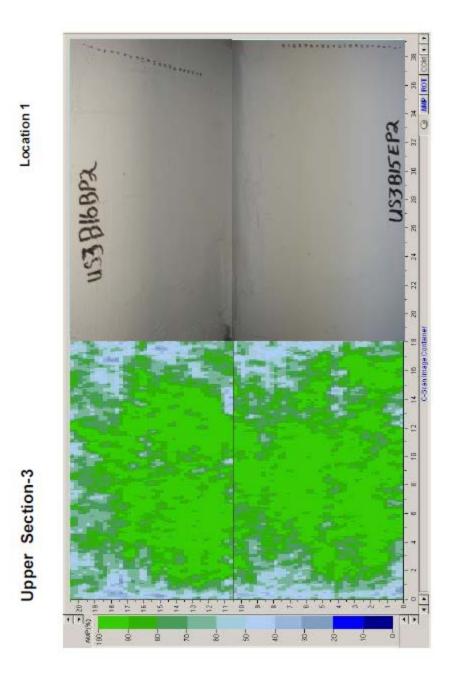


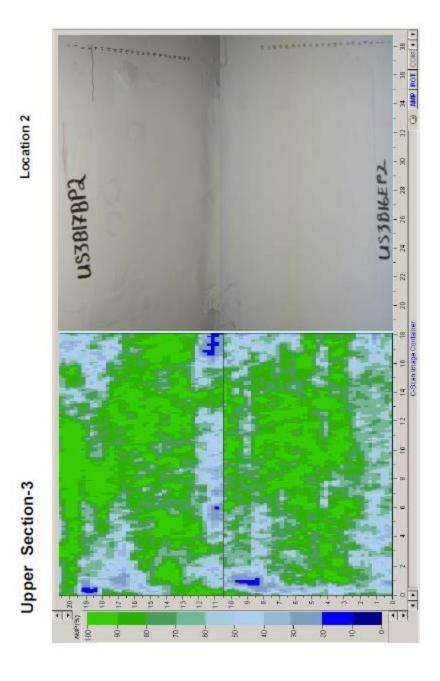


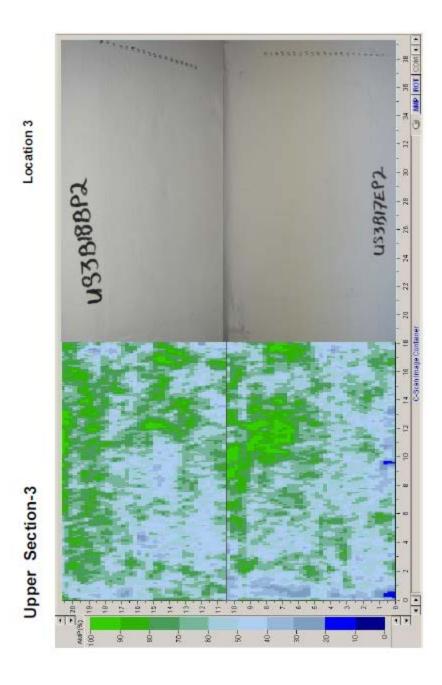


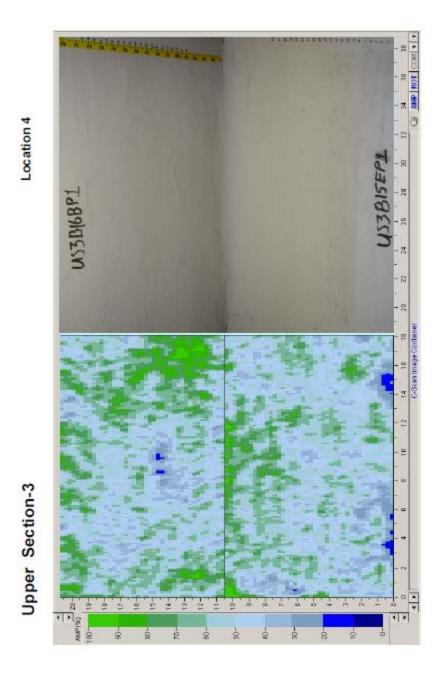


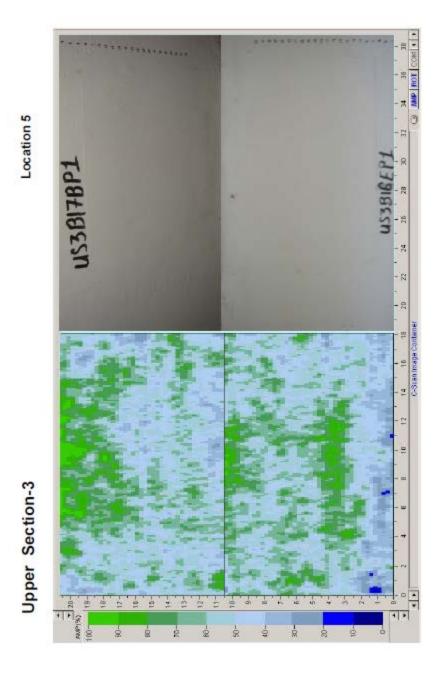


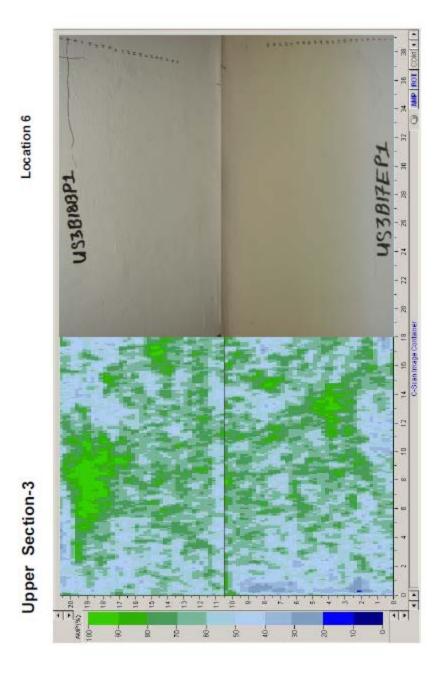


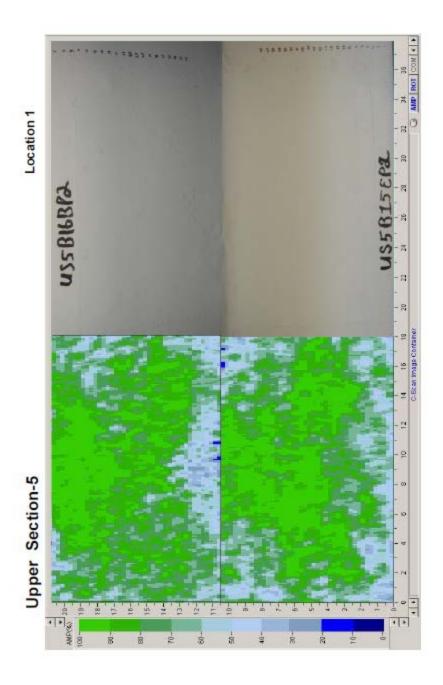


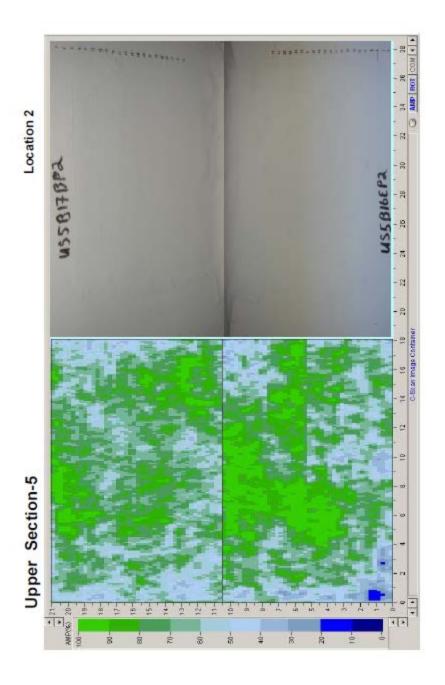


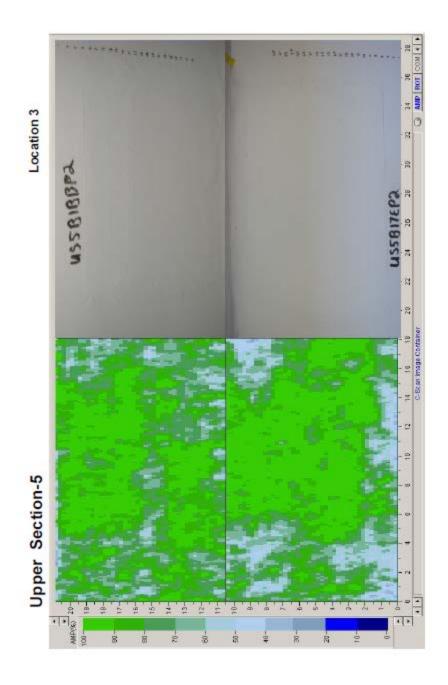


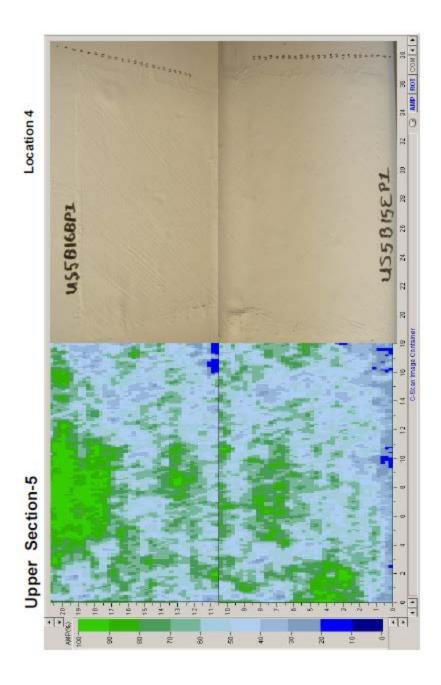


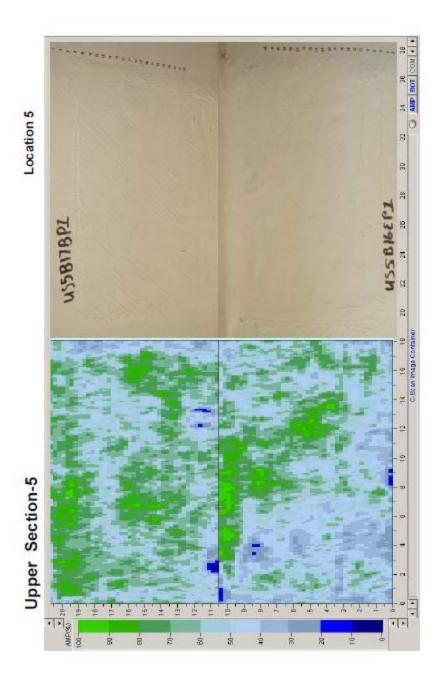


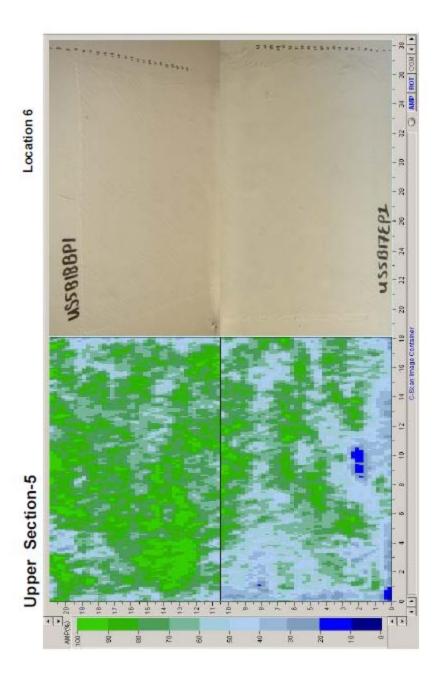


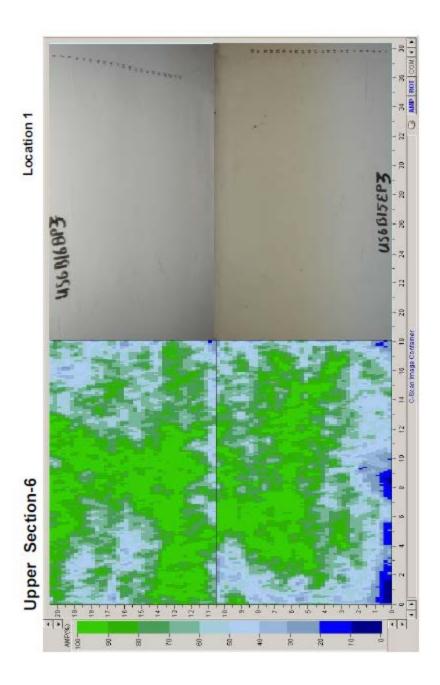


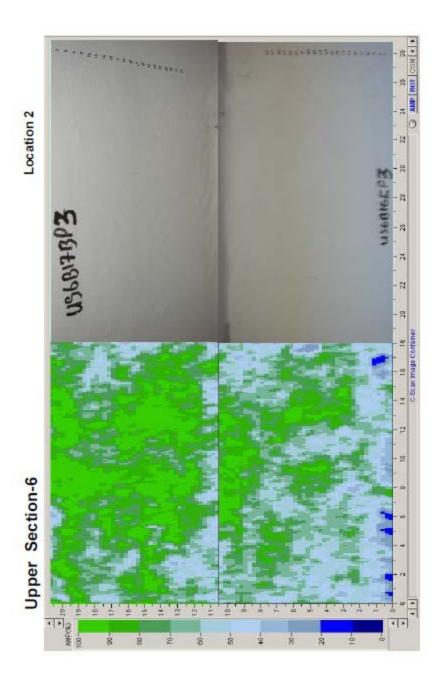


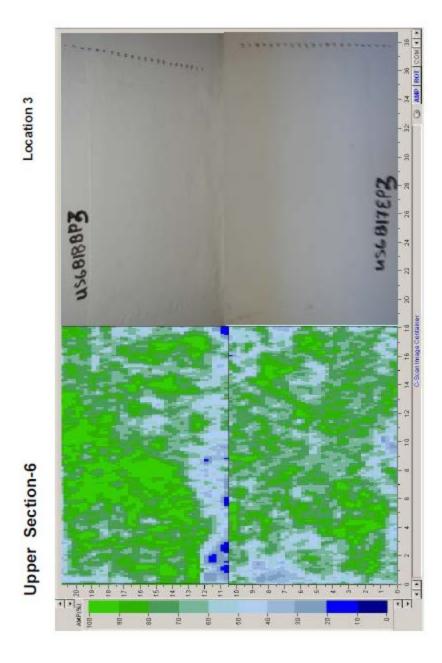


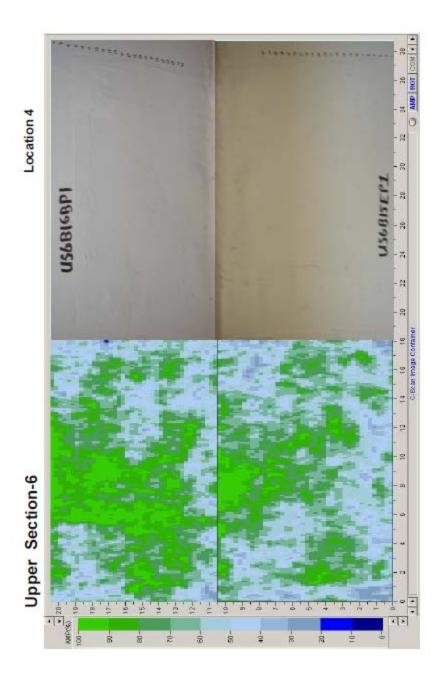


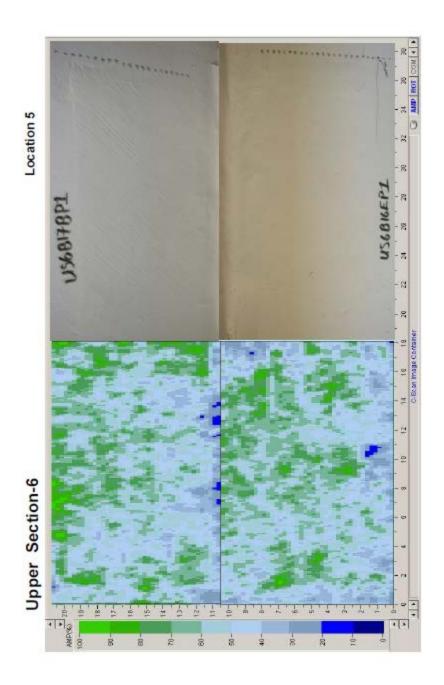


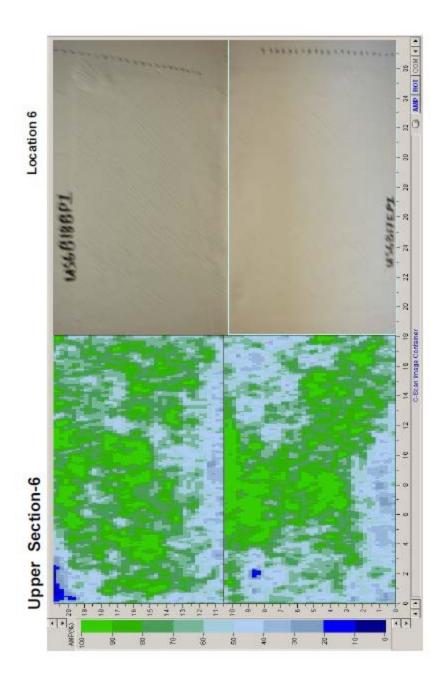


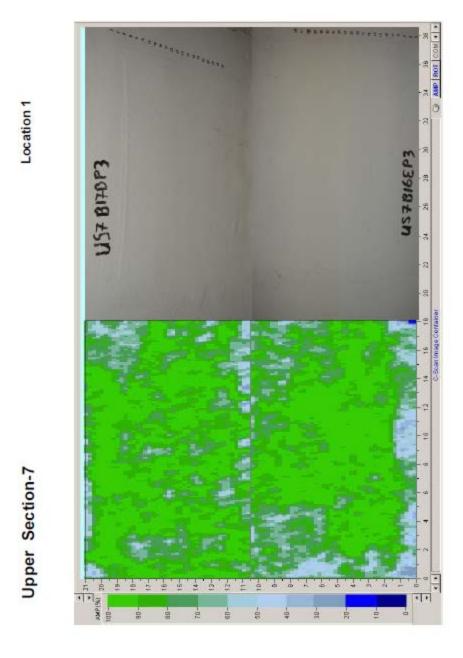


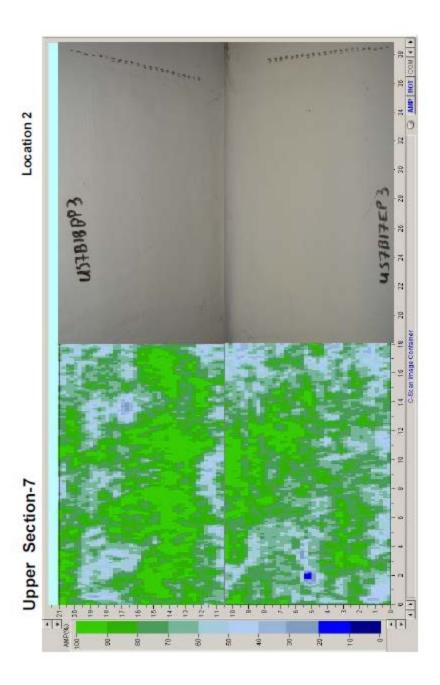


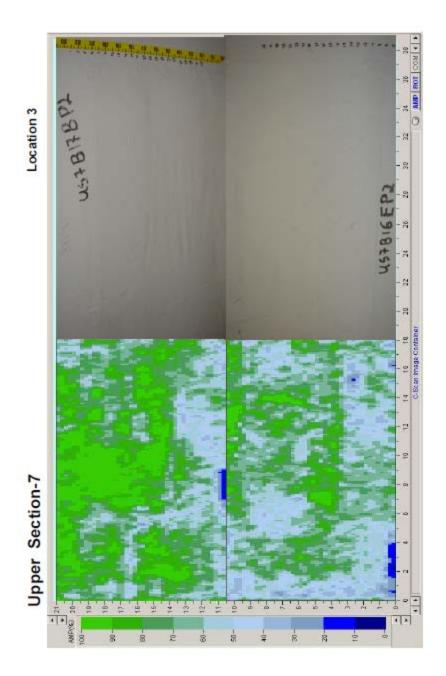


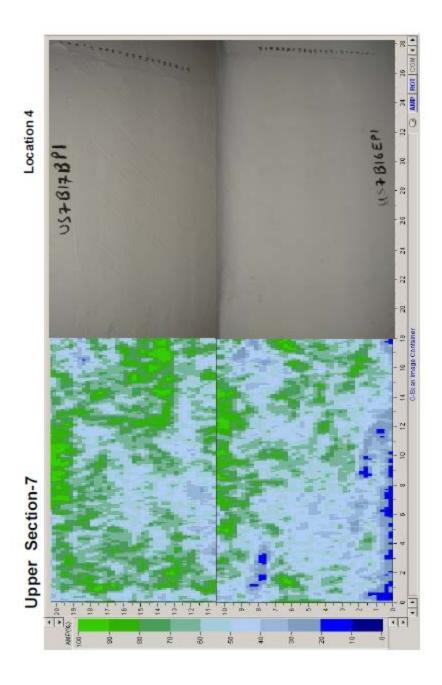


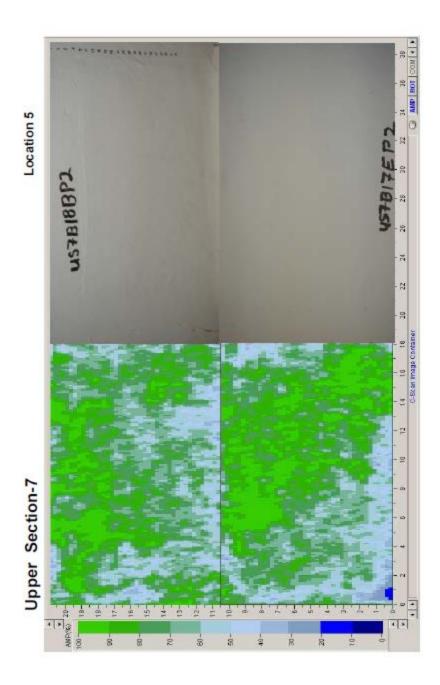


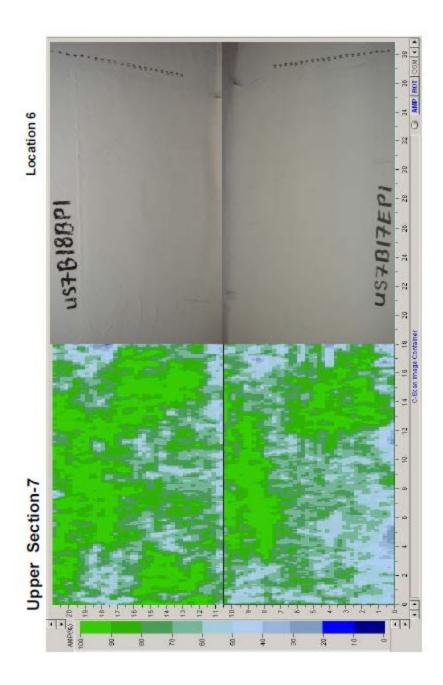


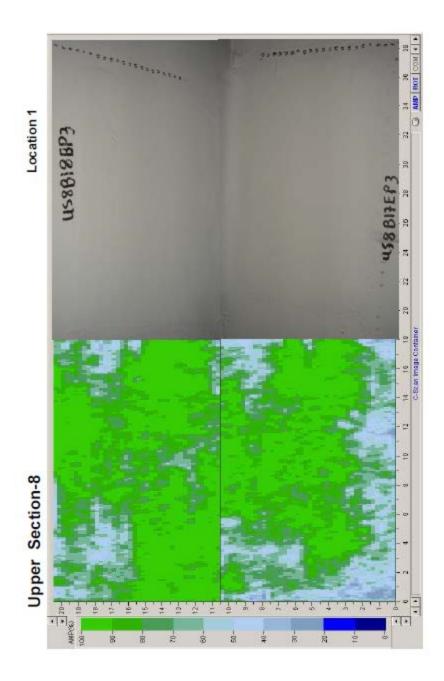


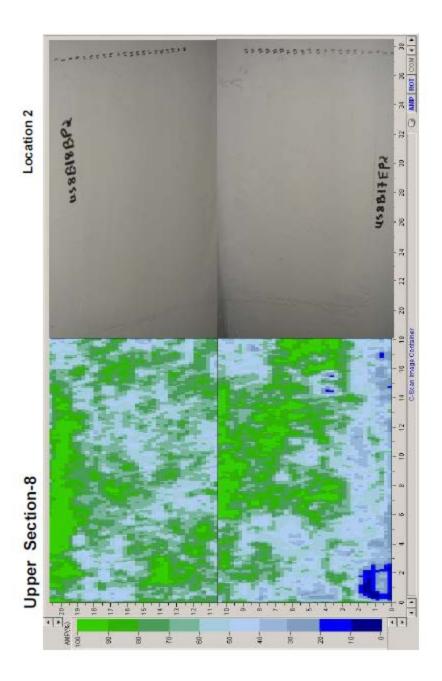


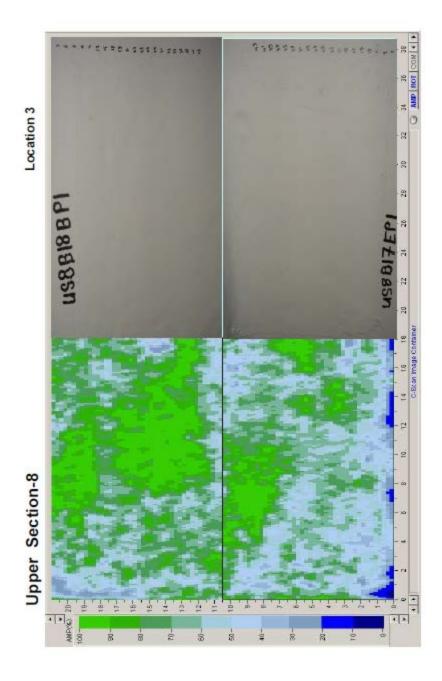


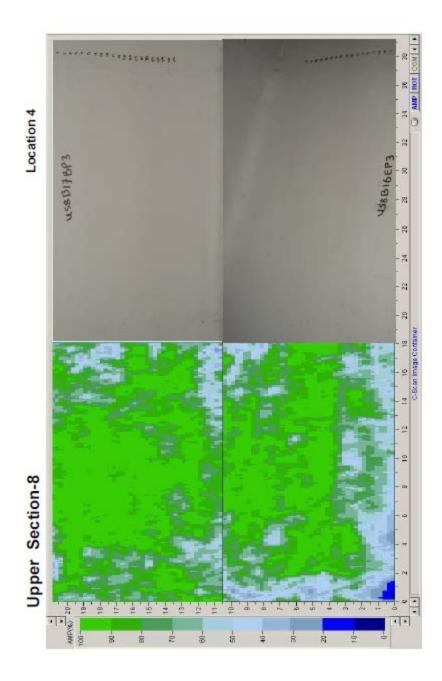


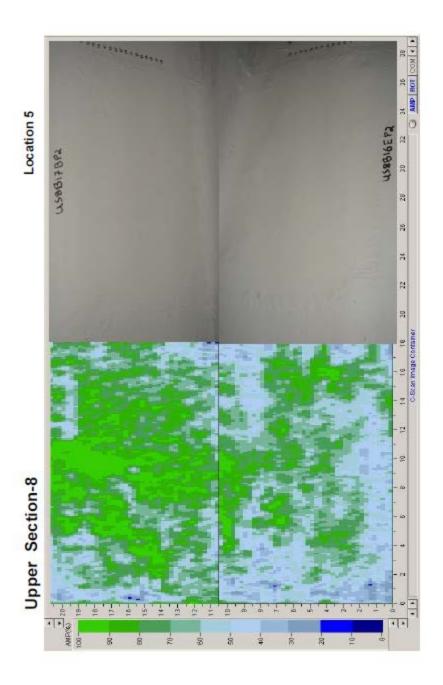


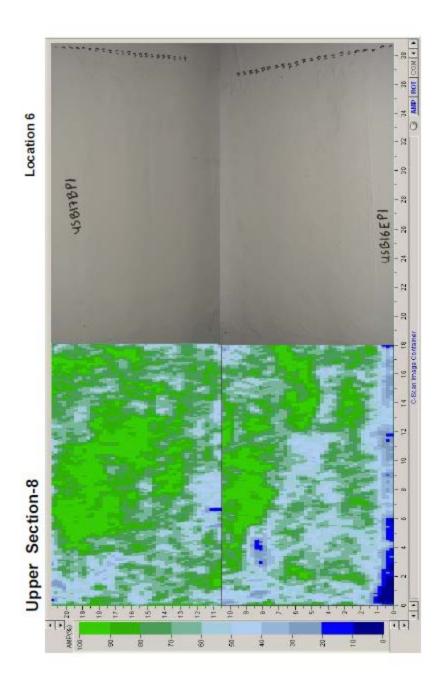


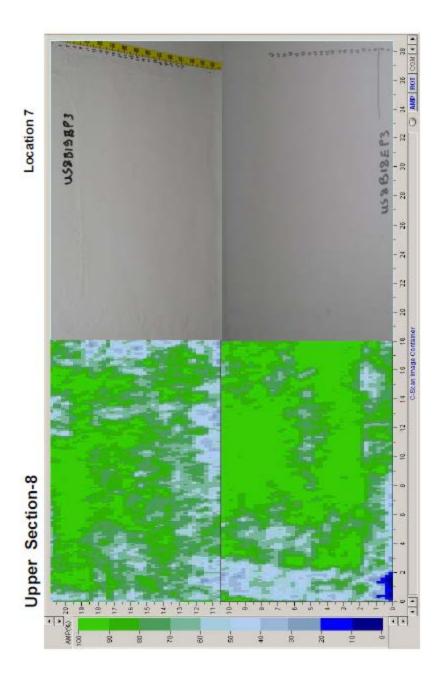


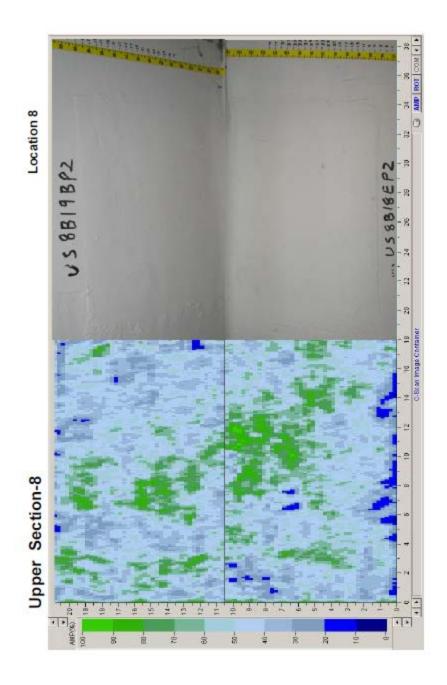


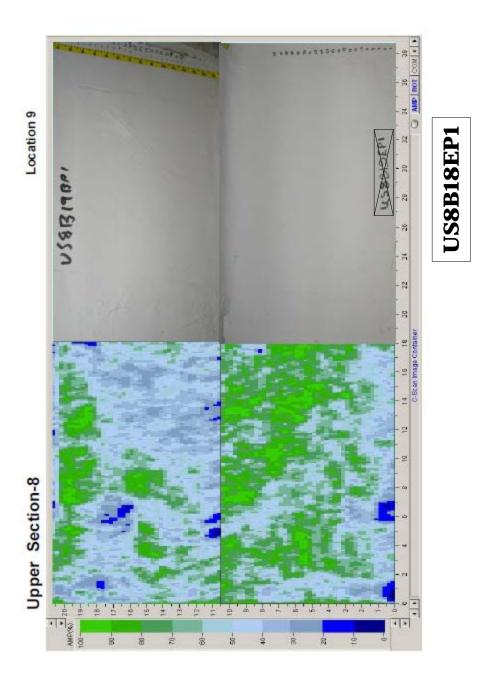


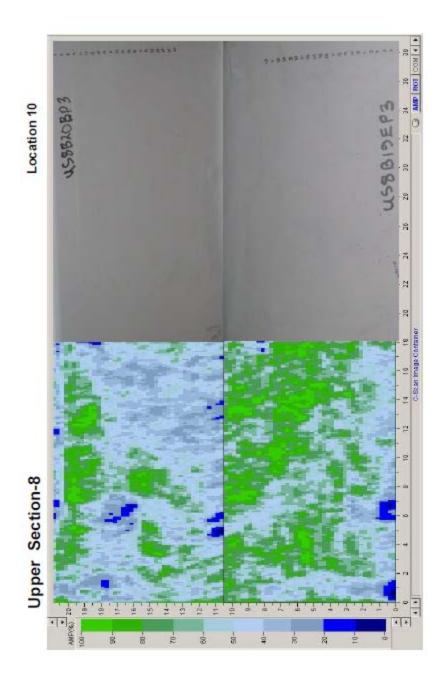


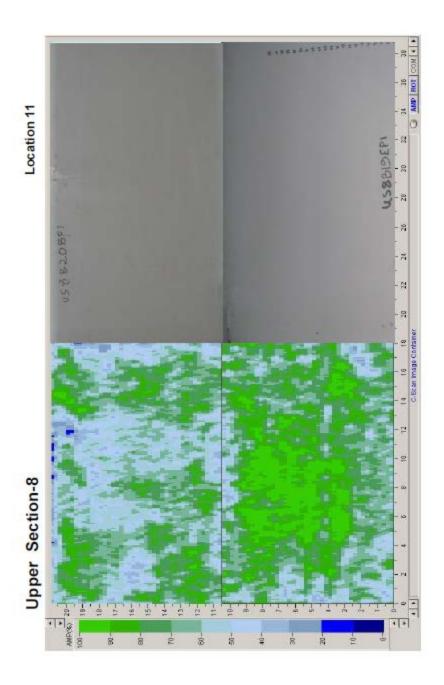


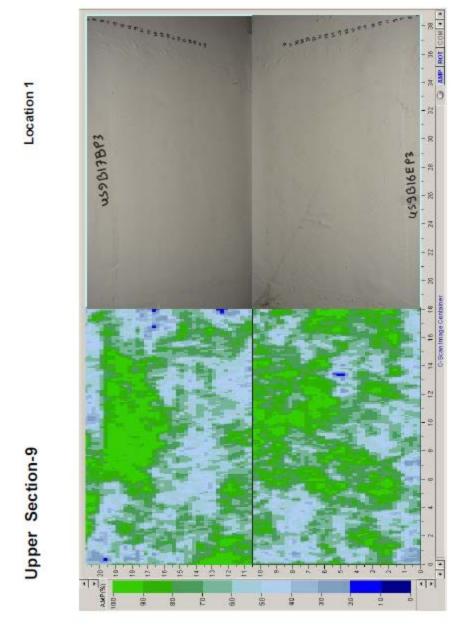


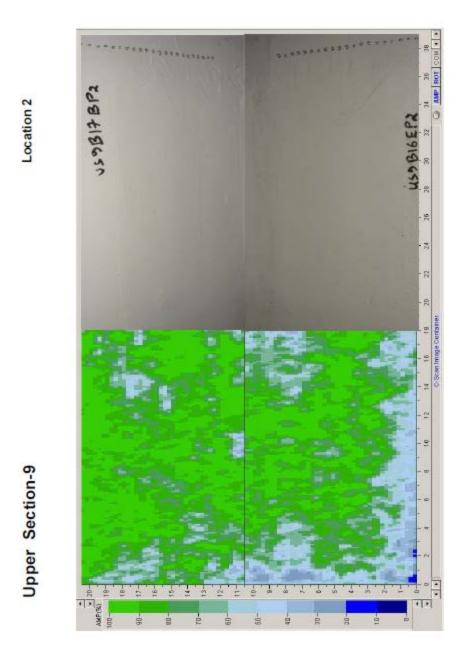


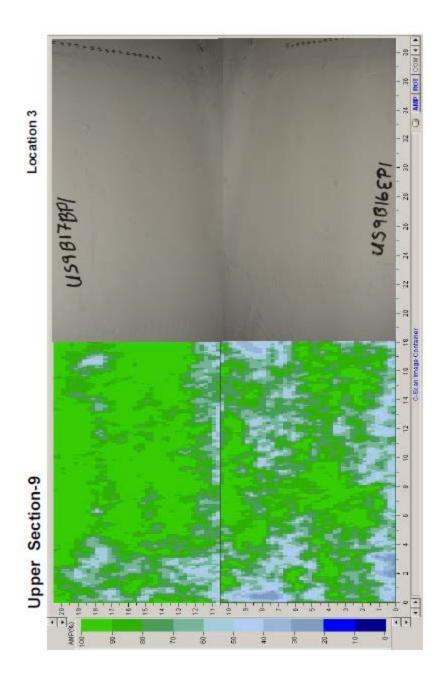


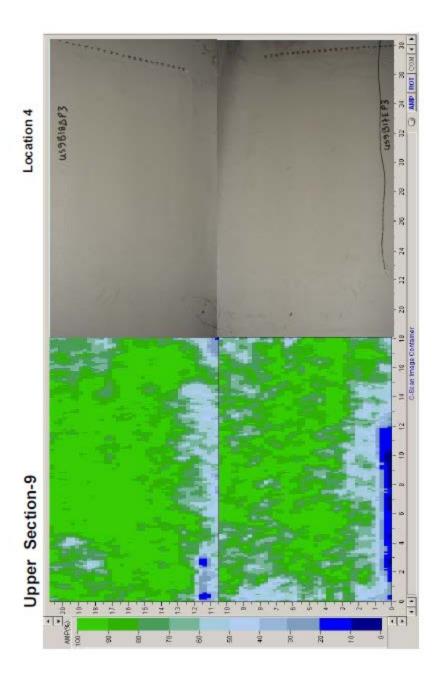


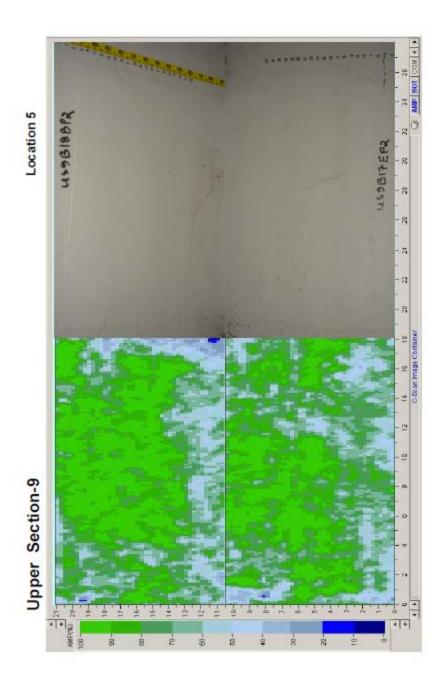


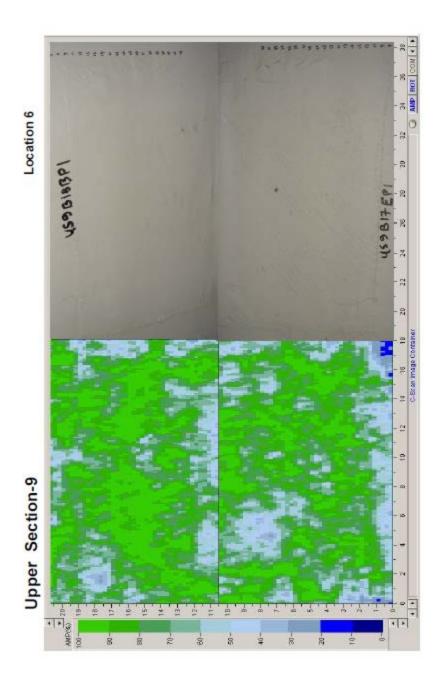


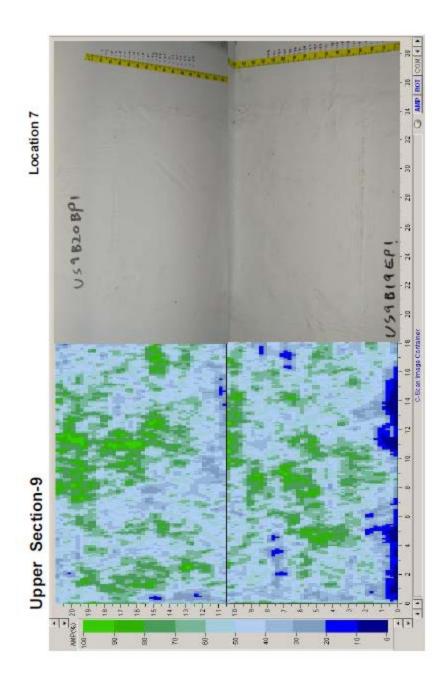


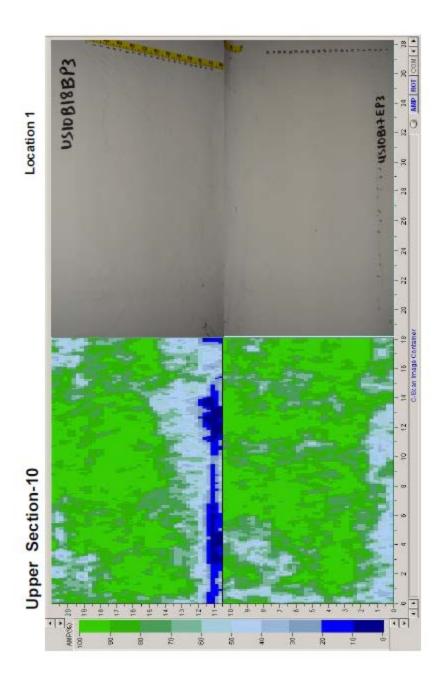


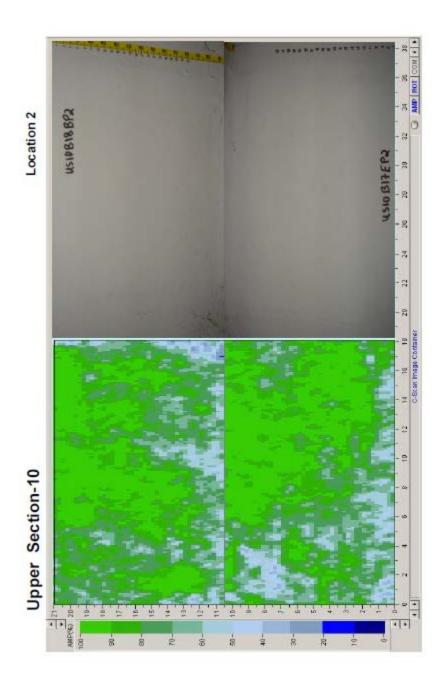


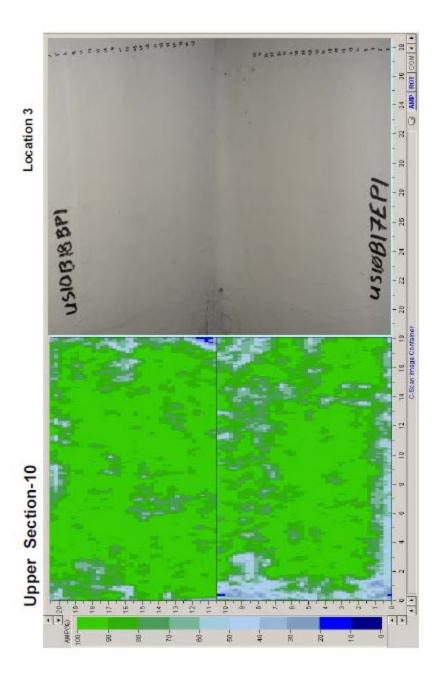


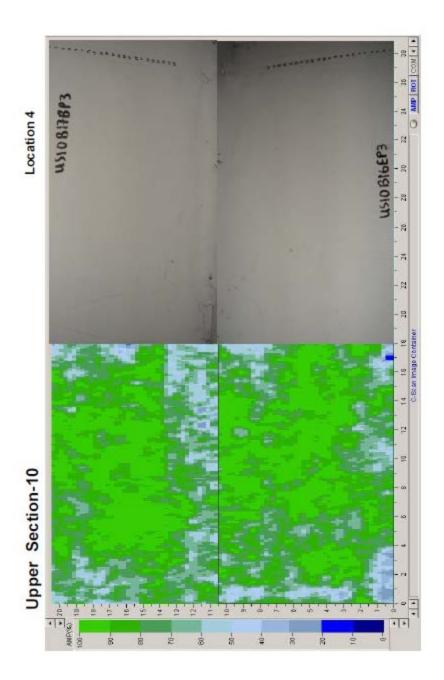


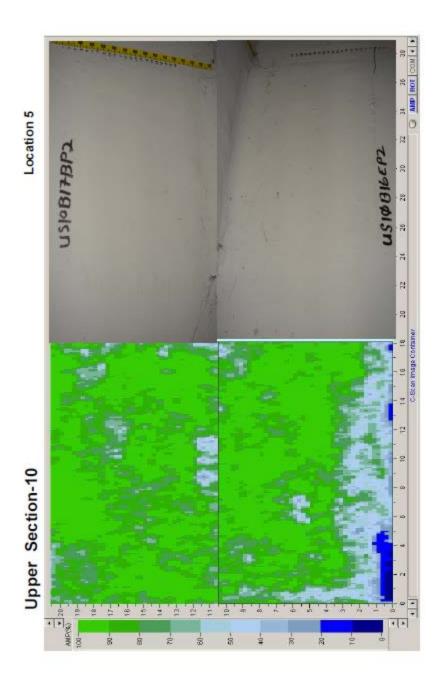


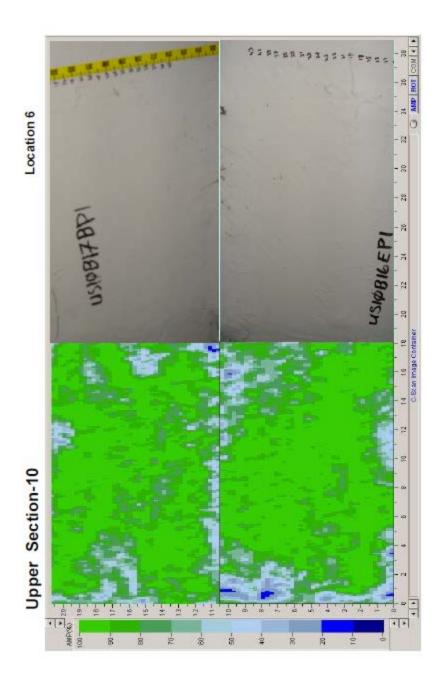


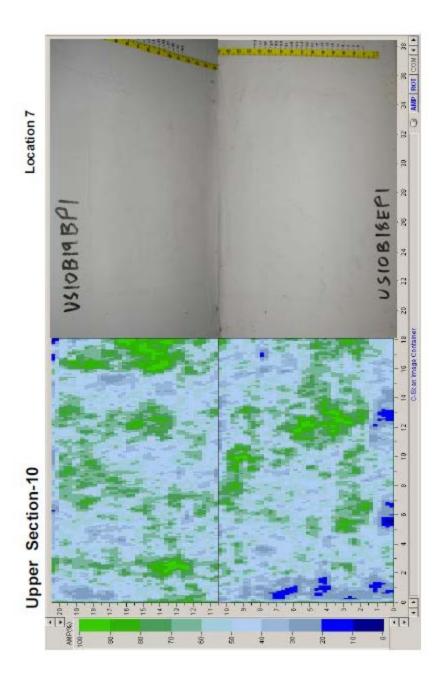


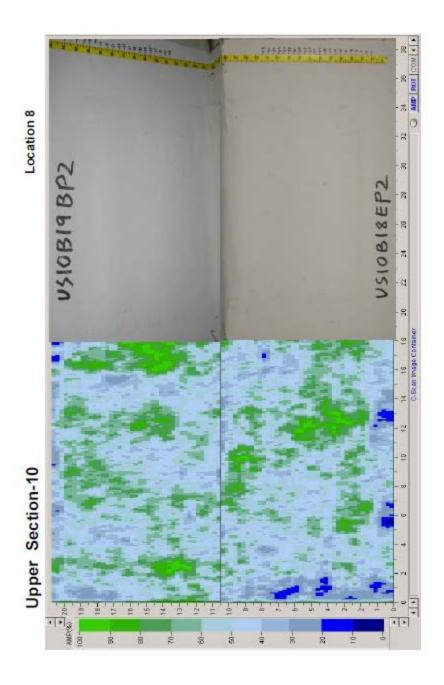


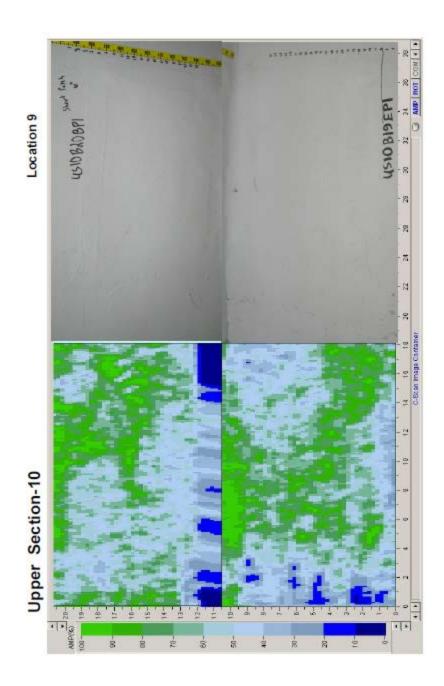


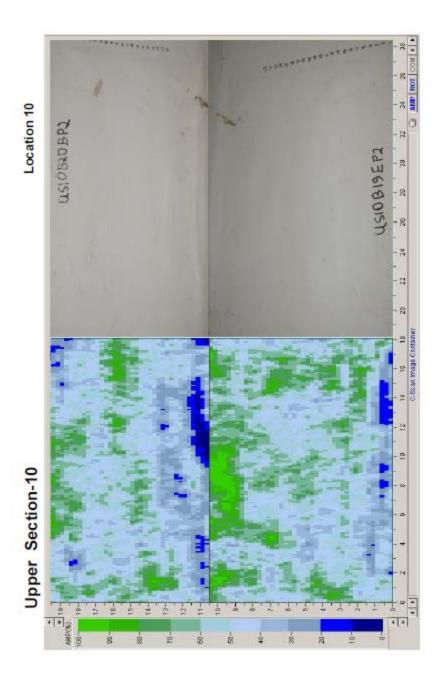


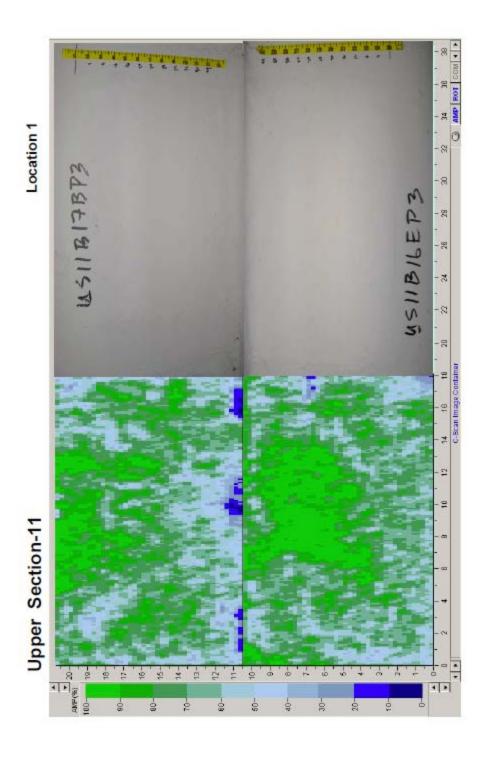


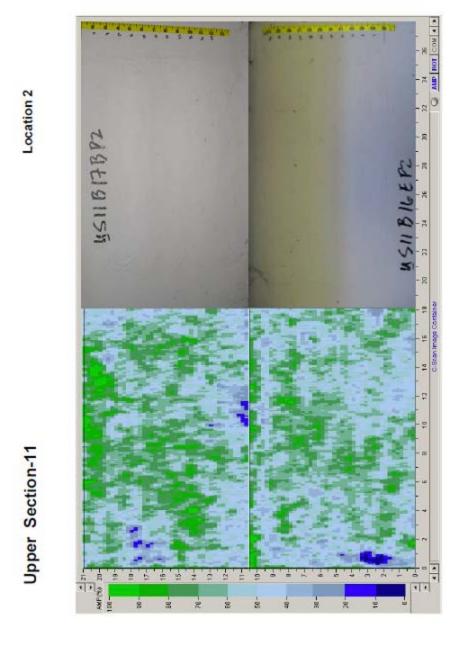


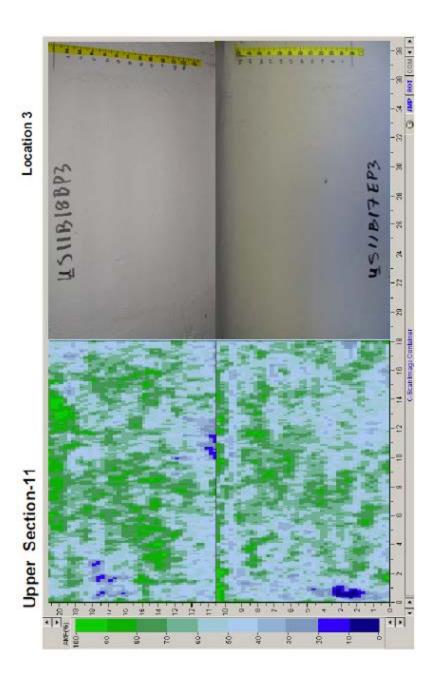


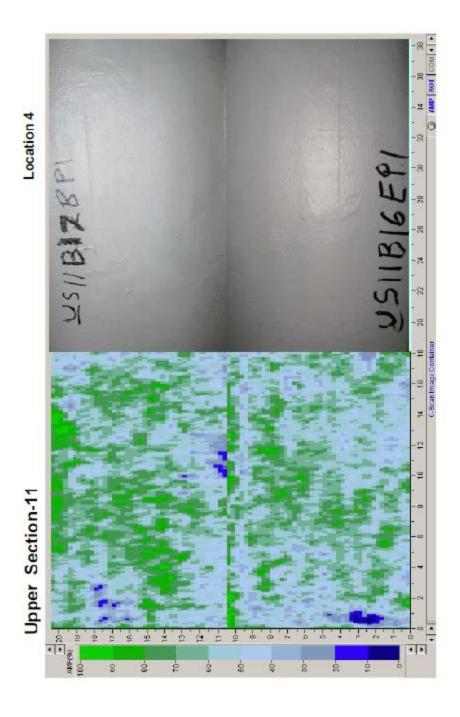


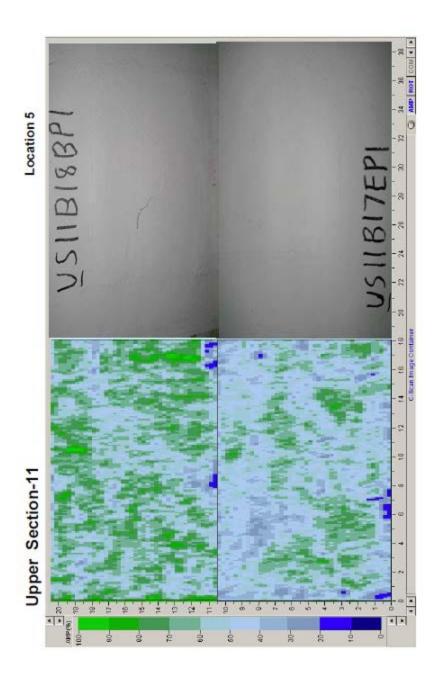


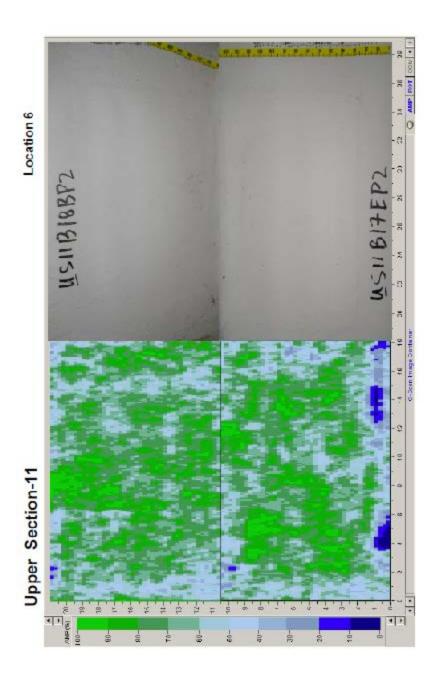


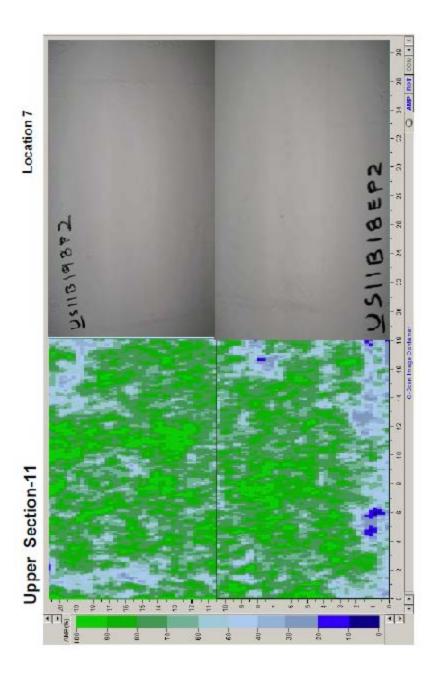


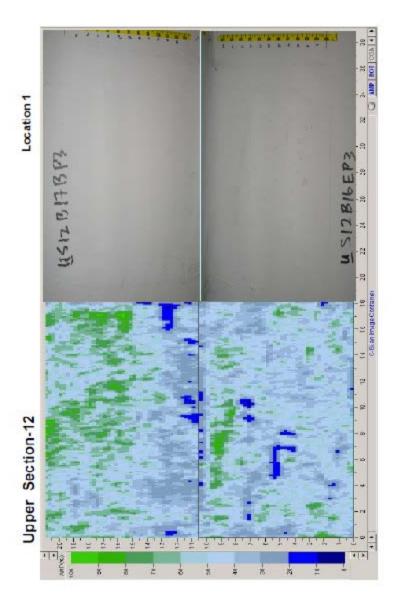


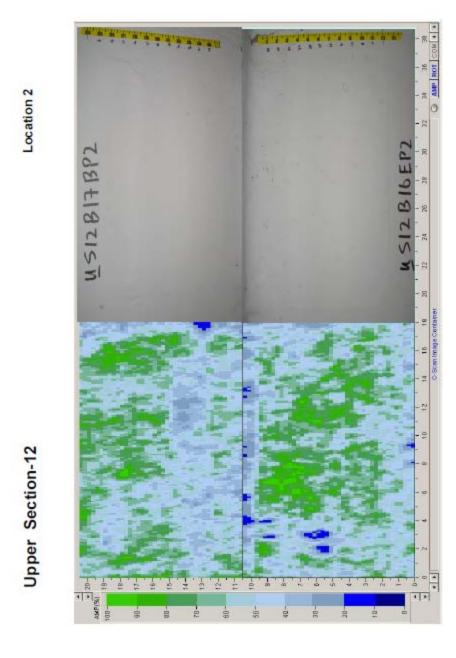


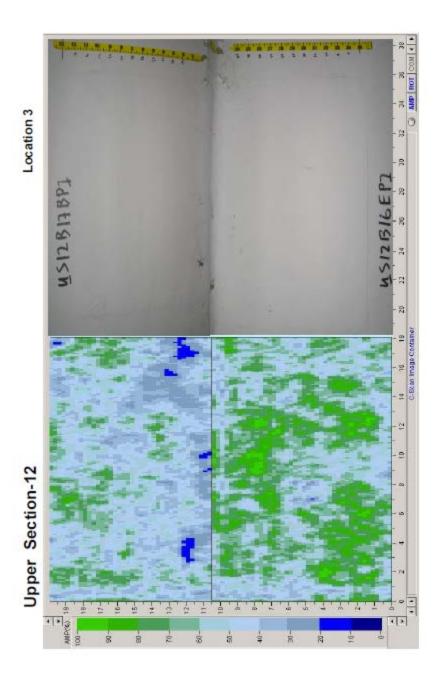


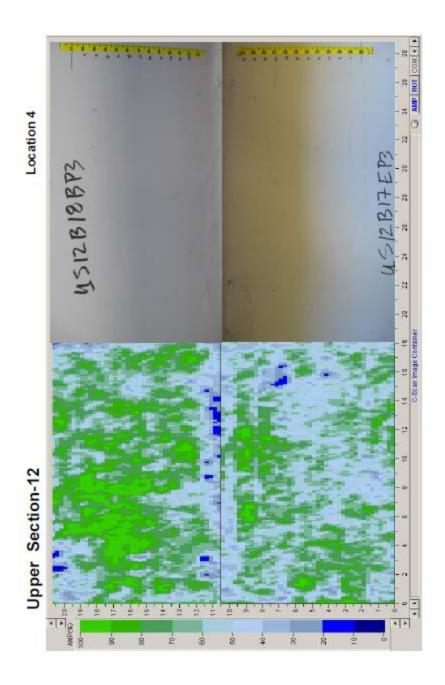


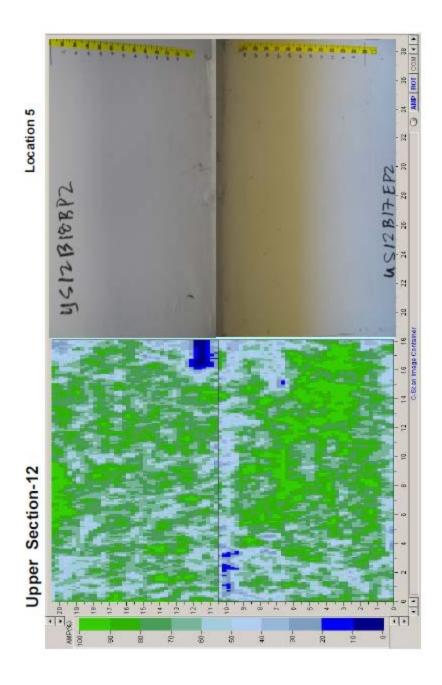


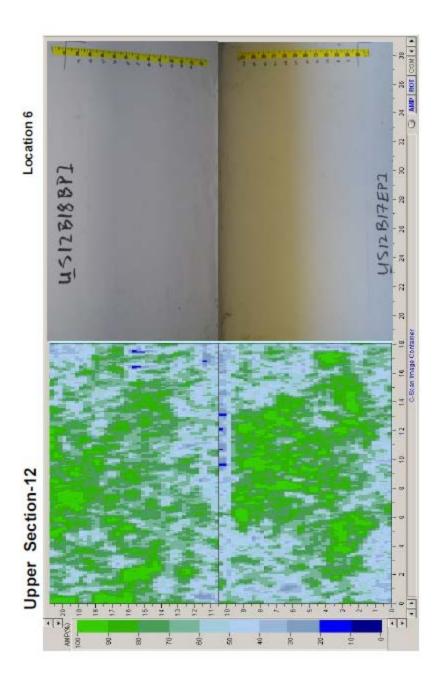


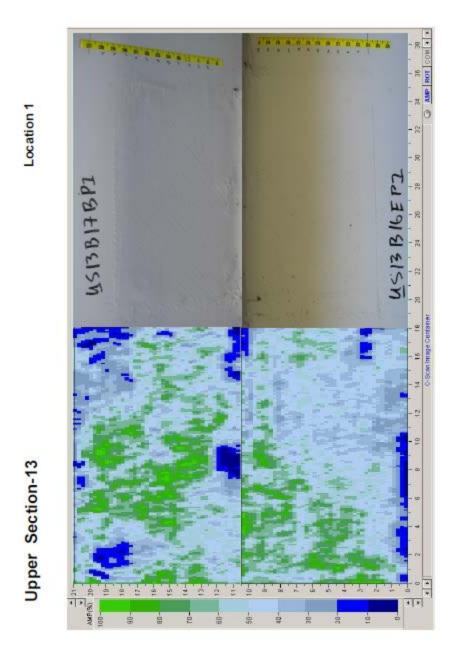


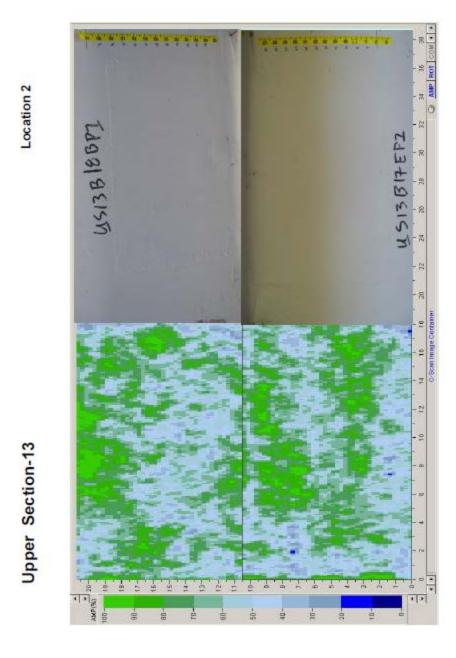


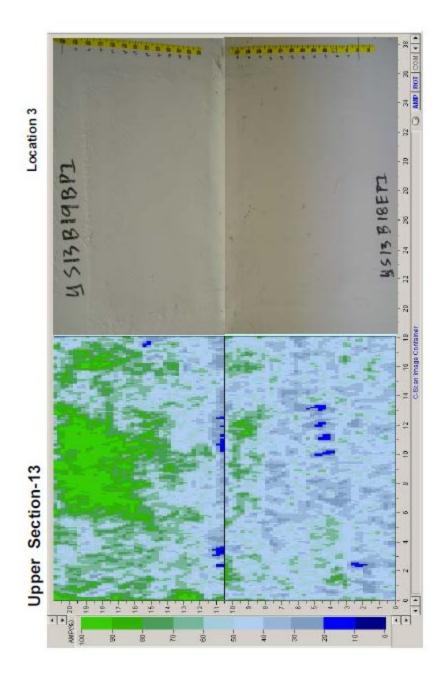


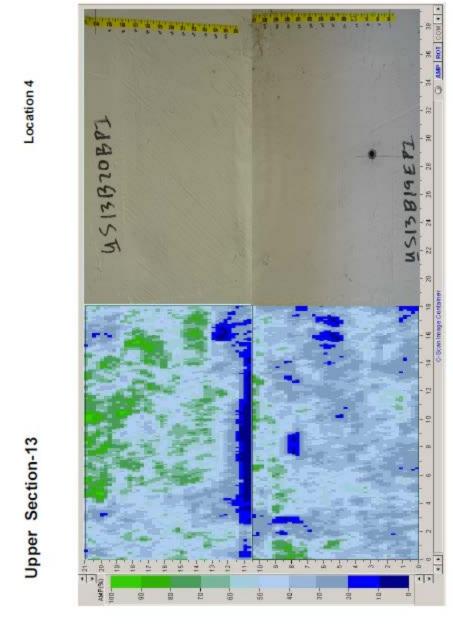


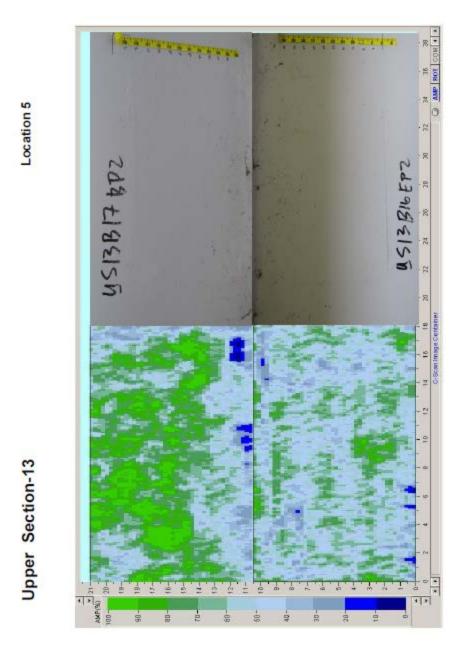


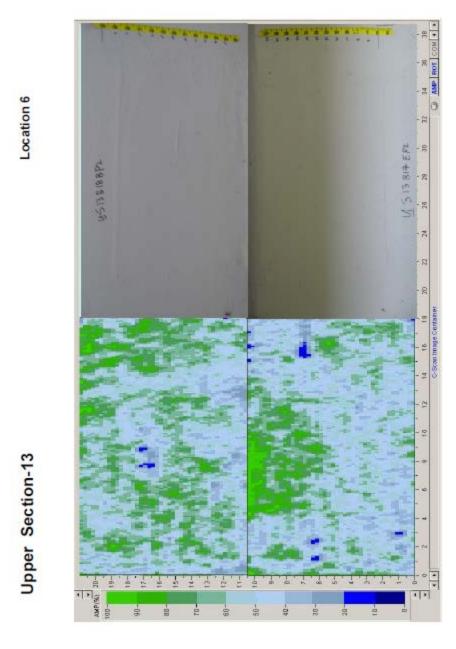


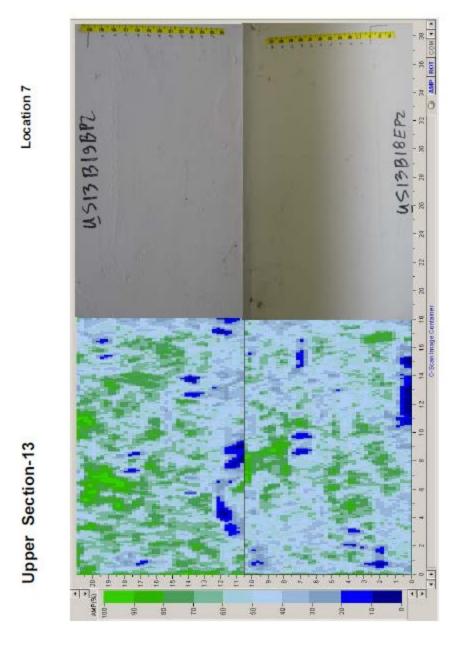


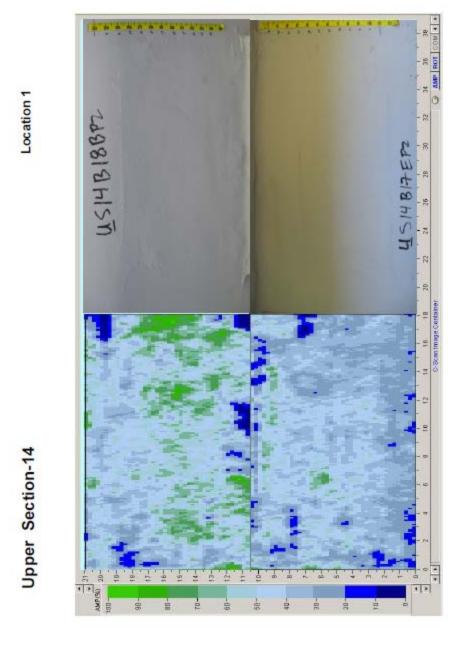


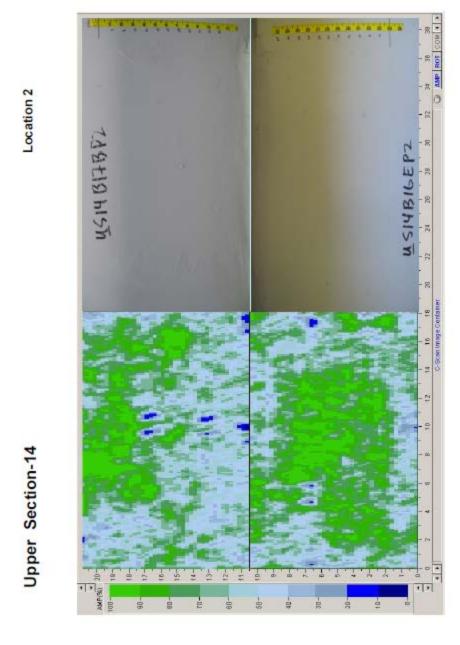




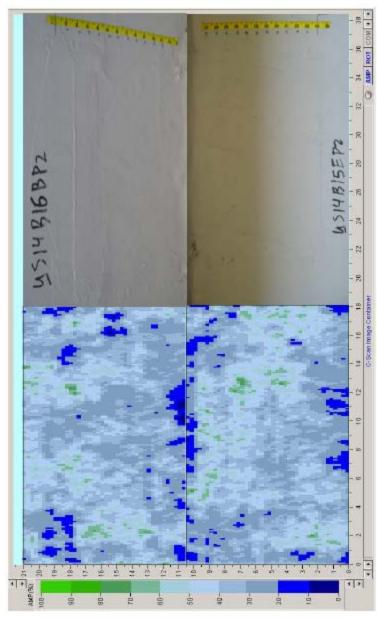


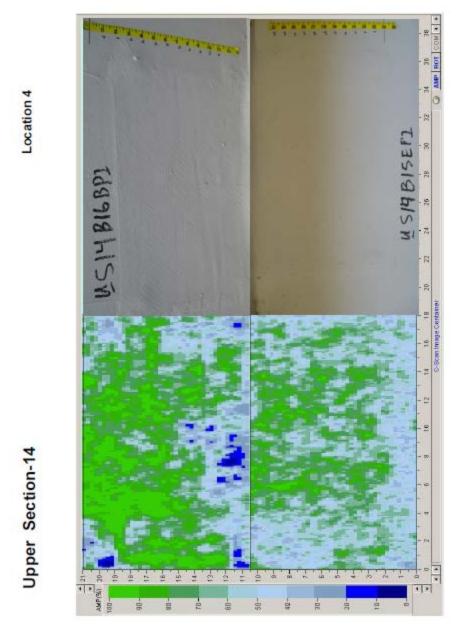


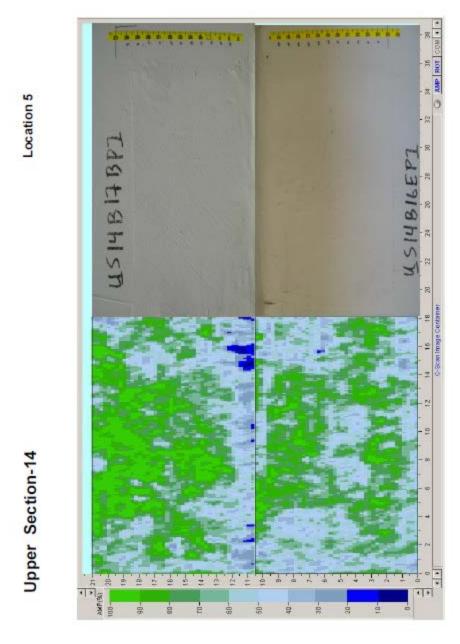




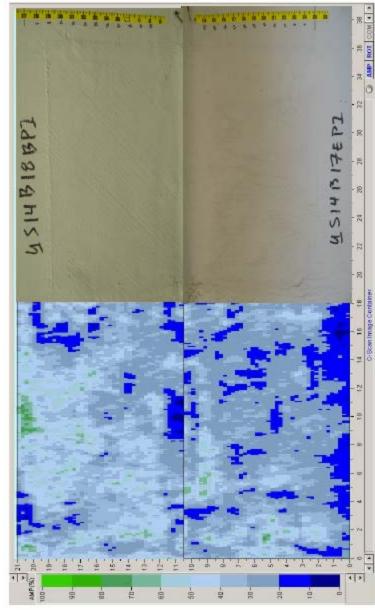


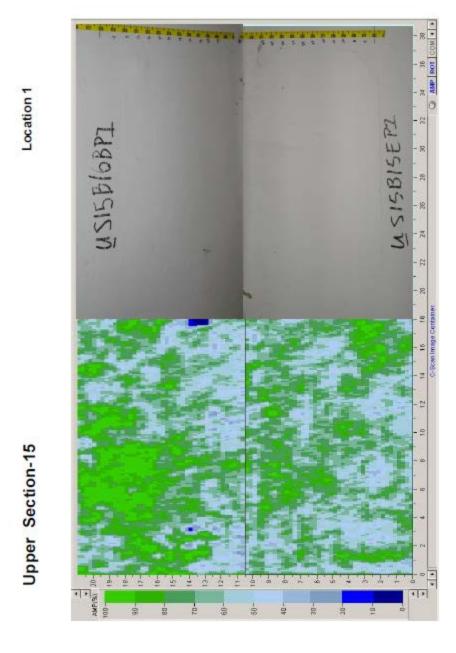




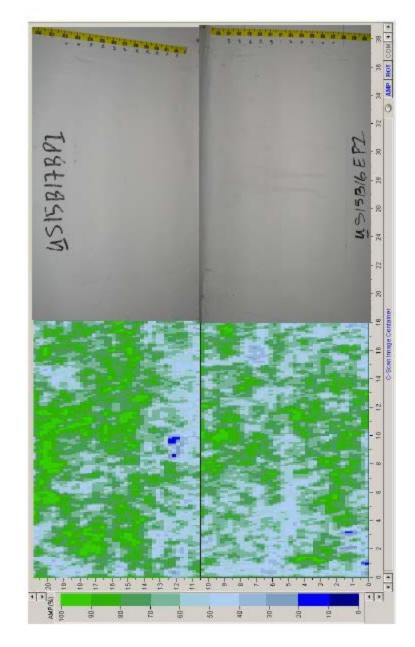


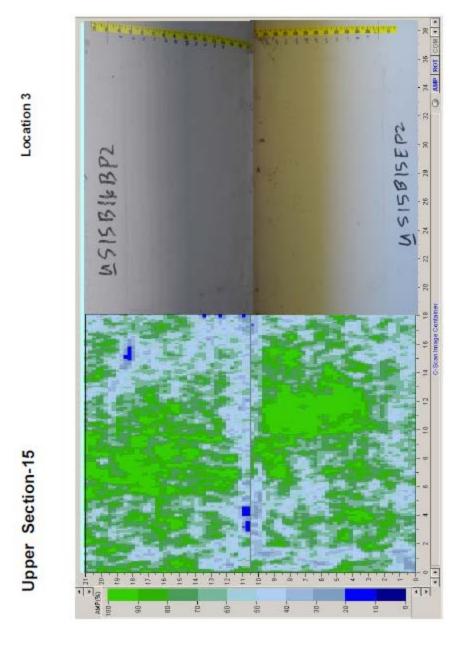


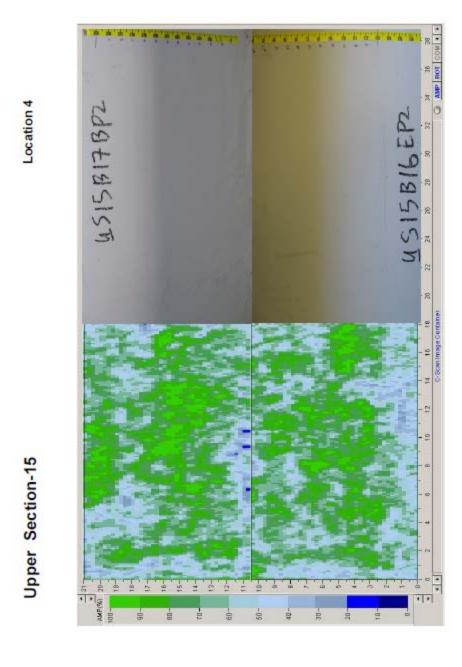


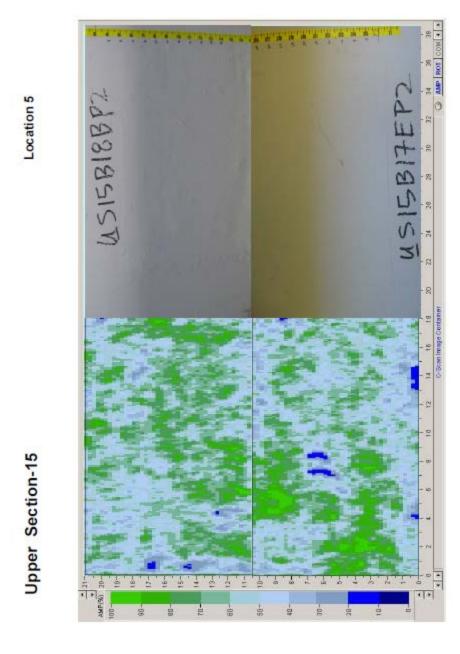


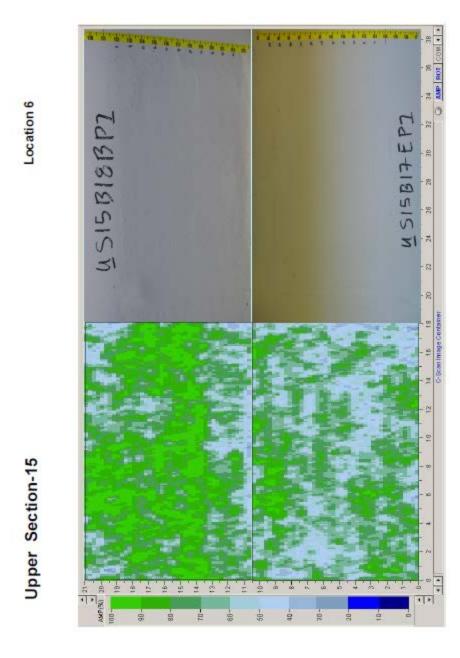


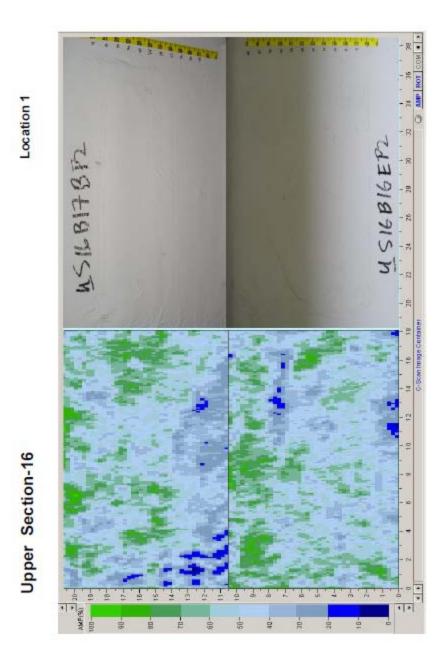


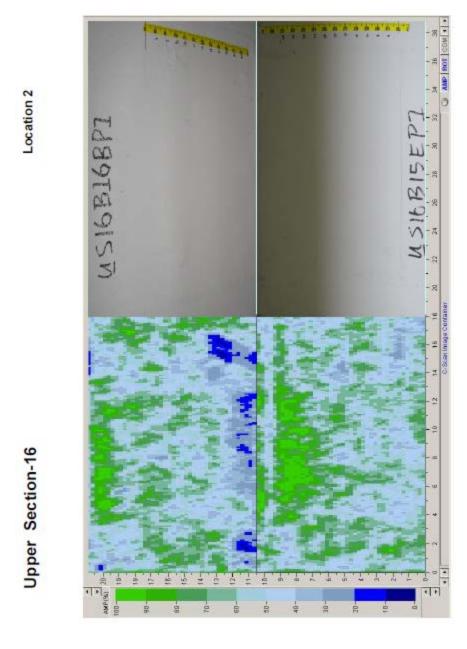


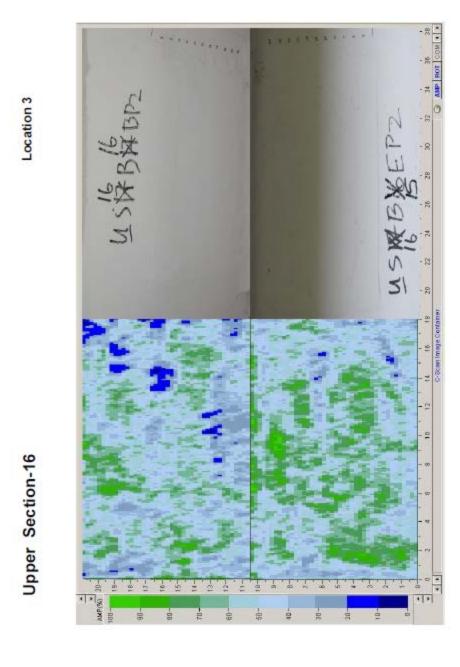


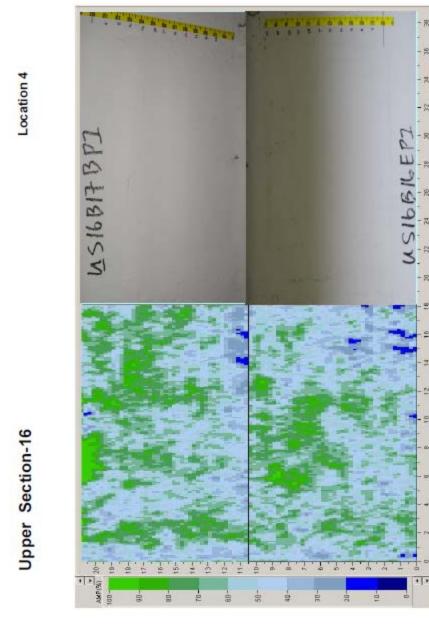


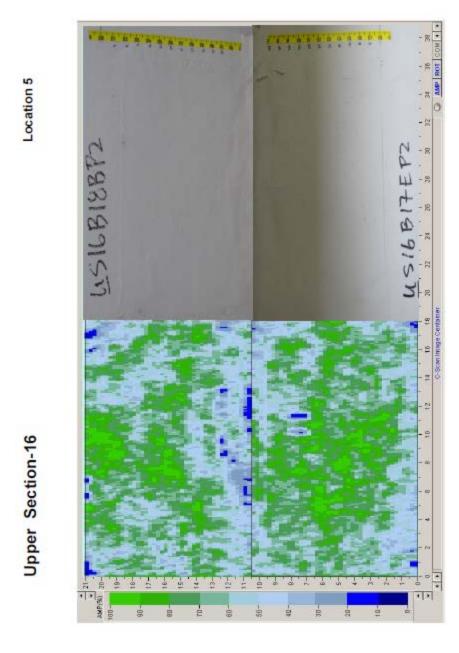


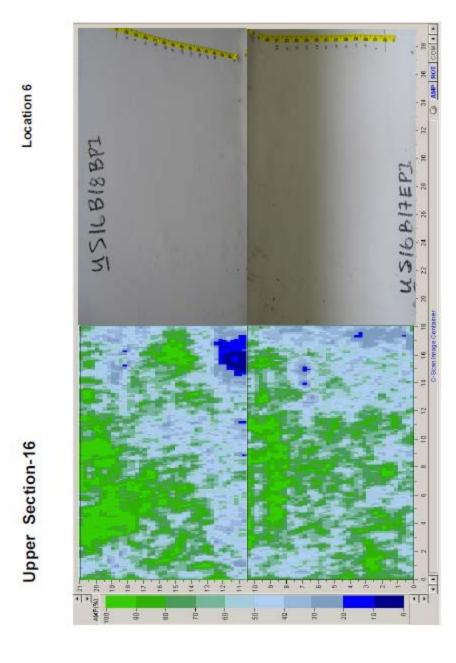


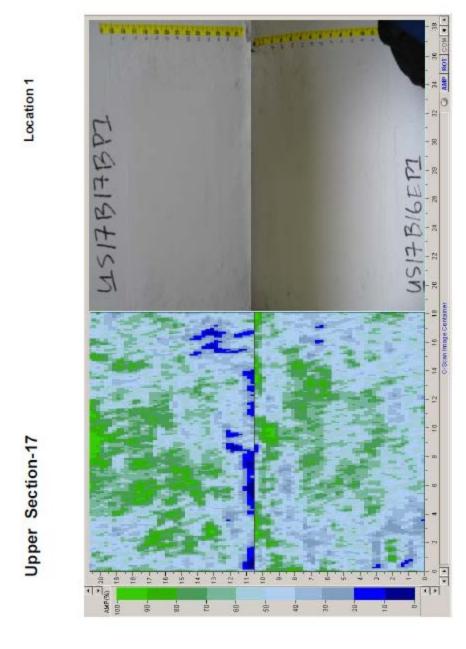


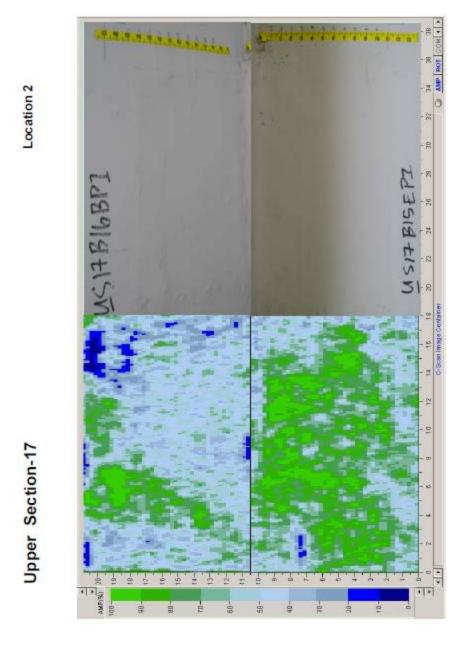


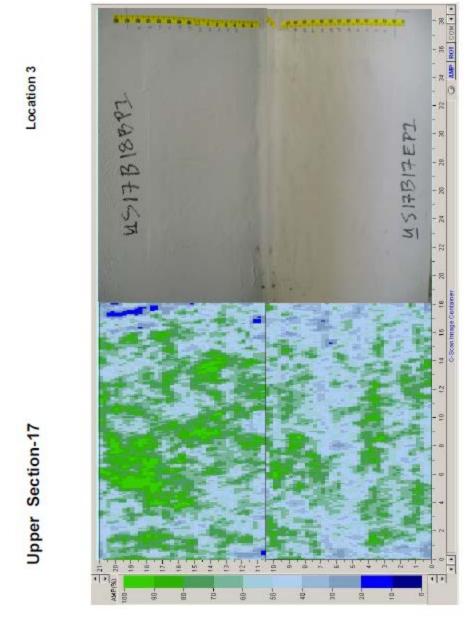




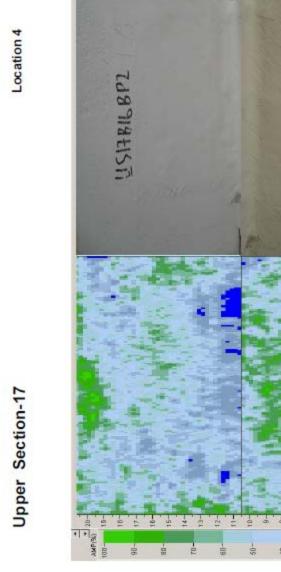


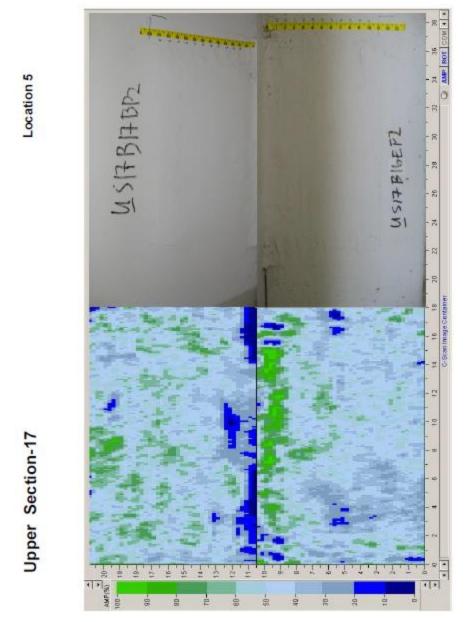


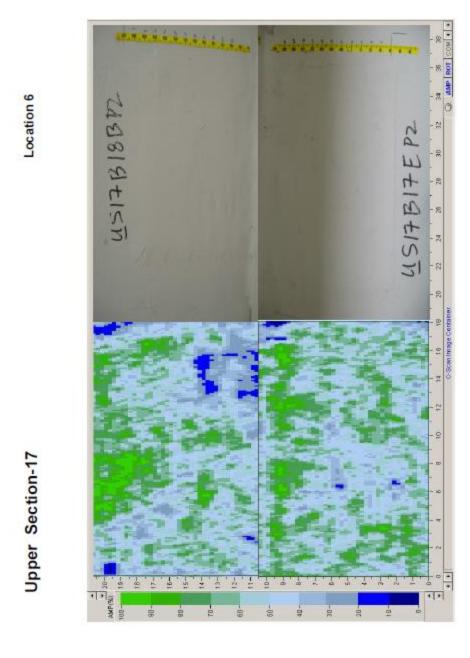




USHBISEPL







Appendix E: Original ROI Projection From Project Management Plan (PMP)

[Note: The text below is extracted from the submitted PMP for CPC Project F07-AR03. It is included for comparison with the post-demonstration economic analysis in Chapter 4.]

The Return on Investment (ROI) for project F07AR03 as computed in the Project Management Plan (PMP), revised 27 September 2006, is presented below.

Assumptions:

Alternative 1: Structural components of the West Point Michie Stadium require replacement 8 years from now, at a cost of \$25.5M, as shown under Baseline Costs. Average annualized maintenance cost of the existing structural components is \$280k, which drops to \$6.5k after replacement of the components, as shown under Baseline Costs. Since the replacement components will use the sensors, the operating cost of these sensors (\$10k) is also included, bringing the total cost to \$16.5k.

Alternative 2: Installing corrosion/degradation monitoring and degradation sensing technologies in year 1 at a project cost of \$940k is projected to extend the life of the structural components over the conventional maintenance schedule by another 30 years. Data from maintenance personnel indicate that early detection and subsequent preventive measures result in maintenance cost savings of 50%, (which means that the new system cost will be \$140k) plus the annual cost of operating the sensors (\$10k) for a total of \$150k as shown under New System Costs. Under this alternative, the structural components must be replaced in Year 30 at a cost of \$25.5M.

Comparing the two alternatives, the potential return-on-investment after implementing the new technology (Alternative 2) is 11.98 [see table below].

Return on Investment Calculation

Investment Required 940,000 Return on Investment Ratio 11.98 Percent 1198% Net Present Value of Costs and Benefits/Savings 5,192,295 16,456,195 11,263,900 С D F Α В Е G Future **Baseline Costs** Baseline New System New System Present Value of Present Value of Total Present Benefits/Savings Benefits/Savings Savings Year Costs Costs Value 280,000 150,000.0 140,190 261,688 121,498 113,542 280,000 150,000.0 131,010 244,552 280.000 150,000.0 122,445 228,564 106,119 99,177 280,000 150,000.0 114,435 213,612 280,000 150,000.0 106.950 199,640 92,690 99,945 86,619 280,000 150,000.0 186,564 280.000 150,000.0 93,405 174,356 80,951 25,500,000 150,000.0 87,300 14,841,000 14,753,700 16,500 150,000.0 81,585 8,974 -72,611 10 16,500 150,000.0 76,245 8,387 -67,858 11 16,500 150,000.0 71,265 7,839 -63,426 12 16,500 150,000.0 66,600 7,326 -59,274 13 16,500 150,000.0 -55,403 16,500 150,000.0 58,170 6,399 -51,771 15 16,500 150,000.0 54,360 5,980 -48,380 16 16,500 150,000.0 5,589 -45,216 50,805 17 16,500 150,000.0 47,490 5,224 -42,266 18 150,000.0 44,385 4,882 -39,503 16,500 19 16,500 150,000.0 41,475 4,562 -36,913 20 16,500 4,264 150,000.0 38.760 -34,496 21 16,500 -32,240 150,000.0 36,225 3,985 22 16,500 150,000.0 33,855 3,724 -30,131 3,480 -28,155 23 16,500 150,000.0 31,635 24 16.500 150,000.0 29.565 3.252 -26.313 25 16,500 150,000.0 27,630 3,039 -24,591 26 16,500 150,000.0 25,830 2,841 -22,989 27 16,500 150,000.0 24,135 2,655 -21,480

150,000.0

150,000.0

25,500,000

22,560

21,090

3,350,700

2.482

2,320

2,168

-20,078

-18,770

-3,348,532

28

29

16,500

16,500

16,500

REPORT DOCUMENTATION PAGE

Form Approved OMB No. 0704-0188

Public reporting burden for this collection of information is estimated to average 1 hour per response, including the time for reviewing instructions, searching existing data sources, gathering and maintaining the data needed, and completing and reviewing this collection of information. Send comments regarding this burden estimate or any other aspect of this collection of information, including suggestions for reducing this burden to Department of Defense, Washington Headquarters Services, Directorate for Information Operations and Reports (0704-0188), 1215 Jefferson Davis Highway, Suite 1204, Arlington, VA 22202-4302. Respondents should be aware that notwithstanding any other provision of law, no person shall be subject to any penalty for failing to comply with a collection of information if it does not display a currently valid OMB control number. PLEASE DO NOT RETURN YOUR FORM TO THE ABOVE ADDRESS.

1. REPORT DATE (DD-MM-YYYY) July 2014	2. REPORT TYPE Final	3. DATES COVERED (From - To)
4. TITLE AND SUBTITLE Corrosion/Degradation Monitoring	5a. CONTRACT NUMBER	
Building Service Life		5b. GRANT NUMBER
		5c. PROGRAM ELEMENT NUMBER Corrosion Prevention and Control
6. AUTHOR(S)	5d. PROJECT NUMBER	
Michael K. McInerney, Orange S. M	CPC F07-AR03	
Lawrence Clark, Chris Olaes, and V	5e. TASK NUMBER	
		5f. WORK UNIT NUMBER
7. PERFORMING ORGANIZATION NAME(8. PERFORMING ORGANIZATION REPORT NUMBER	
U.S. Army Engineer Research and I	ERDC/CERL TR-14-9	
Construction Engineering Research	Laboratory	
P.O. Box 9005		
Champaign, IL 61826-9005		
9. SPONSORING / MONITORING AGENC	10. SPONSOR/MONITOR'S ACRONYM(S)	
Office of the Secretary of Defense (OUSD(AT&L))	
3090 Defense Pentagon Washington, DC 20301-3090		11. SPONSOR/MONITOR'S REPORT NUMBER(S)

12. DISTRIBUTION / AVAILABILITY STATEMENT

Approved for public release; distribution is unlimited.

13. SUPPLEMENTARY NOTES

14. ABSTRACT

Fiber-reinforced polymer (FRP) composites offer cost and performance advantages for patching concrete structures that have corroded reinforcing steel, but the Army largely avoids structural composite repair applications because of the lack of long-term performance data. Established composite patch inspection methods are fast but highly subjective. This report describes the demonstration of acoustic guided wave (AGW) technology as a nondestructive evaluation (NDE) methodology for assessing the condition of FRP composite structural patches. The technology uses a hand-guided rolling probe to collect ultrasonic inspection data that can then be analyzed to determine patch condition.

The technology was used to evaluate more than 250 composite seismic upgrade patches installed in 1999 at historic Michie Stadium, U.S. Military Academy. The amplitude difference between the probe's emitted signal and the measured reflection provides data about bond quality and potential material defects. The technology identified five patches needing follow-up attention and possible rehabilitation. When considering costs for equipment procurement, logistics, labor, and field contingencies, an average patch-inspection time of 1.5 hours was estimated. The calculated life-cycle return on investment for this application was 11.91.

15. SUBJECT TERMS

acoustic guided wave (AGW); nondestructive evaluation (NDE); corrosion/degradation monitoring; fiber-reinforced polymer composites; reinforced concrete

16. SECURITY CLASSIFICATION OF:		17. LIMITATION OF ABSTRACT	18. NUMBER OF PAGES	19a. NAME OF RESPONSIBLE PERSON	
a. REPORT	b. ABSTRACT	c. THIS PAGE			19b. TELEPHONE NUMBER (include
Unclassified	Unclassified	Unclassified		364	area code)